CDF-7708
October 5, 2005

Search for $H \to WW^*$ in the dilepton channel with 360 pb^{-1} of Run II Data

S. Chuang [i], M. Coca [ii], M. Kruse [ii]

[i)] University of Wisconsin
[ii)] Duke University

Abstract

We have searched for $p\bar{p} \to H \to WW^*$ production in the dilepton channel ($W^+W^- \to \ell^+\nu\ell^-\bar{\nu}$, where $\ell = e$ or μ) using approximately 360 pb^{-1} Tevatron Run 2 data collected by the CDF detector. We have further optimized the analysis since blessed in 4.11.1 (using 184 /pb of data, collected up to run 168890) [9], by allowing one lepton leg to be above 10 GeV, a higher $\not\!\!E_T$ threshold, removing the missing significance requirement and using a looser jet veto. This improves significantly the lower mass Higgs expected limits. We construct a likelihood function from the $\Delta\phi(\ell,\ell)$ distribution, which we use to extract cross section limits using a Bayesian procedure. For Higgs masses of 110, 120, 130, 140, 150, 160, 170, 180, 190 and 200 GeV we obtain 95% CL limits on the $p\bar{p} \to H \to WW$ cross section of 8.3, 4.5, 4.4, 4.6, 3.5, 3.2, 3.4, 4.3, 6.4 and 4.6 pb respectively.

Contents

1 Introduction **10**

2 Changes from the previous version of the note **12**
2.1 September 27th, 2005 12

3 Event Selection **13**
3.1 Objects Identification 13
3.2 Lepton identification 14
3.3 Dilepton categories 17
3.4 Event Selection 17
3.5 Selection Optimization 20

4 Monte Carlo Datasets **25**

5 Signal Acceptances **27**

6 Scale Factors **28**

7 Measuring Z$\rightarrow \ell\ell$ cross-sections **29**

8 $H \rightarrow WW$ Acceptance Systematic Uncertainties **30**
8.1 PDF Uncertainty 30
8.2 ISR-more/less 30
8.3 α_s 30
8.4 Jet Energy Scale 31
8.5 Lepton ID 31
8.6 Track Isolation 31
8.7 Trigger Efficiency 31
8.8 Combined Acceptance Systematic 34

9 Background Estimates **34**
9.1 WW background 34
9.2 $t\bar{t}$ background 34
9.3 Drell-Yan background 34
9.4 Fake background 35
9.5 $W\gamma$ background 35
9.6 WZ and ZZ background 35
9.7 Background systematic uncertainties 36

10 Data analysis **37**
10.1 Data samples and luminosity 37
10.2 Energy Scale factors for Plug electrons. 38
10.3 Dilepton table 39

11 Grand Summary **39**

12 Cross-Section Limit Calculation **40**
12.1 $\Delta\phi$ Distributions 40
12.2 The Likelihood function and Posterior Density 52
12.3 Expected Limits from Pseudo-experiments 52
12.4 Cross section Limits from the Data 54

13 Conclusions **57**

A Comparison with the THWG's Prospects **59**

B Expected signal, backgrounds and data candidates per di-lepton channel **59**

C Detailed acceptance tables **64**

List of Tables

1 The SM Higgs production cross section and branching ratios of H→WW are presented [19]. Also we show the number of events produced in 360 pb^{-1}, where ℓ = e or μ. . . . 12
2 Baseline cuts for central high-p_T isolated electrons ($E_T > 20$ GeV) (CEM) [15]. . . 15
3 Baseline cuts for plug isolated electrons (PHX) [15]. . . . 15
4 Baseline cuts for minimum ionizing isolated tracks [12]. After passing these cuts the muon is classified as *CMUP*, *CMX* or *non-triggering* according to the definitions in the text. . . . 16
5 Dilepton categories included in the current analysis. Shown in bold are the triggerable lepton in the data samples studied. The one exception to this is the PHX categories. Both lepton legs are required to be isolated. . . . 18
6 Fraction of events passing various kinematics cuts, as a function of the Higgs mass. 22
8 The DY background as a function of Higgs mass with or without the cut ($\not\!\!E_T > 50$ GeV $||\Delta\phi(\not\!\!E_T$, lep/jet) > 0.35)). . . . 25
7 Results of varying the $\not\!\!E_T$ and 1-jet E_T threshold. Defaults are $\not\!\!E_T < M_H/4$ and ${E_T}^{\text{1-jet}} < 50$ GeV. We show the default expected limits, expected limits when changing the cut for the 1-jet Et from 50 to $50 + 5, +10, +15, +20$ GeV, and also expected limits for $\not\!\!E_T < M_H/4 - 10, -5, +5, +10, +15, +20, +25, +30$ GeV. . . . 25
9 Monte Carlo datasets used for HWW analysis. . . . 26
10 Event Selection for the HWW analysis. . . . 28
11 Summary of trigger efficiencies. The CEM_18 trigger efficiency is run-dependent, number given above being an average over η. We use the MET_PEM trigger efficiency as estimated in 4.11.1. The contribution from dilepton categories triggered by PHX is below 15%. . . . 28
13 PHX charge mis-identification scale factors [7]. . . . 29
12 Summary of lepton data/MC scale factors. . . . 29
14 Summary of Z cross-section measurements. . . . 29
15 Sources of systematic uncertainty on the $H \to WW \to l^+l^-\nu\bar{\nu}$ acceptance. . . . 30
16 Track isolation scale factors (data/MC) for all the lepton types used in the HWW analysis. The statistical error are all below 1%. . . . 31
17 $W\gamma$ MC samples used to estimate the background to HWW. . . . 35
18 Sources of systematic uncertainties on the backgrounds. To all these uncertainties we add in quadrature 6% coming from luminosity. . . . 37
19 Luminosities of the different di-lepton categories used in the analysis. . . . 38
20 Phoenix electron energy scale factors divided by run range, plug side ($\eta > 0$ for east; $\eta < 0$ for west) and data/MC. . . . 39
21 The estimated backgrounds and HWW signal in 360 pb^{-1}, and the number of events observed in the data, for each of the dilepton categories. The HWW expectation uses the theoretical cross-sections and BRs discussed in Section 1. The error on luminosity (6%) it is not included. . . . 40

22 The estimated backgrounds and HWW signal in $360\,\mathrm{pb}^{-1}$, and the number of events observed in the data, for each of the dilepton categories. The HWW expectation uses the theoretical cross-sections and BRs discussed in Section 1. The error on luminosity it is not included. 40
23 95% CL limits on $\sigma(gg \to H) \times BR(H \to WW^*)$ at $\sqrt{\hat{s}} = 1.96\,\mathrm{TeV}$ for the different Higgs obtained using our old 20-20 selection from CDF-6958, for 200 /pb. The expected limits using the new selection are also shown, as discussed above. In all cases the limits correspond to $360\,\mathrm{pb}^{-1}$. 57
24 Comparison between the current status of our analysis and the THWG's prospect for the same integrated luminosity. The THWG's prospect are taken from Table 29 of the Report of the Tevatron Higgs Working Group [19] (originally at fb^{-1} scale) and interpolated to $\mathcal{L}_{\mathrm{int}} = 360\ \mathrm{pb}^{-1}$. 59
25 Summary of the signal and background expectations for a Higgs mass of 110 GeV, for 360 pb^{-1}. Also the observed number of events is shown. The error on luminosity it is not included. 59
26 Summary of the signal and background expectations for a Higgs mass of 120 GeV, for 360 pb^{-1}. Also the observed number of events is shown. The error on luminosity it is not included. 60
27 Summary of the signal and background expectations for a Higgs mass of 130 GeV, for 360 pb^{-1}. Also the observed number of events is shown. The error on luminosity it is not included. 60
28 Summary of the signal and background expectations for a Higgs mass of 140 GeV, for 360 pb^{-1}. Also the observed number of events is shown. The error on luminosity it is not included. 61
29 Summary of the signal and background expectations for a Higgs mass of 150 GeV, for 360 pb^{-1}. Also the observed number of events is shown. The error on luminosity it is not included. 61
30 Summary of the signal and background expectations for a Higgs mass of 160 GeV, for 360 pb^{-1}. Also the observed number of events is shown. The error on luminosity it is not included. 62
31 Summary of the signal and background expectations for a Higgs mass of 170 GeV, for 360 pb^{-1}. Also the observed number of events is shown. The error on luminosity it is not included. 62
32 Summary of the signal and background expectations for a Higgs mass of 180 GeV, for 360 pb^{-1}. Also the observed number of events is shown. The error on luminosity it is not included. 63
33 Summary of the signal and background expectations for a Higgs mass of 190 GeV, for 360 pb^{-1}. Also the observed number of events is shown. The error on luminosity it is not included. 63
34 Summary of the signal and background expectations for a Higgs mass of 200 GeV, for 360 pb^{-1}. Also the observed number of events is shown. The error on luminosity it is not included. 64

35 data acceptance table, assuming $M_H^{\rm SM} = 130$ GeV 65
36 HWW acceptance table, assuming $M_H^{\rm SM} = 130$ GeV 66
37 data acceptance table, assuming $M_H^{\rm SM} = 140$ GeV 67
38 data acceptance table, assuming $M_H^{\rm SM} = 150$ GeV 68
39 data acceptance table, assuming $M_H^{\rm SM} = 160$ GeV 69
40 HWW dilepton MC acceptance table, assuming $M_H^{\rm SM} = 160$ GeV 70
41 WW MC acceptance table, assuming $M_H^{\rm SM} = 160$ GeV 71
42 WZ MC acceptance table, assuming $M_H^{\rm SM} = 160$ GeV 72
43 $t\bar{t}$ MC acceptance table, assuming $M_H^{\rm SM} = 160$ GeV 73
44 Drell-Yan MC acceptance table, assuming $M_H^{\rm SM} = 160$ GeV 74
45 ZZ MC acceptance table, assuming $M_H^{\rm SM} = 160$ GeV 75
46 $W\gamma$ MC acceptance table, assuming $M_H^{\rm SM} = 160$ GeV 76
47 fakesacceptance table, assuming $M_H^{\rm SM} = 160$ GeV 77
48 data acceptance table, assuming $M_H^{\rm SM} = 170$ GeV 78
49 data acceptance table, assuming $M_H^{\rm SM} = 180$ GeV 79

List of Figures

1 SM Higgs production versus the mass of the Higgs boson. 10

2 Relative branching ratios for Higgs boson decays. 11

3 Feynman diagram for the dominant production mechanism, with both final state W's decaying leptonically. 11

4 Four of the variables used in the event selection (for $M_H = 180$ GeV) are shown before cutting on that variable: (upper-left) number of jets; (upper-right) missing energy; (lower-left) dilepton invariant mass and (lower-right) $P_T(lep1)$ + $P_T(lep2)$+$\not\!\!E_T$. 19

5 Highest lepton p_T vs the second highest lepton p_T for a 130 GeV Higgs. 21

6 Highest lepton p_T vs the second highest lepton p_T for a 180 GeV Higgs. 21

7 The fraction of events passing kinematical cuts on $p_T(max)$, $p_T(min)$, for a 130 GeV Higgs. The circled values show that the efficiency increases from 39 to 78 %, when lowering the transverse momentum requirement on the second lepton from 20 to 10 GeV. 22

8 Missing energy for the signal (M_H=160 GeV) and WW background. 23

9 Jet E_T spectrum is shown before the jet veto, for: (upper-left) any number of jets event; (upper-right) only for 1-jet events; (lower-left) the leading jet in 2-jet events; (lower-right) the second jet in 2-jet events. Also the data point are shown, for 360/pb. The plots are made after requiring 2 good leptons, with $m_{\ell\ell} > 16$ GeV. 24

10 Signal acceptance for various Higgs masses. For comparison the generation 4 values are also shown. 27

11 Track isolation distributions per trkIsol-required lepton type and the cut efficiencies from data or MC as a function of lepton p_T. 32

12 Track isolation distributions per trkIsol-required lepton type and the cut efficiencies from data or MC as a function of lepton p_T. 33

13 The mass peak of $Z \to e_{\rm TCE}e_{\rm PHX}$ with phoenix electron energies added plug preradiator energies and scaled up by factors as listed in Table 20. 39

14 Azimuthal angular separation between the leptons, $\Delta\phi(\ell,\ell)$, from the decay of $H \to WW^* \to \ell\nu\ell\nu$. Distributions of data, HWW^* signal ($M_H = 110$ GeV) MC, WW MC and the sum of other considered background MC samples are shown. The MCs are normalized to the expectations for the integrated luminosity for analyzed data, about 360/pb. We use the upper-left $ee + e\mu + \mu\mu$ plot to fit for a limit on the cross-section of SM HWW production at Tevatron, at the Higgs mass of $M_H = 110$ GeV. 42

15 Azimuthal angular separation between the leptons, $\Delta\phi(\ell,\ell)$, from the decay of $H \to WW^* \to \ell\nu\ell\nu$. Distributions of data, HWW^* signal ($M_H = 120$ GeV) MC, WW MC and the sum of other considered background MC samples are shown. The MCs are normalized to the expectations for the integrated luminosity for analyzed data, about 360/pb. We use the upper-left $ee + e\mu + \mu\mu$ plot to fit for a limit on the cross-section of SM HWW production at Tevatron, at the Higgs mass of $M_H = 120$ GeV. 43

16 Azimuthal angular separation between the leptons, $\Delta\phi(\ell,\ell)$, from the decay of $H \to WW^* \to \ell\nu\ell\nu$. Distributions of data, HWW^* signal ($M_H = 130$ GeV) MC, WW MC and the sum of other considered background MC samples are shown. The MCs are normalized to the expectations for the integrated luminosity for analyzed data, about 360/pb. We use the upper-left $ee + e\mu + \mu\mu$ plot to fit for a limit on the cross-section of SM HWW production at Tevatron, at the Higgs mass of $M_H = 130$ GeV. 44

17 Azimuthal angular separation between the leptons, $\Delta\phi(\ell,\ell)$, from the decay of $H \to WW^* \to \ell\nu\ell\nu$. Distributions of data, HWW^* signal ($M_H = 140$ GeV) MC, WW MC and the sum of other considered background MC samples are shown. The MCs are normalized to the expectations for the integrated luminosity for analyzed data, about 360/pb. We use the upper-left $ee + e\mu + \mu\mu$ plot to fit for a limit on the cross-section of SM HWW production at Tevatron, at the Higgs mass of $M_H = 140$ GeV. 45

18 Azimuthal angular separation between the leptons, $\Delta\phi(\ell,\ell)$, from the decay of $H \to WW^* \to \ell\nu\ell\nu$. Distributions of data, HWW^* signal ($M_H = 150$ GeV) MC, WW MC and the sum of other considered background MC samples are shown. The MCs are normalized to the expectations for the integrated luminosity for analyzed data, about 360/pb. We use the upper-left $ee + e\mu + \mu\mu$ plot to fit for a limit on the cross-section of SM HWW production at Tevatron, at the Higgs mass of $M_H = 150$ GeV. 46

19 Azimuthal angular separation between the leptons, $\Delta\phi(\ell,\ell)$, from the decay of $H \to WW^* \to \ell\nu\ell\nu$. Distributions of data, HWW^* signal ($M_H = 160$ GeV) MC, WW MC and the sum of other considered background MC samples are shown. The MCs are normalized to the expectations for the integrated luminosity for analyzed data, about 360/pb. We use the upper-left $ee + e\mu + \mu\mu$ plot to fit for a limit on the cross-section of SM HWW production at Tevatron, at the Higgs mass of $M_H = 160$ GeV. 47

20 Azimuthal angular separation between the leptons, $\Delta\phi(\ell,\ell)$, from the decay of $H \to WW^* \to \ell\nu\ell\nu$. Distributions of data, HWW^* signal ($M_H = 170$ GeV) MC, WW MC and the sum of other considered background MC samples are shown. The MCs are normalized to the expectations for the integrated luminosity for analyzed data, about 360/pb. We use the upper-left $ee + e\mu + \mu\mu$ plot to fit for a limit on the cross-section of SM HWW production at Tevatron, at the Higgs mass of $M_H = 170$ GeV. 48

21 Azimuthal angular separation between the leptons, $\Delta\phi(\ell,\ell)$, from the decay of $H \to WW^* \to \ell\nu\ell\nu$. Distributions of data, HWW^* signal ($M_H = 180$ GeV) MC, WW MC and the sum of other considered background MC samples are shown. The MCs are normalized to the expectations for the integrated luminosity for analyzed data, about 360/pb. We use the upper-left $ee + e\mu + \mu\mu$ plot to fit for a limit on the cross-section of SM HWW production at Tevatron, at the Higgs mass of $M_H = 180$ GeV. 49
22 Azimuthal angular separation between the leptons, $\Delta\phi(\ell,\ell)$, from the decay of $H \to WW^* \to \ell\nu\ell\nu$. Distributions of data, HWW^* signal ($M_H = 190$ GeV) MC, WW MC and the sum of other considered background MC samples are shown. The MCs are normalized to the expectations for the integrated luminosity for analyzed data, about 360/pb. We use the upper-left $ee + e\mu + \mu\mu$ plot to fit for a limit on the cross-section of SM HWW production at Tevatron, at the Higgs mass of $M_H = 190$ GeV. 50
23 Azimuthal angular separation between the leptons, $\Delta\phi(\ell,\ell)$, from the decay of $H \to WW^* \to \ell\nu\ell\nu$. Distributions of data, HWW^* signal ($M_H = 200$ GeV) MC, WW MC and the sum of other considered background MC samples are shown. The MCs are normalized to the expectations for the integrated luminosity for analyzed data, about 360/pb. We use the upper-left $ee + e\mu + \mu\mu$ plot to fit for a limit on the cross-section of SM HWW production at Tevatron, at the Higgs mass of $M_H = 200$ GeV. 51
24 Expected limits obtained from pseudo-experiments drawn from $\Delta\phi(\ell,\ell)$ distributions, for Higgs masses from 110-160 GeV/c^2. The red line represents the 95% CL extracted from data. 53
25 Expected limits obtained pseudo-experiments, drawn from $\Delta\phi(\ell,\ell)$ distributions, for Higgs masses from 170-200 GeV/c^2. The red line represents the 95% CL extracted from data. 54
26 The likelihood functions obtained from $\Delta\phi(\ell,\ell)$ distributions, for Higgs masses from 110-160 GeV/c^2. 55
27 The likelihood functions obtained from $\Delta\phi(\ell,\ell)$ distributions, for Higgs masses from 170-200 GeV/c^2. 56

1 Introduction

In the Standard Model, the Higgs mechanism generates the masses of the elementary particles and also stabilizes the high energy behavior of the electroweak interactions. The Standard Model does not predict the mass of the Higgs model, but there are direct and indirect constrains on the Higgs mass. The current best lower limit is $m_H > 114.4$ GeV, at 95% confidence limit (CL), established by direct searches, through the process $e^+e^- \rightarrow HZ$, by the LEP experiments [17]. The Higgs mass indirect limit, determined from the fit to the known data, is 98^{+52}_{-36} GeV and $m_H < 208$ GeV at 95% confidence level (CL) [18][1].

At the Tevatron the dominant SM Higgs boson production mechanism is gluon-gluon fusion, gg→H (Figure 1). The second Higgs production mechanism, quark-quark fusion, which produces a Higgs in association with a W boson, is about 2 orders of magnitude smaller.

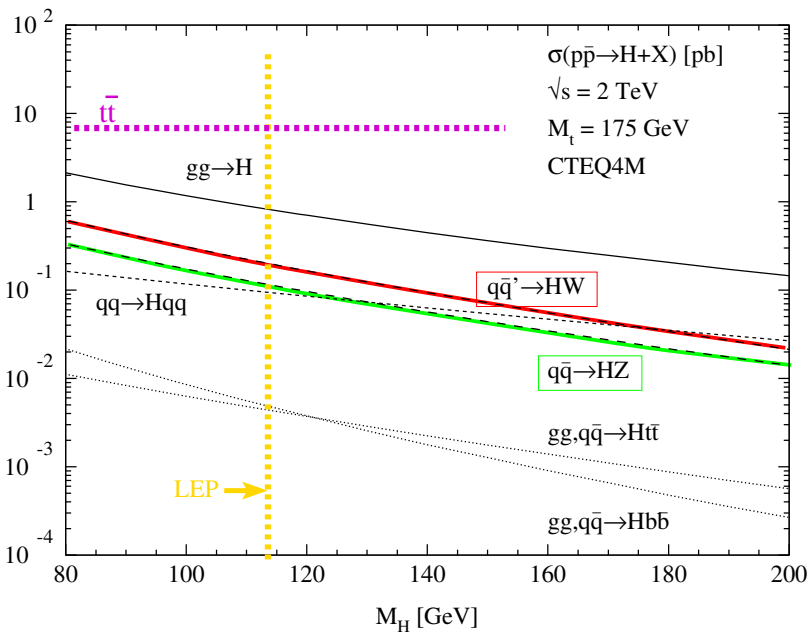

Figure 1: SM Higgs production versus the mass of the Higgs boson.

For Higgs masses greater than about 135 GeV/c^2, the decay branching ratio to W pairs becomes dominant as can be seen in Figure 2. In this analysis we search for $p\bar{p} \rightarrow H \rightarrow WW^*$ for Higgs masses ranging from 110 GeV/c^2 to 200 GeV/c^2, using the leptonic decays of both W bosons (Figure 3).

[1]This limits are obtained using the most recent top mass measurement, $m_{top} = 174.3 \pm 3.4$ GeV.

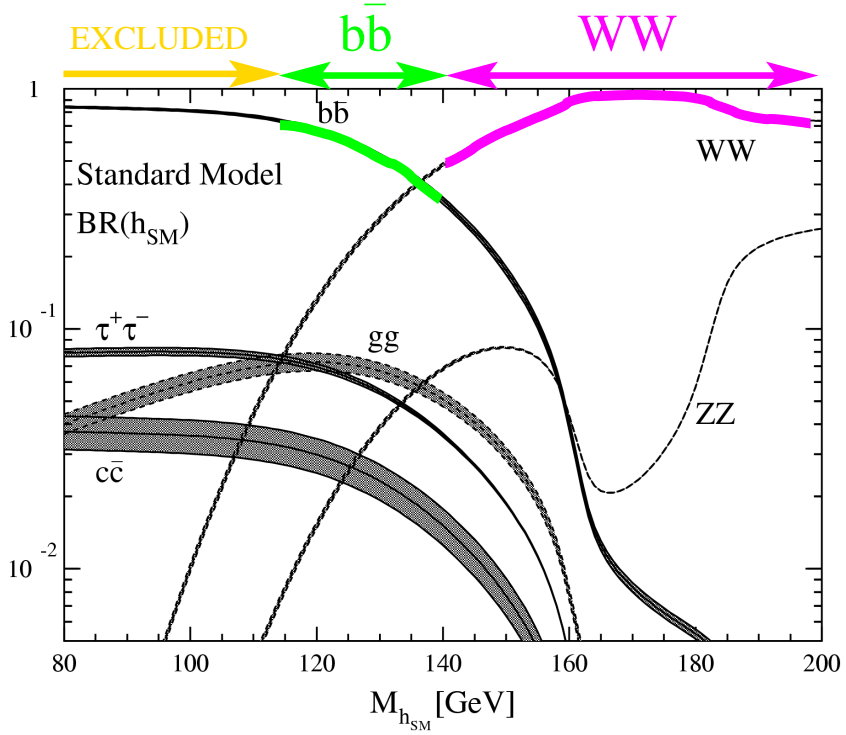

Figure 2: Relative branching ratios for Higgs boson decays.

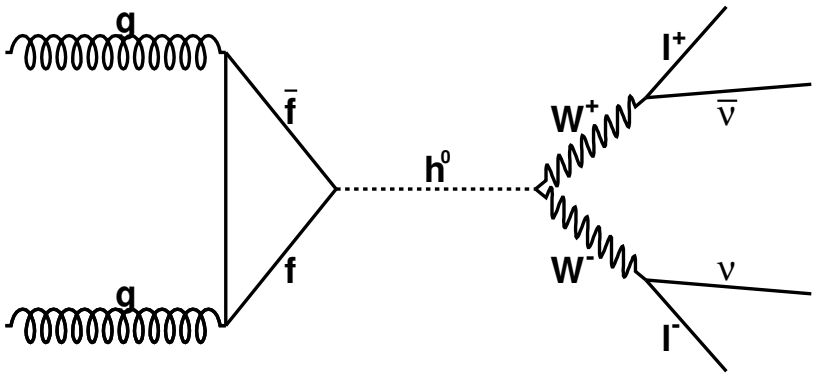

Figure 3: Feynman diagram for the dominant production mechanism, with both final state W's decaying leptonically.

At the LHC gg→H → WW → dileptons is one of the golden channels, so this analysis could be seen as a good training ground for the future, if we cannot discover the Higgs at the Tevatron [2].

[2]In fact near $M_H = 2 * M_W$ the decay mode Higgs to ZZ is suppressed, as can be seen in figure 2.

Also even if the SM cross-section for this channel is small, the new physics might enhance the signal. For example if a 4th SM generation of fermions exists, $\sigma(\mathrm{gg}\rightarrow \mathrm{H})$ could be up to 8 times higher then the SM [2].

The standard model prediction of signal cross-sections and branching ratios, and the expected number of events in 360 pb^{-1} are shown in table 7, for different Higgs masses.

Higgs mass (GeV/c^2)	110	120	130	140	150	160	170	180	190	200
$\sigma(p\bar{p} \rightarrow H)$ (pb)	0.9	0.70	0.56	0.45	0.36	0.30	0.25	0.21	0.17	0.15
$BR(H \rightarrow WW)$	0.04	0.13	0.30	0.48	0.68	0.90	0.97	0.94	0.78	0.74
$H \rightarrow WW$ events in 360 pb^{-1}	13	33	60	78	88	97	87	71	48	34
$HWW\ell\nu\ell\nu$ events in 360 pb^{-1}	0.6	1.5	2.7	3.6	4.0	4.4	4.0	3.2	2.2	1.6

Table 1: The SM Higgs production cross section and branching ratios of H→WW are presented [19]. Also we show the number of events produced in 360 pb^{-1}, where ℓ = e or μ.

Note that what we actually *observe* is the final row of numbers multiplied by the signal acceptance (which is of order 5%). Although the SM Higgs cross sections are at present too small to expect an observation, our search is also sensitive to other models as will be discussed in a later document. In addition this analysis can and will be combined with other searches using different decay channels.

2 Changes from the previous version of the note

2.1 September 27th, 2005

The following are the main changes to the analysis from the September 1st 2005 preblessing:

- We evaluated the pdf uncertainties using the JPM recommended Hessian method [3]. With the new PDF set CTEQ6M, the CTEQ group made available 40 complementary PDF sets CTEQ6M.01...CTEQ6M.40 each of which represents an up/down variation along one of the twenty eigenvectors (corresponding to 20 free parameters used in the fit). They form an orthonormal basis set spanning the full PDF parameter space [1]. Each up and down variation pair represents the range of PDF behavior that is consistent with the current global data. Each event in the Pythia HWW sample is reweighted according to the ratio of the CTEQ6M PDF values and the CTEQ6M.xx PDF values. We add the variations on acceptance in quadrature which results in (+2.76%/-3.44%). Then symmetrize and take 3% as systematic uncertainty.

  Also we compared MRST75 and MRST72, with different α_s values and find a 3.3 % difference taken as systematic error.

- We evaluated the error due to ISR on the acceptance, by generating two samples: ISR-more and ISR-less. A 3% unceratinty is assigned.

- We assign a 20% uncertainty to DY background due to the met modelling. We use the ratio between data and MC cut efficiency to quantify this.

- We updated Z→ $\ell\ell$ cross-section measurements in the electron and muons channels, after some bug fixes. The results agree well with the theoretical NNLO calculation (see section 7).

- Also the rest of the updates to the note are typos or improvements in the description of the analysis.

3 Event Selection

The signal process $p\bar{p} \to H \to W^+W^- \to \ell^+\ell^-\nu\bar{\nu}$, where $\ell = e$ or μ), results in the final state of *two leptons, missing energy (from undetected neutrinos) and no hard jets (possibly soft jets from initial state radiation(ISR)).*

3.1 Objects Identification

Leptons

We discuss lepton selection in detail in section 3.2.

Jets

The jets are the result of the fragmentation and hadronization of colored objects, such as quarks and gluons. There is assumed to be a one-to-one correspondence between a parton and its corresponding jet. The jets are clustered within a 0.4 cone and raw jet energies are applied level 5 energy corrections. We select jets with E_T(L5 corrected) > 15 GeV and $\eta_{detector} < 2.5$[3].

Missing energy

The *raw* $\not\!\!E_T$ is defined as the negative vector sum of the transverse energy in the calorimeter, both electromagnetic and hadronic:

$$\vec{\not\!\!E_T} = -\sum_i [(E_i^{em} + E_i^{had}) sin\theta_i] \times \hat{n_i} \quad (1)$$

where E_i^{em}, E_i^{had} are the electromagnetic, respectively hadronic energy of the i^{th} tower, and $\hat{n_i}$ is a transverse unit vector pointing to the center of each tower. The θ_i is the polar angle of the i^{th} tower with respect to the z=0 coordinate frame. The sum in the above equation extends to $|\eta| < 3.6$, to avoid the forward calorimeter region.

On top of the raw $\not\!\!E_T$ there are few corrections applied, before using $\not\!\!E_T$ for an event selection:

[3]From now on, unless explicitly stated, by *jet* we will refer to such an object, with E_T(L5 corrected) > 15 GeV and $\eta_{detector} < 2.5$.

- *Primary vertex correction*: The raw missing energy stored in CdfMet bank assumes that the event primary vertex is z = 0; using the full offline event information one reconstruct the event primary vertex and then recalculate ($\not\!\!E_{Tx}, \not\!\!E_{Ty}$).

- *Muon correction*: The muons are minimum ionizing particles and they deposit very little energy in the calorimeter. Therefore we add back to ($\not\!\!E_{Tx}, \not\!\!E_{Ty}$) the transverse energy deposited in the electromagnetic and hadronic calorimeter and subtract the COT beam constrained muon momentum components, (P_{Tx}, P_{Ty}). We correct *for all the muons*, passing the dilepton selection cuts; they could be CMUP, CMP-only, CMU-only, CMX or CMIO.

- *Jet correction*: Every jet is corrected for detector effects such as to get closer to parton level energies (as described above), before using it in the event selection. The missing energy is then corrected for the difference between the corrected and uncorrected jet transverse energies.

From this point on $\not\!\!E_T$ will refer to the corrected missing energy, unless explicitly stated otherwise.

3.2 Lepton identification

We select events with two leptons (electrons or muons) satisfying the criteria discussed below. To increase the signal acceptance from previous iteration of the analysis [9], we lowered the E_T requirements on the second leading lepton to 10 GeV, as will be justified in Section 3.5. For the highest p_T lepton, we follow the standard baseline cuts as recommended by the top and electroweak physics groups [15] and require that E_T to 20 GeV. For the lower E_T electron we loosen the p_T to 5 GeV for consistency with E/P cut(for electrons: E/P $>$ 2.0).

In addition to the standard ID cuts, we require both leptons in the event to be isolated (for central electrons and all muons we require both track and calorimeter isolation, and for Phoenix electrons calorimeter isolation only). This simplifies and significantly reduces our fake background calculation and improves $S/\sqrt{B}$. We veto events with 3 leptons.

The identification of *electrons* in the *central part* of the detector is based on the cuts listed in table 2. The electrons are required not to be part of a conversion.

EM E_T	$>$ 20 GeV
E_{HAD}/E_{EM}	$<\ 0.055 + 0.00045 \cdot$E
L_{shr}	< 0.2
Track P_T	$>$10 GeV/c (if EM $E_T \leq$100 GeV) $>$50 GeV/c (if EM $E_T >$100 GeV)
E/p	$<$ 2 (if EM $E_T \leq$100 GeV)
$q \cdot \Delta x$	[-3.0, 1.5] cm
$\lvert\Delta z\rvert$	$<$ 3 cm
χ^2	$<$ 10
track $\lvert z_0\rvert$	$<$ 60 cm
Track quality	3 axial and 2 stereo SL with at least 5 hits out of 12 in each SL
Fiducial	*fidele*=1 (Ces $\lvert X\rvert <$21 cm, 9$<$ Ces $\lvert Z\rvert <$230 cm Tower 9 excluded, most of tower next to chimney included)

Table 2: Baseline cuts for central high-p_T isolated electrons ($E_T > 20$ GeV) (CEM) [15].

The cuts for lower E_T central electrons ($E_T > 10$ GeV) are identical with the baseline high-pt cuts, expect for $p_T > 5$ GeV.

For the identification of *electrons* in the *plug region* of the detector the silicon tracks are reconstructed with the *Phoenix* algorithm [8]. If the plug electron passes all requirements described in table 3, it is classified as Phoenix, denoted *PHX*. The cuts for lower E_T plug electrons ($E_T > 10$ GeV) are identical with the ones for PHX.

EM E_T	$>$ 20 GeV
PhxMatch	true
E_{HAD}/E_{EM}	$<\ 0.05 + 0.026 \cdot \ln(\frac{\mathrm{E_{EM}}}{100})$ (if $E_{EM} >$100 GeV) $<\ 0.05$ (if $E_{EM} \leq$100 GeV)
PEM 3$\times$3 Fit tower	$\neq 0$
PEM 3$\times$3 Fit χ^2	$<$10
PES 5$\times$9 U and V	$>$0.65
PES based Fiducial	1.2$<\lvert\eta\rvert<$2.0
Silicon track	2D Phoenix track
Number of Silicon Hits	$\geq$3
Track $\lvert z_0^{PHX}\rvert$	$<$ 60 cm
ΔR(Track, PES)	$<$3

Table 3: Baseline cuts for plug isolated electrons (PHX) [15].

All central electrons are required to be isolated:

- $I_{cal} < 0.1$: the ratio of calorimeter energy, excluding the electron EM energy, in a cone of 0.4 around the electron, to the electron tower energy be less than 0.1. The isolation is leakage corrected.

Track P_T	>20 GeV/c
Track $\|z_0\|$	< 60 cm
E_{EM}	< 2+Max(0,0.0115(P-100)) GeV
E_{HAD}	< 6+Max(0,0.028(P-100)) GeV
Track $\|d_0\|$	0.2 cm (if no silicon hits attached by OI) 0.02 cm (if silicon hits attached by OI)
$\|\Delta x_{CMU}\|$	< 3.0 cm (CMUP or CMU)
$\|\Delta x_{CMP}\|$	< 5.0 cm (CMUP or CMP)
$\|\Delta x_{CMX}\|$	< 6.0 cm (CMX)
Track quality	3 axial and 2 stereo SL with at least 5 out of 12 in each SL
Track $\|z_0\|$	< 60.0 cm
Fiducial Cuts ([12])	
For CMUP: For CMU-only: For CMP-only: For CMX	x-fid(CMP) < 0 cm, z-fid(CMP) < -3 cm - x-fid(CMP) < 0 cm, z-fid(CMP) < -3 cm x-fid(CMX) < 0 cm, z-fid(CMX) < -3 cm

Table 4: Baseline cuts for minimum ionizing isolated tracks [12]. After passing these cuts the muon is classified as *CMUP*, *CMX* or *non-triggering* according to the definitions in the text.

- $I_{trk} < 0.1$: the ratio of the sum of the transverse momenta for all tracks in a cone of 0.4 around the lepton in the $\eta - \phi$ plane, excluding the lepton track, to the P_T of the lepton be less than 0.1.

A muon is a minimum ionizing high-P_T track passing the baseline *muon* cuts (Table 4). All these tracks must be *calorimeter isolated* and *track isolated* following the same definitions as for electron above.

In addition we require in the data the following:

- a cosmic ray veto,
- the standard curvature correction applied for the beam position, and
- for CMX the triggering CMX leg is required to have a COT exit radius > 140 cm.

This minimum ionizing high-P_T isolated track will be classified as:

- A *CMUP* muon, if there are stubs in both the CMU and CMP detectors, with $|\Delta X|_{\rm CMU}$ <3 cm and $|\Delta X|_{\rm CMP} < 5$ cm respectively.
- A *CMX* muon, if there is one stub in the CMX detector, with $|\Delta X|_{\rm CMX} < 6$ cm.
- A *non-triggering muon*: this can be 3 different sub-categories, the information for which we will maintain for detailed studies of candidates, and internal consumption, etc., but which for presentation purposes we might lump into this one category for simplicity. A

non-triggering muon can only be the second leg in a dilepton event, and can appear in the following ways:

1. *CMU-only* (*CMP-only*) with a stub in the CMU (CMP) detector and non fiducial in the CMP (CMU) detector according to the muon fiduciality checking tool.
2. If there are no muon detector stubs, the minimum ionizing high P_t isolated track will be classified as a *CMIO*.

The cuts for lower P_T muons ($p_T > 10$ GeV) are identical to [6] and identical to those for high p_T except

- $E_{em} + E_{had} > 0.1$ GeV for CMIO;
- $E_{em} < 2$ GeV;
- $E_{had} < p_T/8 + 3.5$ GeV;
- $d_0 < 0.2$ cm;
- $\rho_{\mathrm{COT\ exit}} > 140$ cm for CMIO and trigger CMX;
- trkFiducial==4 for CMIO;
- AxSeg >= 3 and StSeg >= 3 for all non-trigger muons.

3.3 Dilepton categories

We build a dilepton event with two baseline isolated leptons according to the categorizations in table 5. Compared with 4.11.1 categories, we took out PHX-PHX di-leptons, as they represent about 2% of acceptance, while bringing in large fake background.

3.4 Event Selection

After requiring events have 2 isolated leptons, of opposite charge, kinematic cuts are applied to reduce the background contributions while maintaining the bulk of the signal acceptance.

A cut on the lower bound of the $M_{\ell\ell}$ is applied to eliminate backgrounds from J/Ψ's, Upsilons and $b\bar{b}$. This does not significantly impact our Higgs signal.

The jet veto is applied to tight jets: *reclustered* jets with the JetClu 0.4 algorithm using the primary vertex and excluding towers from TCE and PHX isolated electrons, with corrected $E_T > 15$ GeV and $|\eta| < 2.5$. We correct jets using level 5 corrections. The high jet E_T threshold used increases our signal acceptance without significantly impacting our backgrounds. Only the events with 0, 1 and 2 jets, with further energy requirements, are selected. About 4% of the signal events ($M_H = 180$ GeV/c^2) have more than one jet, while only 0.1% have at least 3 jets.

ee		$\mu\mu$		$e\mu$	
1st leg	2nd leg	1st leg	2nd leg	1st leg	2nd leg
TCE	**TCE**	**CMUP**	**CMUP**	**TCE**	**CMUP**
	PHX		**CMX**		**CMX**
			CMU		CMU
			CMP		CMP
			CMIO		CMIO
		CMX	**CMX**	**CMUP**	PHX
			CMU	**CMX**	PHX
			CMP		
			CMIO		
				PHX	CMU
					CMP
					CMIO

Table 5: Dilepton categories included in the current analysis. Shown in bold are the triggerable lepton in the data samples studied. The one exception to this is the PHX categories. Both lepton legs are required to be isolated.

The $\not\!\!E_T$ is corrected for the primary vertex position and for the isolated muons identified in the dilepton category. The $\not\!\!E_T$ is also corrected for the jet corrections affecting tight jets (greater than 15 GeV).

The leptons are required to have opposite sign and trileptons are rejected.

An upper bound cut on $M_{\ell\ell}$ is made, which is a function of the Higgs mass.

These selection cuts depend on the mass of the Higgs and are summarized in table 10.

These cuts are very efficient for the Higgs signal (see table 40), while eliminating a significant amount of background. The exact values of the upper $M_{\ell\ell}$ bounds used were determined from maximizing $S/\sqrt{S+B}$ and then looking at the expected limits. As small variations around the maximum $S/\sqrt{S+B}$ have little impact on the expected limits, we tried to make them as simple and easy to remember as possible. So for $M_{\ell\ell}$ upper cut chosen the functional form of $M_H/2$-5.

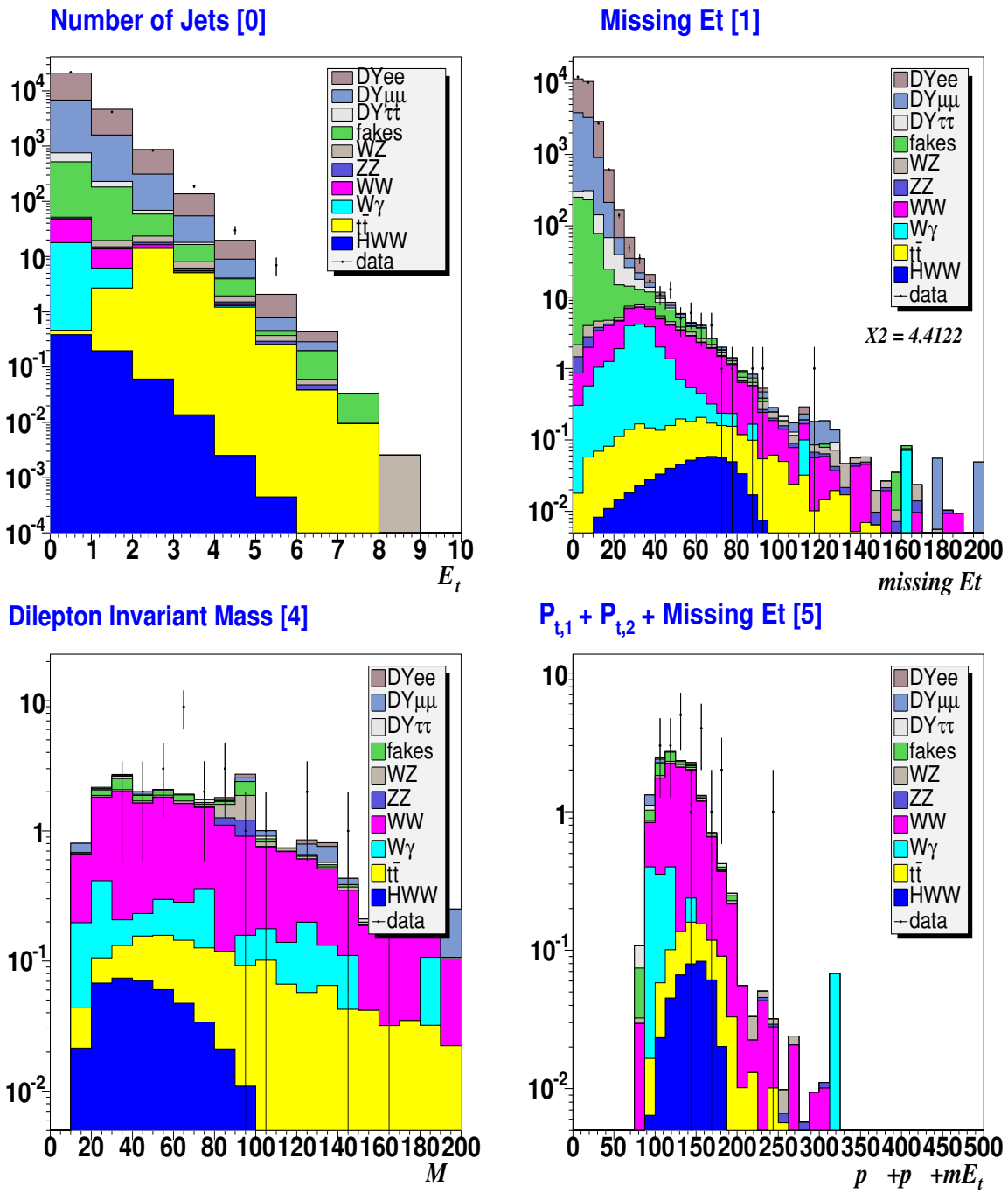

Figure 4: Four of the variables used in the event selection (for $M_H = 180$ GeV) are shown before cutting on that variable: (upper-left) number of jets; (upper-right) missing energy; (lower-left) dilepton invariant mass and (lower-right) $P_T(lep1) + P_T(lep2)+\not\!\!E_T$.

Events passing these cuts are then used in the fits of the $\Delta\phi(\ell,\ell)$ distributions, discussed

later.

Event selection steps are summarized in table 10.

3.5 Selection Optimization

The previous version of this analysis (which will be referred in the paper as *generation 4*) raised from the WW cross-section measurement, and therefore was not fully optimized for a Higgs search. We performed various optimizations, of which the most important ones are detailed below.

- *Lowering one of the lepton transverse momentum*

  The Higgs decays to two W boson, one on-shell, while the second is off-shell. The leptons coming from the off-shell W decay are softer than the ones from on-shell W decay, so an asymmetric cut is expected to help in this situation than the old (20, 20) cut. Figures 5, 6 show the highest vs the lowest lepton transverse momentum for two Higgs masses: 130 and 180 GeV. Figure 7 shows how the cut efficiency changes for various ($p_T(max)$, $p_T(min)$) cuts, for a M_H =130 GeV. Lowering the $p_T(min)$ from 20 to 10 GeV increases the fraction of events passing the kinematical cuts by 100%. Also the plots show that lowering the highest lepton p_T threshold is *not necessary*[4], as the acceptance gain is minimal, while the backgrounds are expected to increase. Table 6 summarizes the fraction of events passing various kinematical cuts, for three choices of
  ($p_T(max)$, $p_T(min)$): (20, 20), (20, 10) and (10, 10).
  (20, 10) is our choice as allows us to use the same triggers as in 4.11.1 and also increases the acceptance by 26-100% as compared with Gen 4.

[4]In doing the optimization we always have in mind the masses of the Higgs were we have the largest sensitivity: 160 and 170 GeV. Sure, lowering the highest lepton p_T would help for lower Higgs masses: 130 GeV or below.

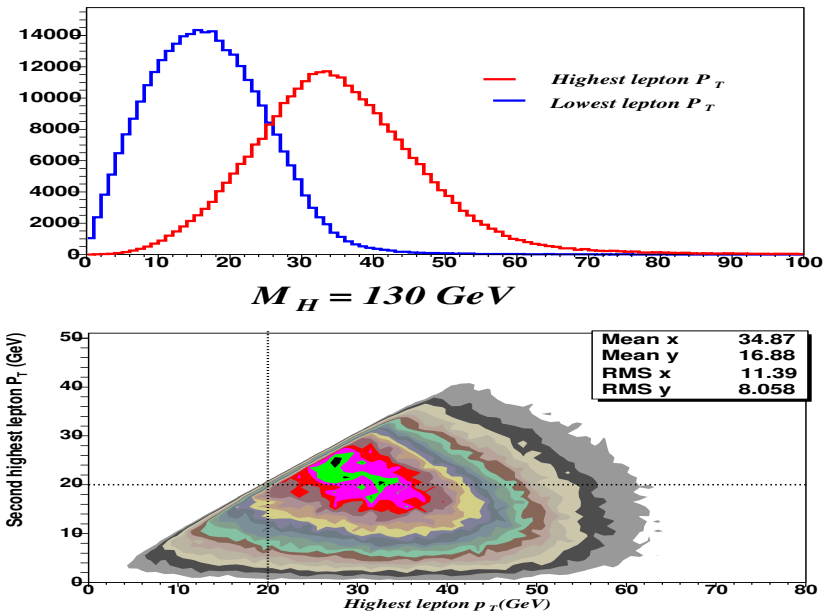

Figure 5: Highest lepton p_T vs the second highest lepton p_T for a 130 GeV Higgs.

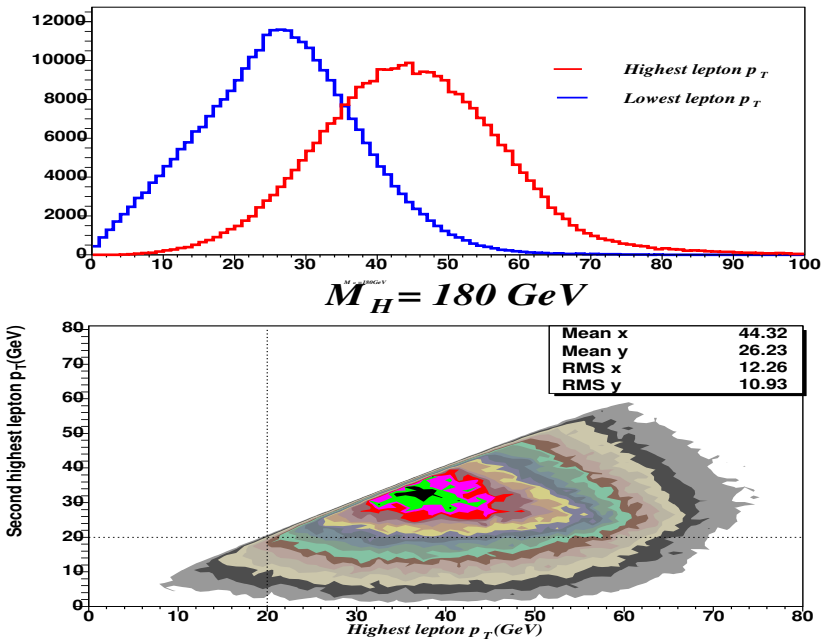

Figure 6: Highest lepton p_T vs the second highest lepton p_T for a 180 GeV Higgs.

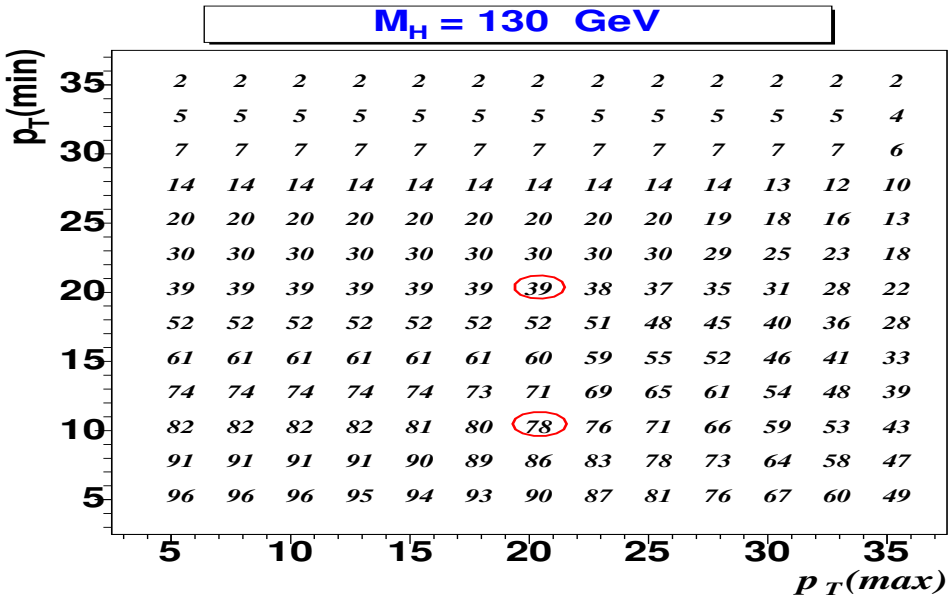

Figure 7: The fraction of events passing kinematical cuts on $p_T(max)$, $p_T(min)$, for a 130 GeV Higgs. The circled values show that the efficiency increases from 39 to 78 %, when lowering the transverse momentum requirement on the second lepton from 20 to 10 GeV.

$p_T(max)$, $p_T(min)$	ϵ(130 GeV)	ϵ(140 GeV)	ϵ(150 GeV)	ϵ(160 GeV)	ϵ(170 GeV)	ϵ(180 GeV)
(20, 20)	0.39	0.50	0.60	0.71	0.74	0.74
(20, 10)	0.78	0.84	0.88	0.83	0.92	0.93
(10, 10)	0.82	0.87	0.90	0.91	0.94	0.94

Table 6: Fraction of events passing various kinematics cuts, as a function of the Higgs mass.

- *Optimizing the missing energy*

  In the Higgs $\rightarrow$ W^+W^- $\rightarrow$ $\ell^+\nu\ell^-\bar{\nu}$, decay channel ($l = e$ or μ), the neutrinos are almost parallel (Higgs has spin 0), therefore signal missing energy tends to be higher then for WW, as also shown in figure 8. Increasing the missing energy threshold allows us to significantly reduce the total background, for a small reduction in the signal, improving $S/\sqrt{S+B}$ and the expected limits.

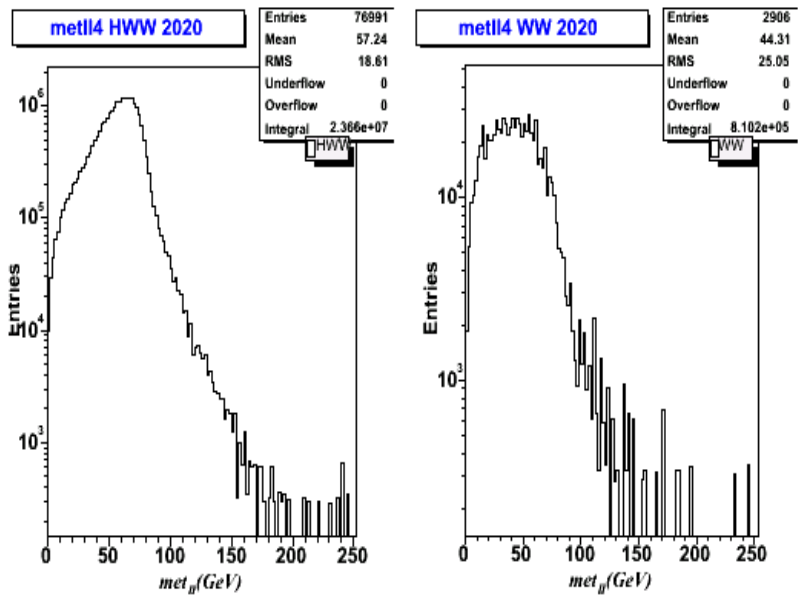

Figure 8: Missing energy for the signal (M_H=160 GeV) and WW background.

- *Changing the jet veto* The signal events tend to have very little jet activity. Only 4% of events have more than 1 jet (see section 3.1 for *jet* definition), while only 0.1% have 3 or more jets. Also the jets come from ISR, therefore are softer than the hard jets from $t\bar{t}$. Based on the above facts, we proposed to select the events with

  – 0 jets *or*

  – 1 jet $E_T < 55$ GeV *or*

  – 2 jets each $E_T < 40$ GeV.

  The jet E_T spectrum for 1 jet and 2 jet events is shown in figure 9. Signal mass is 160 GeV. The new jet cut efficiency for the signal is about 90%.

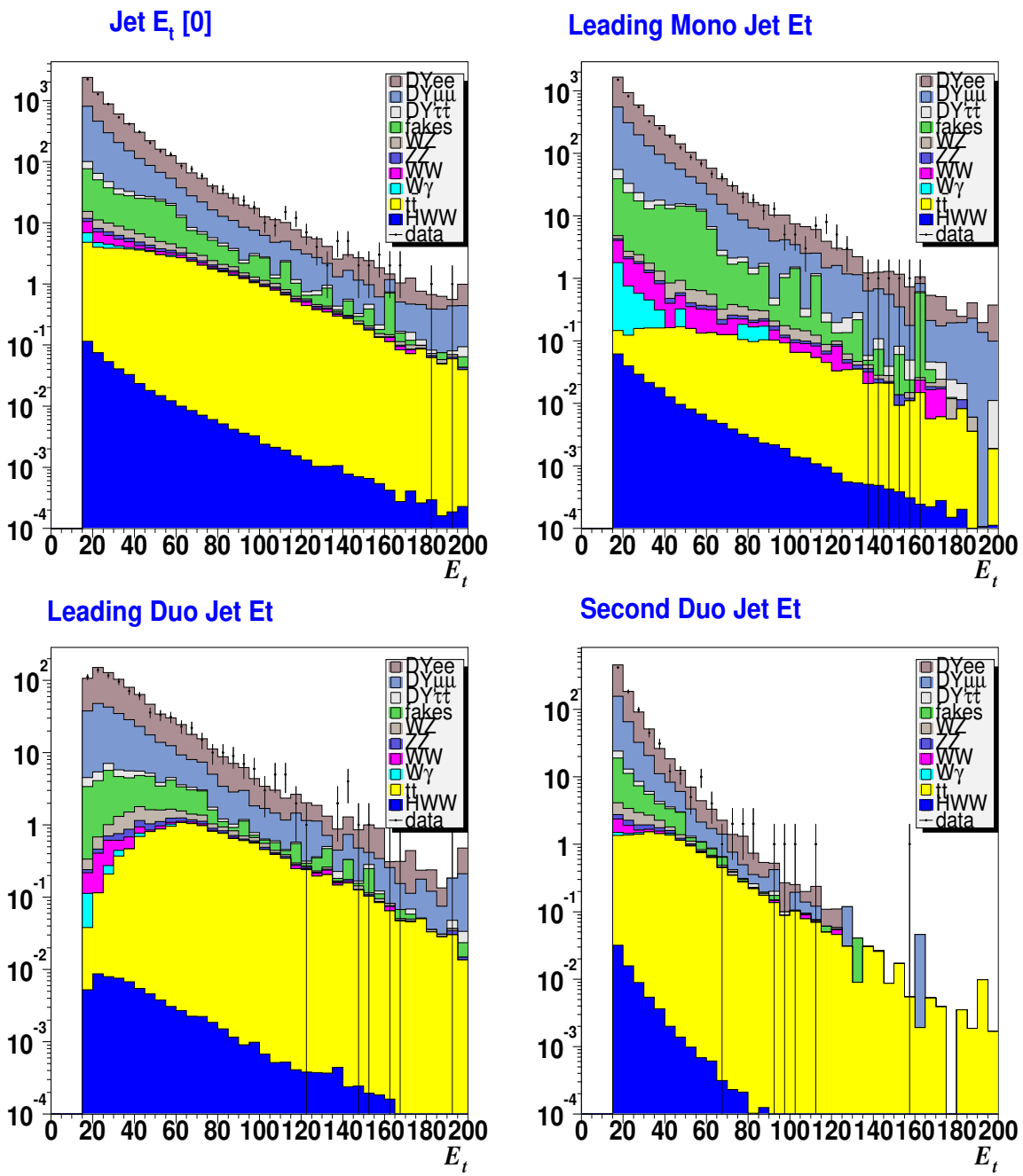

Figure 9: Jet E_T spectrum is shown before the jet veto, for: (upper-left) any number of jets event; (upper-right) only for 1-jet events; (lower-left) the leading jet in 2-jet events; (lower-right) the second jet in 2-jet events. Also the data point are shown, for 360/pb. The plots are made after requiring 2 good leptons, with $m_{\ell\ell} > 16$ GeV.

- *2D Optimization: Missing energy versus Jet E_T threshold*

Higgs mass (GeV)	110	120	130	140	150	160	170	180	190	200
DY (without $\Delta\phi$)	16.12	16.69	10.95	7.24	5.47	3.32	2.26	1.70	1.29	0.97
DY bg (with $\Delta\phi$)	2.29	1.88	1.57	1.31	1.44	0.85	0.91	0.86	0.93	0.97

Table 8: The DY background as a function of Higgs mass with or without the cut ($\not\!\!E_T > 50$ GeV $||\Delta\phi(\not\!\!E_T$, lep/jet$) > 0.35$)).

The final $\not\!\!E_T$ and jet thresholds were chosen based on the expected limits. For this we perform 1000 pseudo-experiments for each 2D point, histogram the 95% CL and use the median of the distribution as the most probable 95% CL.

M_H	$\not\!\!E_T$ def	$E_T j$+5	$E_T j$+10	$E_T j$+15	$E_T j$+20	$\not\!\!E_T$-10	$\not\!\!E_T$-5	$\not\!\!E_T$+5	$\not\!\!E_T$+10	$\not\!\!E_T$+15	$\not\!\!E_T$+20	$\not\!\!E_T$+25	$\not\!\!E_T$+30
110	10.85	10.78	10.91	11.49	11.36	12.13	11.30	10.72	11.43	13.77	23.33	39.22	46.08
120	8.4	8.2	8.305	8.341	8.53	8.586	8.716	8.02	8.283	9.746	13.55	26.68	42.58
130	6.84	6.879	6.738	6.77	7.016	7.253	6.962	6.535	7.111	7.86	10.79	16.43	31.74
140	5.7	5.669	5.742	5.856	5.596	6.357	6.107	5.77	6.111	6.636	8.219	12.38	25.35
150	5.05	4.926	5.089	4.966	5.083	5.338	5.25	4.910	5.125	5.487	6.328	8.953	14.51
160	3.95	4	3.904	3.95	3.92	4.280	4.135	3.896	3.946	4.157	4.510	5.529	7.840
170	3.72	3.678	3.677	3.694	3.618	4.196	3.847	3.672	3.670	3.826	4.142	4.95	6.529
180	3.988	3.896	3.97	3.9	3.937	4.261	4	3.9	3.844	3.91	4.287	5.3	6.952

Table 7: Results of varying the $\not\!\!E_T$ and 1-jet E_T threshold. Defaults are $\not\!\!E_T < M_H/4$ and ${E_T}^{\text{1-jet}} < 50$ GeV. We show the default expected limits, expected limits when changing the cut for the 1-jet Et from 50 to $50 + 5, +10, +15, +20$ GeV, and also expected limits for $\not\!\!E_T < M_H/4 - 10, -5, +5, +10, +15, +20, +25, +30$ GeV.

- *DY background suppression for low masses*

  We retained the cut ($\not\!\!E_T > 50$ GeV $||\Delta\phi(\not\!\!E_T$, lep/jet$) > 0.35$) from previous top, WW and HWW dilepton analyses to suppress the large DY background spared by the lower $\not\!\!E_T$ cut for lower Higgs masses. See Table 8.

4 Monte Carlo Datasets

Monte Carlo datasets were simulated using mcProduction package, runMC executable, in release 5.3.2. The samples used for signal and backgrounds, the MC generator, their dataset ids and the cross-sections are shown in table 9.

Process	Generator	Dataset ID	$\sigma(pb)$	# Events
Signal				
H→WW (M_H = 110 GeV)	PYTHIA	wexobw	0.004	1143420
H→WW (M_H = 120 GeV)	PYTHIA	wexocw	0.009	1137034
H→WW (M_H = 130 GeV)	PYTHIA	wexo5w	0.017	1199597
H→WW (M_H = 140 GeV)	PYTHIA	wexo6w	0.022	1136447
H→WW (M_H = 150 GeV)	PYTHIA	wexo7w	0.025	1162684
H→WW (M_H = 160 GeV)	PYTHIA	wexo8w	0.028	1118660
H→WW (M_H = 170 GeV)	PYTHIA	wexo9w	0.025	1106451
H→WW (M_H = 180 GeV)	PYTHIA	wexoaw	0.020	1153345
H→WW (M_H = 190 GeV)	PYTHIA	wexodw	0.014	1093662
H→WW (M_H = 200 GeV)	PYTHIA	wexoew	0.011	1092527
Backgrounds				
Z/$\gamma \rightarrow$ ee	PYTHIA	zewk6d	355.2 × 1.4	3108482.
Z/$\gamma \rightarrow \mu\mu$	PYTHIA	zewk6m	355.2 × 1.4	3216951
Z/$\gamma \rightarrow \tau\tau$	PYTHIA	zewk8t	355.2 × 1.4	3338836
Z/$\gamma \rightarrow \ell\ell$	PYTHIA	sexo8t	17354.0 × 1.4	3164279
WW	PYTHIA	wtop1w	12.4	419728
WZ	PYTHIA	wtop1z	3.65	407438
ZZ	PYTHIA	ztopcz	1.39	397086
W $\gamma \rightarrow e^+\nu\ \gamma$	PYTHIA	ktop2e	22.35	68273
W $\gamma \rightarrow e^+\nu\ \gamma$	PYTHIA	ktop3e	22.35	102473
W $\gamma \rightarrow \mu^+\nu\gamma$	PYTHIA	ktop2m	22.35	93073
W $\gamma \rightarrow \mu^+\nu\ \gamma$	PYTHIA	ktop3m	22.35	103608
t$\bar{t}$	PYTHIA	ttopel	6.7	1142339

Table 9: Monte Carlo datasets used for HWW analysis.

5 Signal Acceptances

The signal acceptance was evaluated using PYTHIA MC samples for each Higgs mass (110-200 GeV). The samples used are wexo5w-wexoew, and consist of about 1.2M events each, with both W bosons forced to decay leptonically: $W \to l\nu$, where $l = e, \mu, \tau$. The HWW acceptances with respect to the numbers of events decaying leptonically, are shown in Fig 10. Also on the same plot the values from 4.11.1 analysis are shown. After the optimization we increased the acceptance up to a factor of 3, for lower Higgs masses.

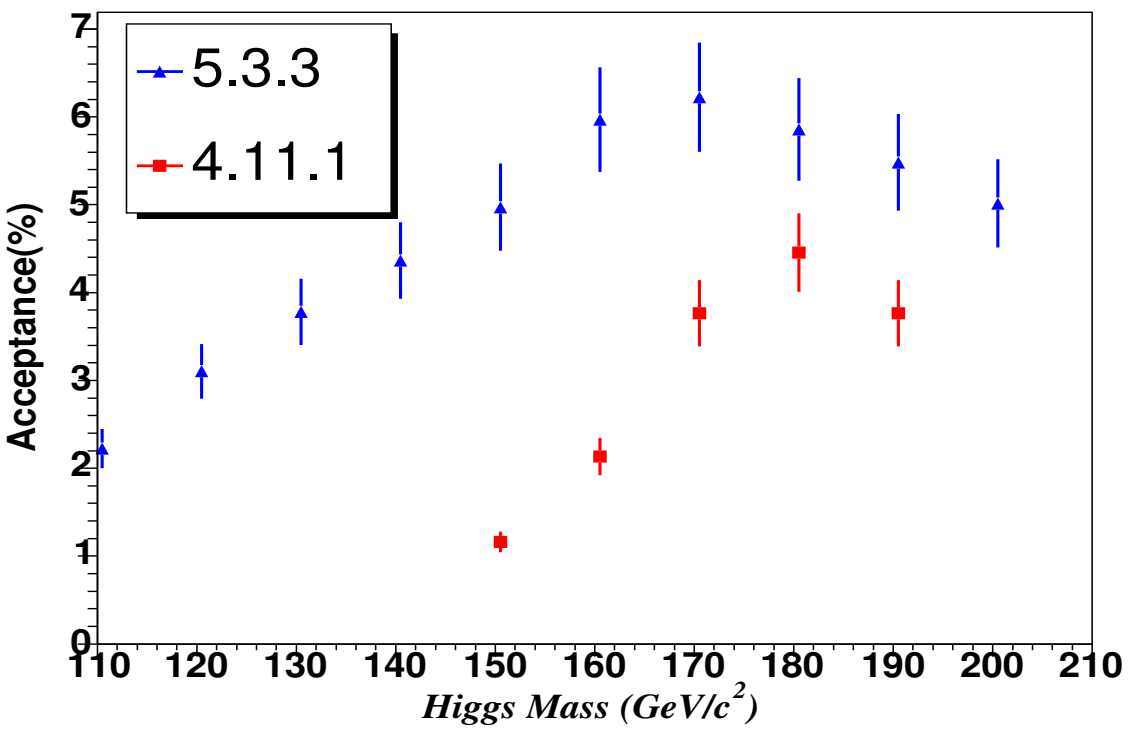

Figure 10: Signal acceptance for various Higgs masses. For comparison the generation 4 values are also shown.

Table 40 shows the detailed signal efficiencies after every single cut, for a Higgs of 160 GeV.

Index	Event Selection
1	two leptons with ${p_T}^{\ell_{\text{trigger, non-trigger}}} > 20$, 10 GeV
2	$M_{\ell\ell} > 16$ GeV
3	nJets($E_T > 15$ GeV) $= 0$ || nJets($E_T < 55$) $= 1$ || nJets($E_T < 40$) $= 2$
4	$\not\!\!E_T > M_H/4$
5	$M_H > 150$ GeV || ($\not\!\!E_T > 50$ GeV || $\Delta\phi(\not\!\!E_T$, lep/jet) > 0.35)
6	opposite lepton charge signs
7	$M_{ll} < M_H/2 - 5$ GeV
8	${E_T}^{\ell_1} + {E_T}^{\ell_2} + \not\!\!E_T < M_H$

Table 10: Event Selection for the HWW analysis.

6 Scale Factors

We correct for trigger inefficiencies (see Table 11) using the official blessed values.We correct for the difference in lepton identification efficiencies between data and MC by applying the scale factors shown in Table 12. We also correct PHX for charge mis-identification as shown in Table 13 after requiring the event selection cut [6] as in Table 10.

Lepton Type	Trigger Efficiency
TCE	0.962 ± 0.066 [10]
PHX	0.955 ± 0.019 [11]
CMUP	0.908 ± 0.005 [12]
CMX	0.965 ± 0.004 [12]

Table 11: Summary of trigger efficiencies. The CEM_18 trigger efficiency is run-dependent, number given above being an average over η. We use the MET_PEM trigger efficiency as estimated in 4.11.1. The contribution from dilepton categories triggered by PHX is below 15%.

$\lvert\eta_{\text{PHX PES}}\rvert$ Range	Data/MC Scale Factor
$1.2 < \lvert\eta\rvert < 1.4$	$(1-0.061)/(1-0.061)$
$1.4 < \lvert\eta\rvert < 1.6$	$(1-0.099)/(1-0.097)$
$1.6 < \lvert\eta\rvert < 1.8$	$(1-0.150)/(1-0.143)$
$1.8 < \lvert\eta\rvert < 2.0$	$(1-0.168)/(1-0.138)$

Table 13: PHX charge mis-identification scale factors [7].

Lepton Type	ID×Reconstruction Scale Factor	
	$p_T < 20$ GeV	$p_T > 20$ GeV
TCE	1.03 ± 0.02 [5]	0.996 ± 0.005 [7]
PHX	-	0.948 ± 0.016 [7]
CMUP	0.85 ± 0.05 [6]	0.892 ± 0.009 [12]
CMX	0.90 ± 0.05 [6]	0.999 ± 0.006 [12]
CMU	-	0.889 ± 0.010 [12]
CMP	-	0.907 ± 0.009 [12]
CMIO	1.00 ± 1.00 [6]	0.995 ± 0.003 [12]

Table 12: Summary of lepton data/MC scale factors.

7 Measuring Z$\rightarrow \ell\ell$ cross-sections

To validate the scale factors discussed in section 6, we measured four Z cross-sections, two in the electron and two in the muon channels. The results are shown in table 14.

For the muon cross-sections, the first muon in the trigger one, while the second can be any muon, used in current analysis: CMUP/CMX/CMU/CMP/CMIO, all defined in section 3. The results agree very well with an independent measurement, performed using the same amount of data, $\sigma(\text{Z}\rightarrow_{\mu\mu}) = 261.2 \pm 2.7 \pm^{5.8}_{6.9} \pm 15.1\text{pb}$([4]).

Also the measurements agree with the NNLO calculation: $\sigma(\text{Z}\rightarrow_{\ell\ell}) = 250.5 \pm 3.8$ pb.

Dilepton Type	σ_Z (pb)
TCE-TCE	$259.3 \pm 3.3(stat) \pm 5.4(syst) \pm 15.4(lumi)$
TCE-PHX	$262.6 \pm 3.2(stat) \pm 23.0(syst) \pm 15.5(lumi)$
CMUP-CM(UP/X/U/P/IO)	$260.9 \pm 3.5(stat) \pm 5.8(syst) \pm 15.4(lumi)$
CMX-CM(UP/X/U/P/IO	$259.7 \pm 4.6(stat) \pm 5.4(syst) \pm 15.3(lumi)$

Table 14: Summary of Z cross-section measurements.

8 $H \to WW$ Acceptance Systematic Uncertainties

Potential sources of systematic uncertainty on the $H \to WW \to l^+l^-\nu\bar{\nu}$ acceptance are summarized in table 15 and described below.

	Systematic Error (%)
ISR	3
α_s	3.3
PDF Acceptance	3
Jet Energy Scale	1
Lepton ID	2
Track Isolation	2
Trigger Efficiency	1
Combined	6

Table 15: Sources of systematic uncertainty on the $H \to WW \to l^+l^-\nu\bar{\nu}$ acceptance.

8.1 PDF Uncertainty

We evaluated the pdf uncertainties using the JPM recommended Hessian method [3]. With the new PDF set CTEQ6M, the CTEQ group made available 40 complementary PDF sets CTEQ6M.01...CTEQ6M.40, each of which represents an up/down variation along one of the twenty eigenvectors (corresponding to 20 free parameters used in the fit). They form an orthonormal basis set spanning the full PDF parameter space [1]. Each up and down variation pair represents the range of PDF behavior that is consistent with the current global data used in the fit. Each event in the Pythia HWW sample is reweighted according to the ratio of the CTEQ6M PDF values and the CTEQ6M.xx PDF values. We add the variations on acceptance in quadrature, which results in (+2.76%/-3.44%). Then symmetrize and take 3% as systematic uncertainty.

8.2 ISR-more/less

We generated two samples, for 160 GeV Higgs mass, with more/less initial state radiation settings, kindly provided by Un-ki Yang. We estimate the change in the acceptance and find to be 3%, which is assigned as a systematic uncertainty.

8.3 α_s

We compare the acceptance for two sets of PDFs: MRST72 ($\alpha_s = 0.1175$) and MRST75 ($\alpha_s = 0.1125$), with different α_s. There is a 3.3 % difference, which is assigned as a uncertainty.

8.4 Jet Energy Scale

To estimate the systematic uncertainty associated with the jet energy scale, we follow the prescription described in [16]: Vary each jet correction factor by +1 σ, respectively -1 σ, and sum the variations on acceptance in quadrature to get up/down errors. This prescription is used for all the Higgs masses signal samples. The uncertainties are within 1%, and this is due to the fact that we raised the jet threshold compared with generation 4.11.1 analysis to 50 GeV and all jets in the signal events come from ISR.

8.5 Lepton ID

Using the identification and reconstruction efficiencies scale factors (data/MC) shown in table 12, we estimate an uncertainty of 2%.

8.6 Track Isolation

We determine the track isolation efficiency ϵ_{triso} using Z→ ee and Z→ mm data samples.

$$\epsilon_{triso} = \frac{N_{\ell\text{id+caliso+trkiso}}}{N_{\ell\text{id+caliso}}} \tag{2}$$

where the denominator represent the number of leptons passing all the id cuts, including calorimeter isolation; the numerator consist of all the denominator leptons passing also the track isolation. The scale factors shown in table 16 are well within 1% of unity. See also figures 11 and 12, where "prediction" refers to Monte Carlo-based efficiency, while "observation" is the data track isolation efficiency. We take the uncertainty on single lepton 1%, and total uncertainty 2%.

Lep.Type	Data/MC SF
TCE	1.00
CMUP	1.00
CMX	0.99
CMP	1.00
CMU	0.99
CMIO	0.99

Table 16: Track isolation scale factors (data/MC) for all the lepton types used in the HWW analysis. The statistical error are all below 1%.

8.7 Trigger Efficiency

Central trigger efficiencies are all below 1%, the largest one is on MET_PEM trigger [13]. This affects only categories triggered by the PHX electrons, representing about 15% of the total. The overall uncertainty becomes 1%.

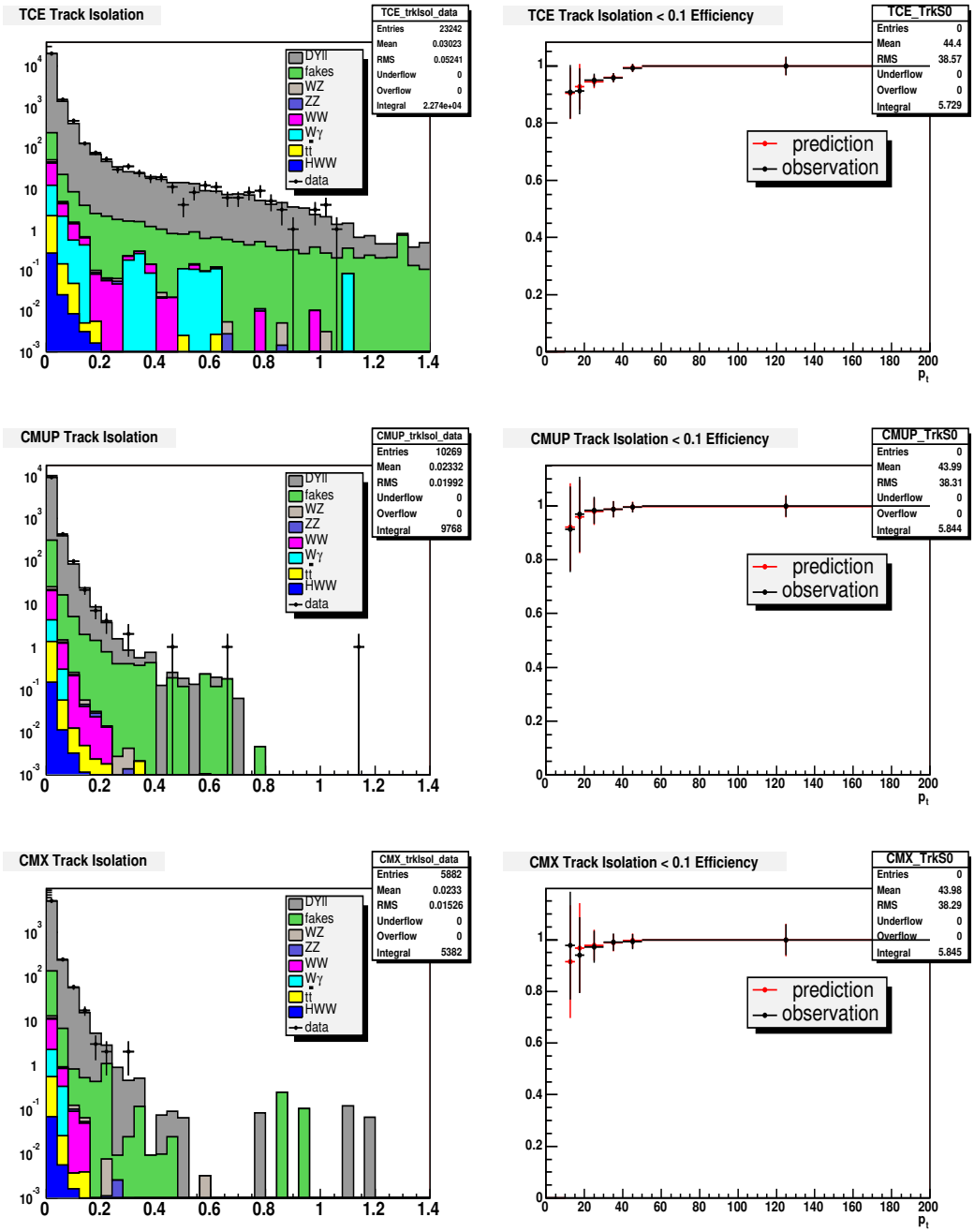

Figure 11: Track isolation distributions per trkIsol-required lepton type and the cut efficiencies from data or MC as a function of lepton p_T.

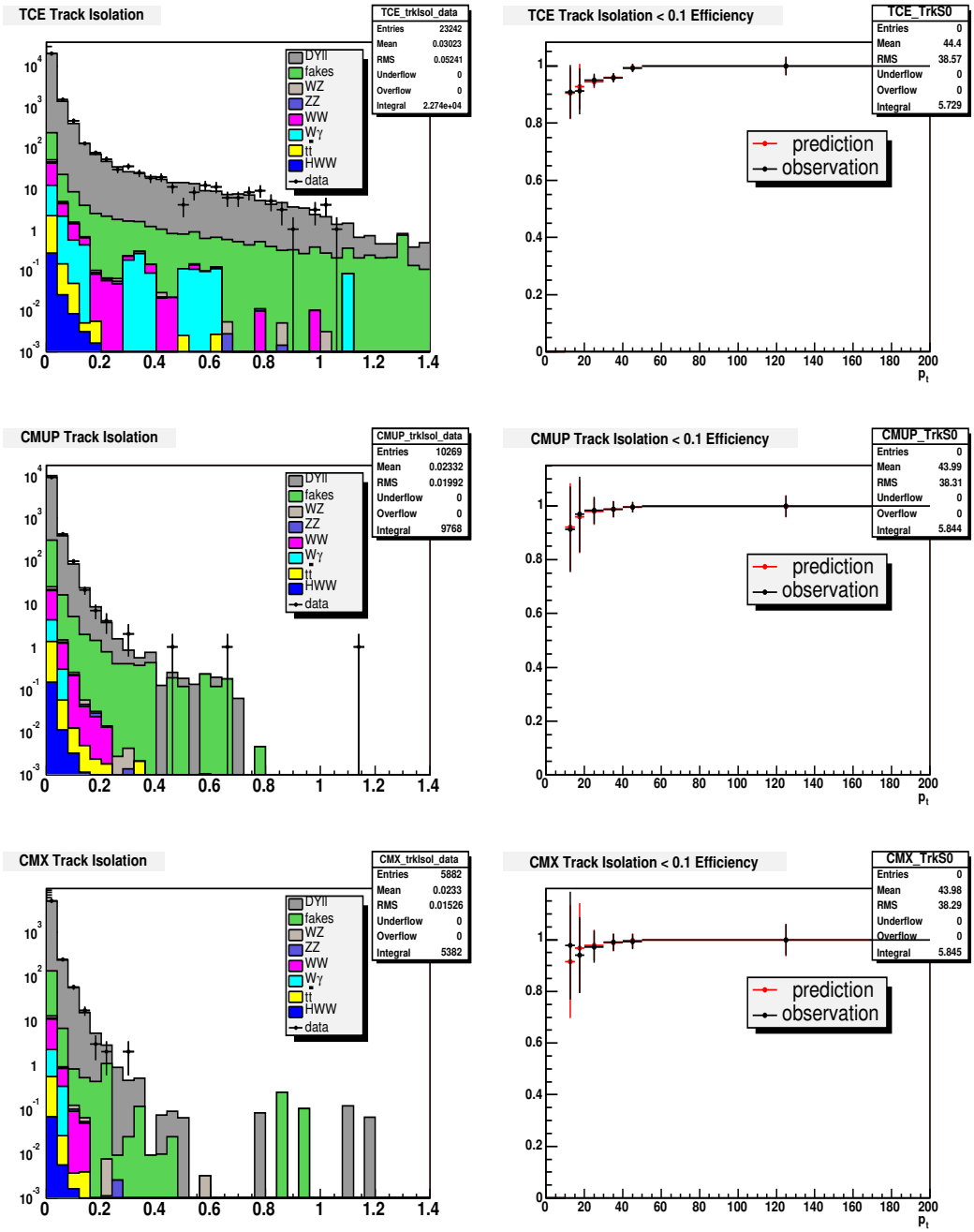

Figure 12: Track isolation distributions per trkIsol-required lepton type and the cut efficiencies from data or MC as a function of lepton p_T.

8.8 Combined Acceptance Systematic

The sources of systematic uncertainties from table 15, added in quadrature, result in an uncertainty of 6% of the HWW signal.

9 Background Estimates

The main background (50 to 60% of the total) is from SM WW production. Smaller contributions arise from $t\bar{t}$, WZ, ZZ, $W\gamma$, Drell-Yan e^+e^-, $\mu^+\mu^-$ and $\tau^+\tau^-$, and $W + jets$ events, where a jet fakes a lepton. All the backgrounds are estimated using Monte Carlo samples, except for the fake contribution, determined entirely from data.

9.1 WW background

To estimate the WW background, we used a PYTHIA MC sample (dataset ID: wtop1w) of 0.4M inclusive WW events. A cross-section $\sigma(p\bar{p} \to WW) = 12.4 \pm 0.8$ pb is assumed to estimate the sample luminosity. The efficiencies of the WW background after each of the cuts for HWW search are shown in Table 41, for $M_H = 160$ GeV criteria. The cuts $M_{\ell\ell} < M_H/2$ and requiring large missing energy are relatively effective on reducing the inclusive WW dilepton background.

9.2 $t\bar{t}$ background

$t\bar{t}$ background is estimated using a PYTHIA MC sample (dataset ID: ttopel) consisting of 1.2M $t\bar{t}$ events. The sample assumed the mass of top quark $m_{\rm top} = 178$ GeV and the (theoretical best) cross-section $\sigma(p\bar{p} \to t\bar{t}) = 6.7$ pb. Acceptance of the $t\bar{t}$ background through each of the cuts for HWW search is in Table 43, for $M_H = 160$ GeV criteria. We see that the 0-jet cut is very effective in reducing the $t\bar{t}$ background. We will switch to a 175 GeV sample soon.(closer to top mass world average.)

9.3 Drell-Yan background

To estimate the Drell-Yan ll background, we used a PYTHIA MC sample (dataset id: sexo8t), of 3M $Z/\gamma^* \to ll$ events. ee, $\mu\mu$, and $\tau\tau$ were generated together. The sample was HEPG-filtered, with the efficiency around 2.9%, requiring two leptons, e or μ; the electrons with p_T >3.6 GeV and $|\eta|$ <1.4, the muons with pt>4.8 GeV and $|\eta|$ <1.4. The process was leading order only, so a factor $k_{\rm NNLO/LO} \simeq 1.38$ was applied. The process cross-section was determined to be 17354 pb. Acceptance of the DY ll background through each of the cuts for HWW search is in Table 44, for $M_H = 160$ GeV criteria . Also we cross-checked the estimate using electroweak samples with extra min bias, *zewk6d, zewd6m* and *zewk8t*. The estimates are consistent. We see that the cut on the upper $M_{\ell\ell}$ mass bound is the most effective on reducing the Drell-Yan background.

9.4 Fake background

The main source of fakes is W + multi-jet processes, with one jet/track misidentified as a lepton. To estimate the background due to fakes we use the following procedure:

- Step 1: calculate the jet-like-objects faking a lepton probability, i.e.fake ratio, for each lepton type using Jet 20, Jet 50, Jet 70 and Jet 100 samples. Use the average fake ratio over all four jet samples in step 2.

- Step 2: search the high-p_t electron/muon inclusive data samples for jet-like objects (defined in step 1) that might fake a lepton and passing the event selection criteria (described in section 3) – let's call such events "fakeable events".

- Step 3: apply the fake ratios to the fakeable objects to estimate how many events in data might be fakes.

The fake background, with few associated cross-checks, has been evaluated using data, and written up in a separate note [11]. In this document we just give the results for brevity.

9.5 $W\gamma$ background

The samples used to estimate this background were generated using Baur and Berger's WGAMMA program [21], using the following cuts: $|\eta^{lepton}| < 10$, $E_T^{\gamma} > 5.0$ GeV, $|\eta^{gamma}| < 10$ and $\Delta R(l,\gamma) > 0.2$ [20]. The details about four samples used are shown in table 46. The systematic uncertainties on $W\gamma$ are shown in table 18. The first three uncertainties are taken from the W+γ PRL. [22].

Sample	Events	Cross-section (pb)	DFC ID
W$\gamma \to e^+\nu$	70k	22.35	ktop2e
W$\gamma \to e^-\nu$	100k	22.35	ktop3e
W$\gamma \to \mu^+\nu$	90k	22.35	ktop2m
W$\gamma \to \mu^-\nu$	100k	22.35	ktop3m

Table 17: $W\gamma$ MC samples used to estimate the background to HWW.

9.6 WZ and ZZ background

To estimate the WZ background we used a PYTHIA MC sample (dataset ID: wtop1z) of 0.4M inclusive WZ events. The cross-section is $\sigma(p\bar{p} \to WZ) = 3.96$ pb. Acceptance of the WZ background through each of the cuts for HWW search is in Table 42, for $M_H = 160$ GeV criteria. A ZZ PYTHIA sample containing 0.4M events (dataset id: ztopcz) was used to estimate the background from ZZ. The ZZ cross-section is $\sigma(p\bar{p} \to WZ) = 1.39$ pb (NLO).

9.7 Background systematic uncertainties

We summarize the systematic uncertainties on the backgrounds in table 18.

For WW/WZ we determined the jet energy scale uncertainty to be 1%.

The fake uncertainty and details of the fake calculation are described in [11].

We are in the process of checking the systematic uncertainty due to MC generators for $t\bar{t}$. The current value (6%) was determined in the context of top dilepton analysis [23]. Similarly for ISR/FSR uncertainties. Also we are redoing the jet energy scale systematic uncertainty.

For Wγ we use an uncertainty due to the events unweighting and K-factor error, described in [20], page 14. This is appropriate as we used the same 4.11.1 samples used in [20], stripped for HEPG and reprocessed with 5.3.2 Simulation.

For Drell-Yan we were worried about the missing energy or jet multiplicity modeling of the MC. We selected events with 2 leptons passing the analysis cuts. We checked the ratio of missing energy cut efficiency for data and MC for various thresholds. The numbers agree well within the errors, however the statistics is very limited beyond 30 GeV. We use the statistical errors as an estimate of the potential difference in the met cut efficiency between data and MC; we quote a 20 % uncertainty on DY due to missing energy cut.

- $\frac{\epsilon_{data}}{\epsilon_{MC}} = 0.92 \pm 0.06$, for $\not\!\!E_T > 20$ GeV

- $\frac{\epsilon_{data}}{\epsilon_{MC}} = 1.02 \pm 0.15$, for $\not\!\!E_T > 30$ GeV

- $\frac{\epsilon_{data}}{\epsilon_{MC}} = 1.13 \pm 0.13$, for $\not\!\!E_T > 40$ GeV

Also we compared the cut efficiency for data and MC for jet veto cut and they agree well. We restrict to the events with 0, 1 or two jets.

Background	Source	Uncertainty (%)
WW	Jet Veto ("jet modeling")	6
	PDF/Q^2 Effect on $\sigma(WW)$	5
	Generator/Parton Shower Model	4
	Lepton ID SF	2
	Jet Energy Scale	1
	PDFs on Acceptance	1
	Track Isolation	2
	Trigger Efficiency	1
WW	Total	9
WZ/ZZ	Total (same as WW)	9
Fakes	Different Jet Samples	50
$t\bar{t}$	Lepton ID SF	2
	Jet Energy Scale	5
	MC Generators (Pythia vs Herwig)	6
	PDF's	1
	ISR/FSR	1.7
$t\bar{t}$	Total	8
Drell-Yan	Jet Energy Scale	1
	Lepton ID SF	2
	Track Isolation	2
	PDF on Acceptance	2
	Trigger Efficiency	1
	Missing Energy Data/MC	20
Drell-Yan	Total	20
W γ	Factorization scale	2
	Renormalization scale	3
	PDF	5
	Jet Energy Scale	1
	Unweighting and k-factor error	2
W γ	Total	7

Table 18: Sources of systematic uncertainties on the backgrounds. To all these uncertainties we add in quadrature 6% coming from luminosity.

10 Data analysis

10.1 Data samples and luminosity

We use the inclusive high-P_T lepton triggered samples, processed with version 5.3.1 Production. The central electrons (CEM) came in on $ELECTRON_CENTRAL_18$ trigger and correspond to the datasets bhel0d. The muons were collected on the two triggers: $MUON_CMUP18$ and $MUON_CMX18$ and are in the bhmu0d dataset. The plug electron samples we use were also processed with 5.3.1 Production; they were collected with MET_PEM trigger, which additionally requires large missing energy ($\not\!\!E_T > 15$ GeV), to keep the rates low. The associated dataset is ptop00, stripped from bpel0d.

Version 7 of the DQM good run list of the Top, EWK and Exotics groups is applied [5]. This covers all the runs numbers up to 186598 and does not include the "COT-compromised" period, where the lower gains affected the COT tracking efficiency (run range 179096-182842). However we note the following:

- In the *ee* channel we apply the good run list without muon requirements.
- We have applied the good run list without silicon checks to the events that do not contain a PHX in the dilepton category.
- For dilepton events with a PHX (TCE-PHX, PHX-PHX, CMUP-PHX, CMX-PHX, PHX-CMU, PHX-CMP, PHX-CMIO) the good run list with good silicon has been applied. Only about 15% of the acceptance comes from events with a plug electron.

Dilepton Combination Type	Good Run List	Offline $\mathcal{L}_{int}$ (pb^{-1}) +1.9% correction and ±5.9% errors
TCE-TCE	1001	374 ± 22
PHX-{TCE, PHX}	1101	343 ± 21
TCE-{CMUP, CMU, CMP, CMIO}	1031	366 ± 22
TCE-CMX	1021	333 ± 20
PHX-{CMUP, CMU, CMP, CMIO}	1131	337 ± 20
PHX-CMX	1121	310 ± 19
CMUP-{CMUP, CMU, CMP, CMIO}	0031	378 ± 23
CMX-{CMUP, CMX, CMU, CMP, CMIO}	0011	339 ± 20

Table 19: Luminosities of the different di-lepton categories used in the analysis.

.

The luminosities relevant for our dilepton categories are summarized in table 19. These luminosities, together with the relative acceptances in the HWW dilepton categories, gives us an average luminosity of:

$$\mathcal{L}_{HWW} \quad = \quad (360 \ \pm \ 22)\,\mathrm{pb}^{-1}$$

10.2 Energy Scale factors for Plug electrons.

We correct phoenix electron energy with scale factors after adding plug pre-radiator (PPR) energy as listed in Table 20, bringing the $Z \rightarrow e_{\mathrm{TCE}} e_{\mathrm{PHX}}$ mass peak to 91 GeV as shown in Figure 13. The run range division was inherited from 4.11.1 diboson analyses [13, 14].

[5] http://www-cdf.fnal.gov/internal/dqm/goodrun/v7/goodv7.html

run range	Data		MC	
	east	west	east	west
141544-168889	1.041	1.033	1.019	1.019
168890-186598	1.041	1.045	1.019	1.020

Table 20: Phoenix electron energy scale factors divided by run range, plug side ($\eta > 0$ for east; $\eta < 0$ for west) and data/MC.

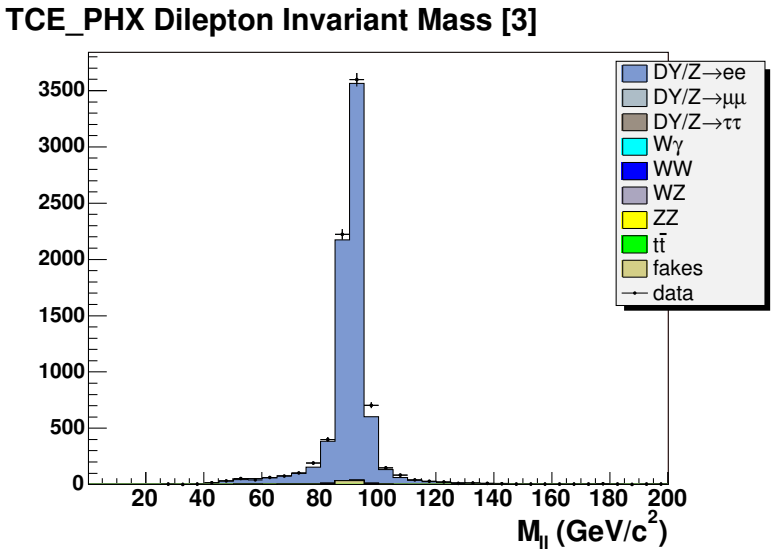

Figure 13: The mass peak of $Z \to e_{\rm TCE}e_{\rm PHX}$ with phoenix electron energies added plug preradiator energies and scaled up by factors as listed in Table 20.

10.3 Dilepton table

The result of the event selection described in Section 2, applied to the datasets described above, are shown in tables 21, 22, 25-34. The number of candidates depend on the particular mass of the Higgs boson we search for.

11 Grand Summary

The summary of all the backgrounds, signal acceptances, and data analysis for $360\,{\rm pb}^{-1}$ are shown in table 21 and 22. The tables 27-32 show the distributions of the signal and backgrounds per ee, $e\mu$ and $\mu\mu$ channels.

M_H	110	120	130	140	150
WW	3.838 ± 0.403	5.491 ± 0.576	6.826 ± 0.717	7.983 ± 0.838	9.132 ± 0.959
WZ	0.144 ± 0.019	0.230 ± 0.030	0.284 ± 0.037	0.338 ± 0.044	0.372 ± 0.048
ZZ	0.023 ± 0.004	0.025 ± 0.005	0.029 ± 0.005	0.032 ± 0.006	0.036 ± 0.007
$t\bar{t}$	0.080 ± 0.009	0.118 ± 0.013	0.152 ± 0.017	0.210 ± 0.023	0.281 ± 0.031
W γ	2.837 ± 0.209	2.895 ± 0.213	2.217 ± 0.163	1.967 ± 0.145	1.477 ± 0.109
DY$\ell\ell$	2.114 ± 0.529	1.635 ± 0.409	1.265 ± 0.316	1.014 ± 0.254	1.200 ± 0.300
Fakes	1.595 ± 0.797	1.672 ± 0.836	1.780 ± 0.890	1.526 ± 0.763	1.507 ± 0.754
Total back	10.632 ± 1.059	12.066 ± 1.116	12.554 ± 1.198	13.071 ± 1.172	14.005 ± 1.262
HWW	0.028 ± 0.002	0.095 ± 0.006	0.205 ± 0.012	0.326 ± 0.020	0.436 ± 0.026
Data	8	7	9	14	14

Table 21: The estimated backgrounds and HWW signal in $360\,\mathrm{pb}^{-1}$, and the number of events observed in the data, for each of the dilepton categories. The HWW expectation uses the theoretical cross-sections and BRs discussed in Section 1. The error on luminosity (6%) it is not included.

M_H	160	170	180	190	200
WW	9.794 ± 1.028	9.967 ± 1.046	9.892 ± 1.039	9.623 ± 1.010	9.193 ± 0.965
WZ	0.365 ± 0.047	0.379 ± 0.049	0.433 ± 0.056	0.577 ± 0.075	0.860 ± 0.112
ZZ	0.036 ± 0.007	0.044 ± 0.008	0.062 ± 0.012	0.139 ± 0.026	0.302 ± 0.057
$t\bar{t}$	0.349 ± 0.038	0.399 ± 0.044	0.459 ± 0.050	0.518 ± 0.057	0.576 ± 0.063
W γ	1.142 ± 0.084	0.969 ± 0.071	0.816 ± 0.060	0.654 ± 0.048	0.477 ± 0.035
DY$\ell\ell$	0.763 ± 0.191	0.827 ± 0.207	0.827 ± 0.207	0.843 ± 0.211	0.958 ± 0.239
Fakes	1.334 ± 0.667	1.242 ± 0.621	0.884 ± 0.442	0.800 ± 0.400	0.722 ± 0.361
Total back	13.784 ± 1.245	13.826 ± 1.238	13.373 ± 1.152	13.154 ± 1.112	13.089 ± 1.068
HWW	0.577 ± 0.035	0.541 ± 0.032	0.409 ± 0.025	0.238 ± 0.014	0.214 ± 0.013
Data	16	18	19	19	17

Table 22: The estimated backgrounds and HWW signal in $360\,\mathrm{pb}^{-1}$, and the number of events observed in the data, for each of the dilepton categories. The HWW expectation uses the theoretical cross-sections and BRs discussed in Section 1. The error on luminosity it is not included.

12 Cross-Section Limit Calculation

Now we proceed to extract 95% credibility limits (C.L.) on the Standard Model $\sigma \times BR(p\bar{p} \to H \to WW^*)$.

12.1 $\Delta\phi$ Distributions

The distributions of $\Delta\phi$ between the 2 leptons in events passing the selection criteria described in Section 2, are used to set limits on the $p\bar{p} \to H \to WW^*$ cross section. These distributions are given in Figures 14-21. The scalar nature of the Higgs boson gives a tendency of the leptons to be closer in ϕ than that from WW production, making this variable a good discriminator.

Rather than simply cut on the variable (and hence loose some signal acceptance), we form a binned likelihood of the observed spectrum to a combination of signal and background, and use this to extract cross section limits. This procedure is discussed in detail below.

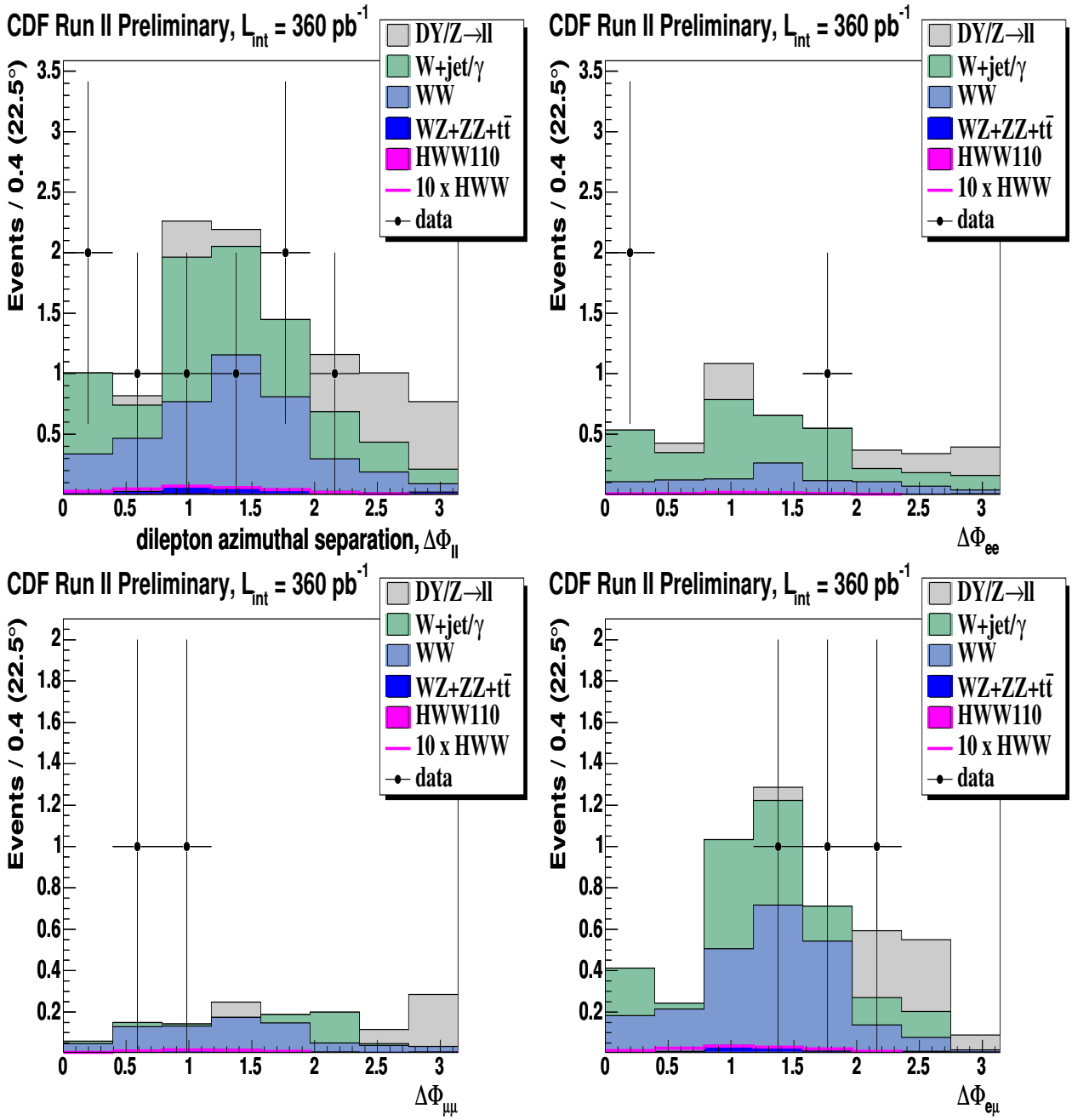

Figure 14: Azimuthal angular separation between the leptons, $\Delta\phi(\ell,\ell)$, from the decay of $H \rightarrow WW^* \rightarrow \ell\nu\ell\nu$. Distributions of data, HWW^* signal ($M_H = 110$ GeV) MC, WW MC and the sum of other considered background MC samples are shown. The MCs are normalized to the expectations for the integrated luminosity for analyzed data, about 360/pb. We use the upper-left $ee + e\mu + \mu\mu$ plot to fit for a limit on the cross-section of SM HWW production at Tevatron, at the Higgs mass of $M_H = 110$ GeV.

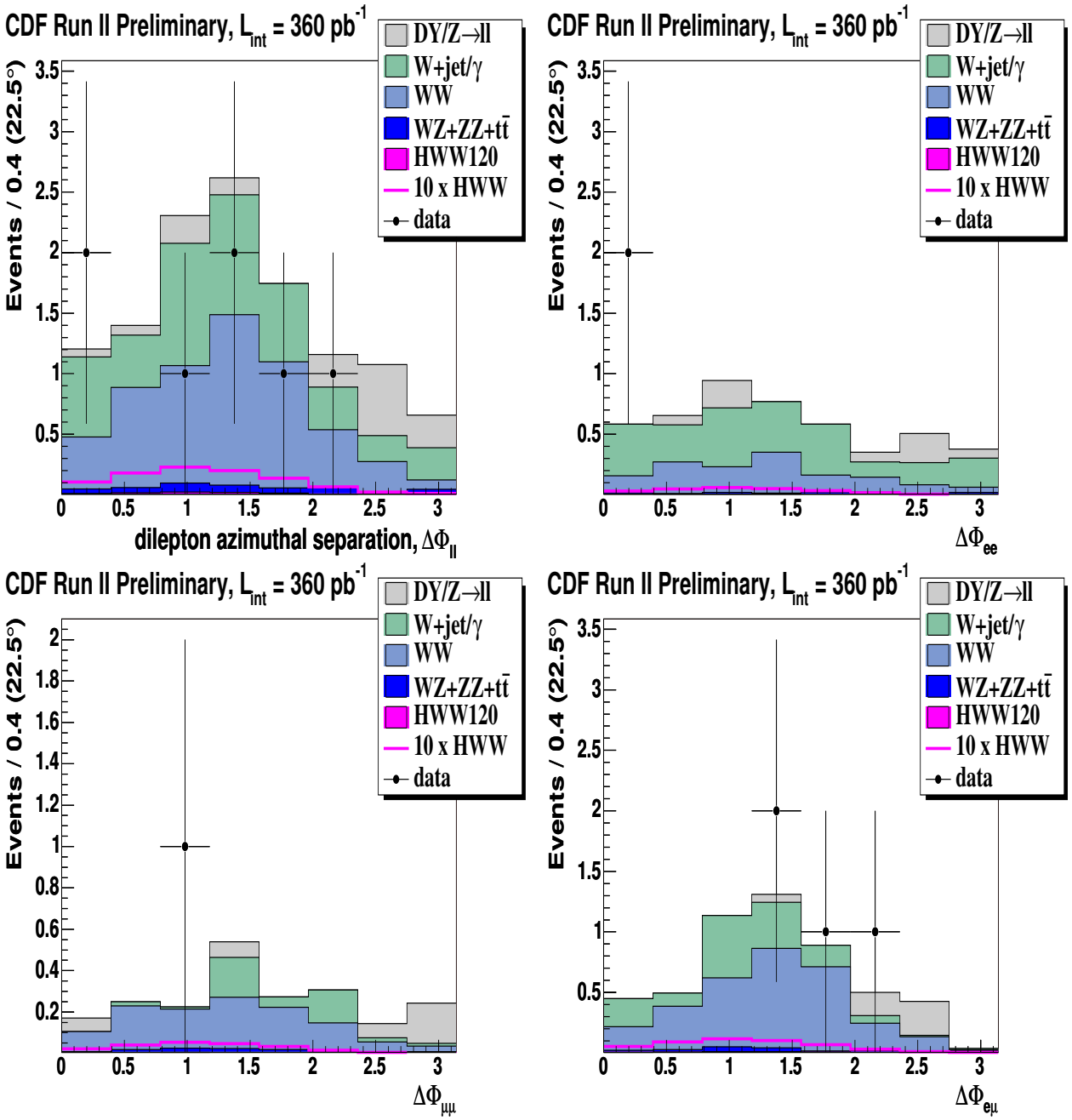

Figure 15: Azimuthal angular separation between the leptons, $\Delta\phi(\ell,\ell)$, from the decay of $H \to WW^* \to \ell\nu\ell\nu$. Distributions of data, HWW^* signal ($M_H = 120$ GeV) MC, WW MC and the sum of other considered background MC samples are shown. The MCs are normalized to the expectations for the integrated luminosity for analyzed data, about 360/pb. We use the upper-left $ee + e\mu + \mu\mu$ plot to fit for a limit on the cross-section of SM HWW production at Tevatron, at the Higgs mass of $M_H = 120$ GeV.

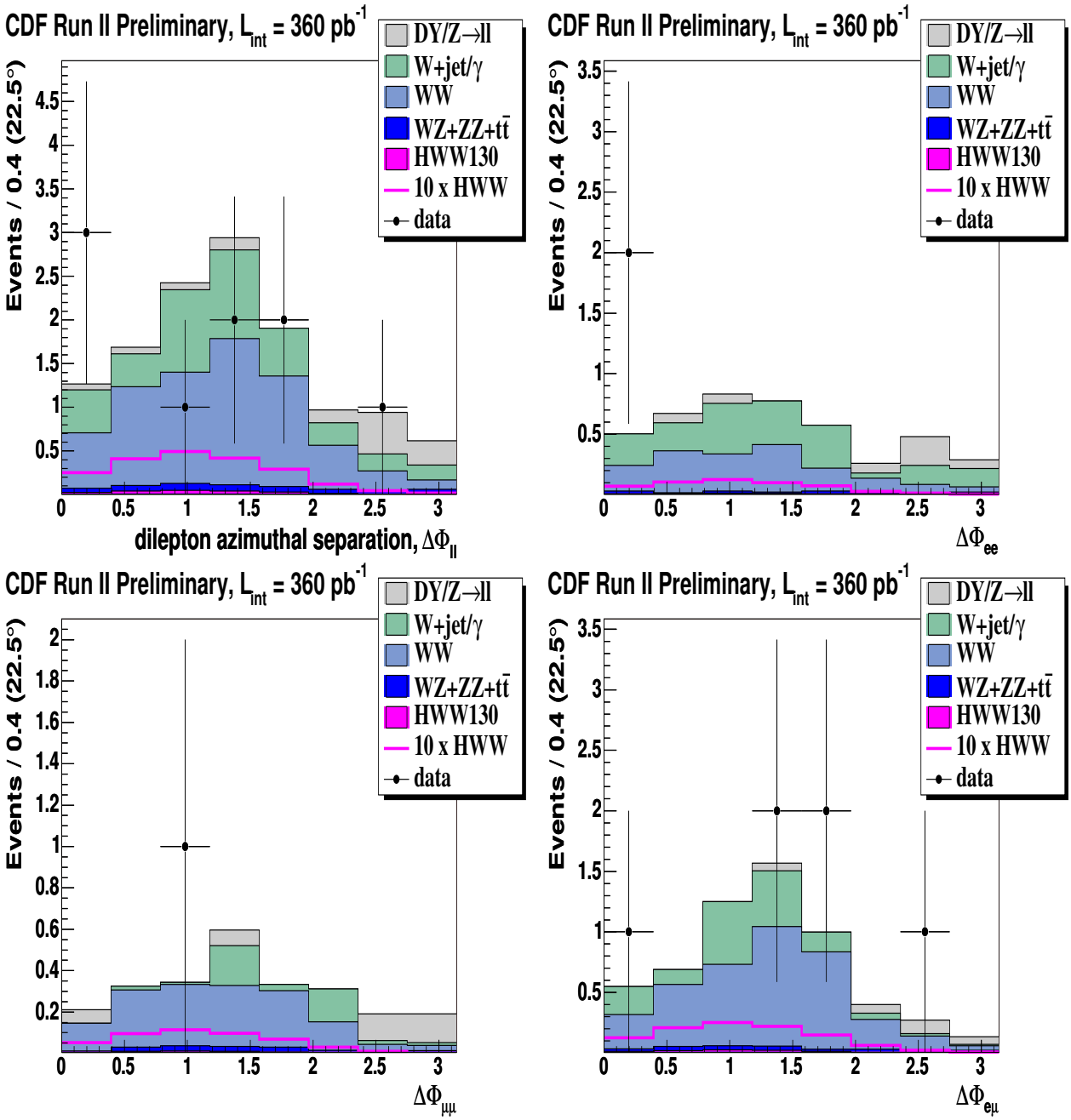

Figure 16: Azimuthal angular separation between the leptons, $\Delta\phi(\ell,\ell)$, from the decay of $H \to WW^* \to \ell\nu\ell\nu$. Distributions of data, HWW^* signal ($M_H = 130$ GeV) MC, WW MC and the sum of other considered background MC samples are shown. The MCs are normalized to the expectations for the integrated luminosity for analyzed data, about 360/pb. We use the upper-left $ee + e\mu + \mu\mu$ plot to fit for a limit on the cross-section of SM HWW production at Tevatron, at the Higgs mass of $M_H = 130$ GeV.

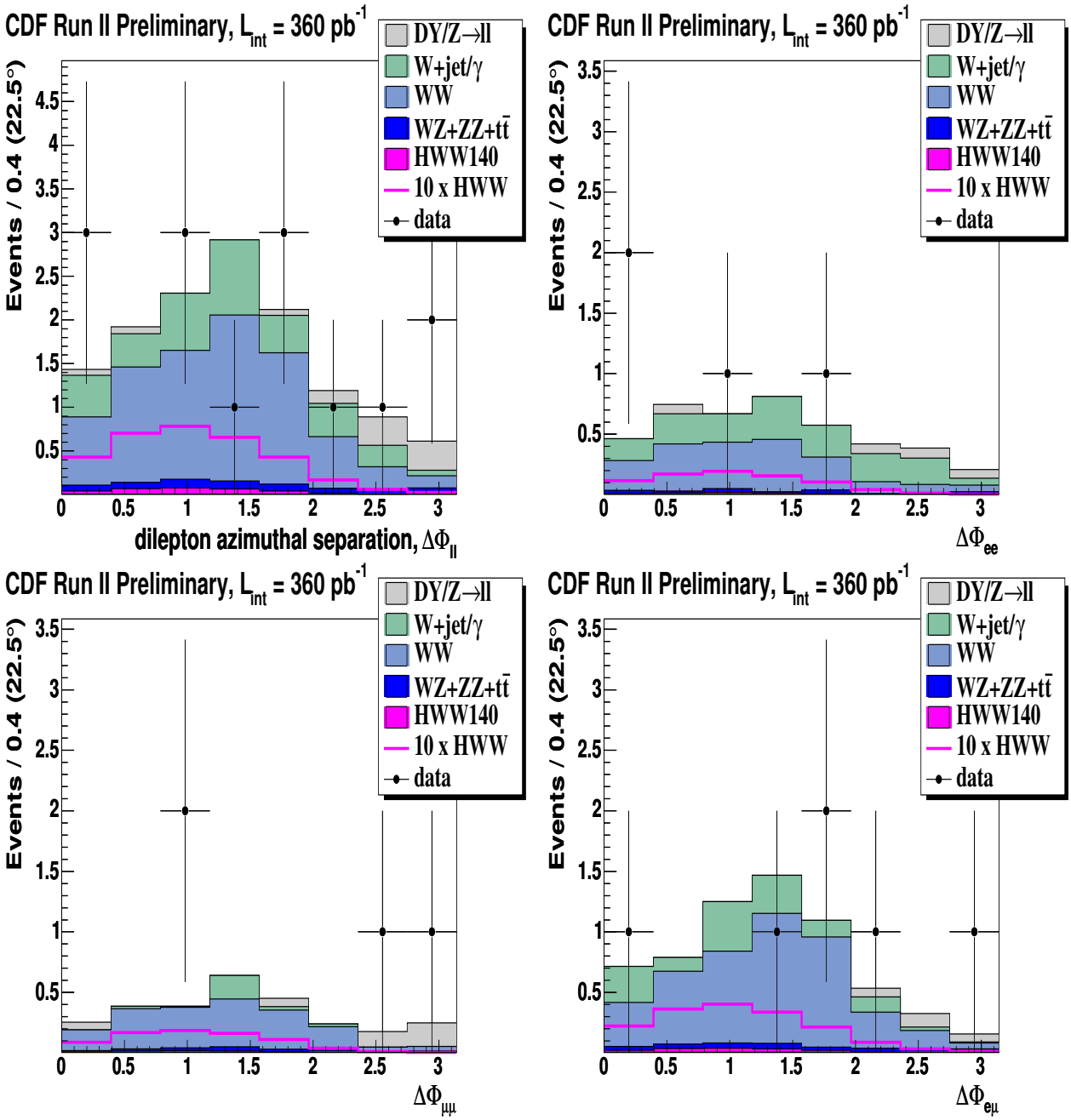

Figure 17: Azimuthal angular separation between the leptons, $\Delta\phi(\ell,\ell)$, from the decay of $H \to WW^* \to \ell\nu\ell\nu$. Distributions of data, HWW^* signal ($M_H = 140$ GeV) MC, WW MC and the sum of other considered background MC samples are shown. The MCs are normalized to the expectations for the integrated luminosity for analyzed data, about 360/pb. We use the upper-left $ee + e\mu + \mu\mu$ plot to fit for a limit on the cross-section of SM HWW production at Tevatron, at the Higgs mass of $M_H = 140$ GeV.

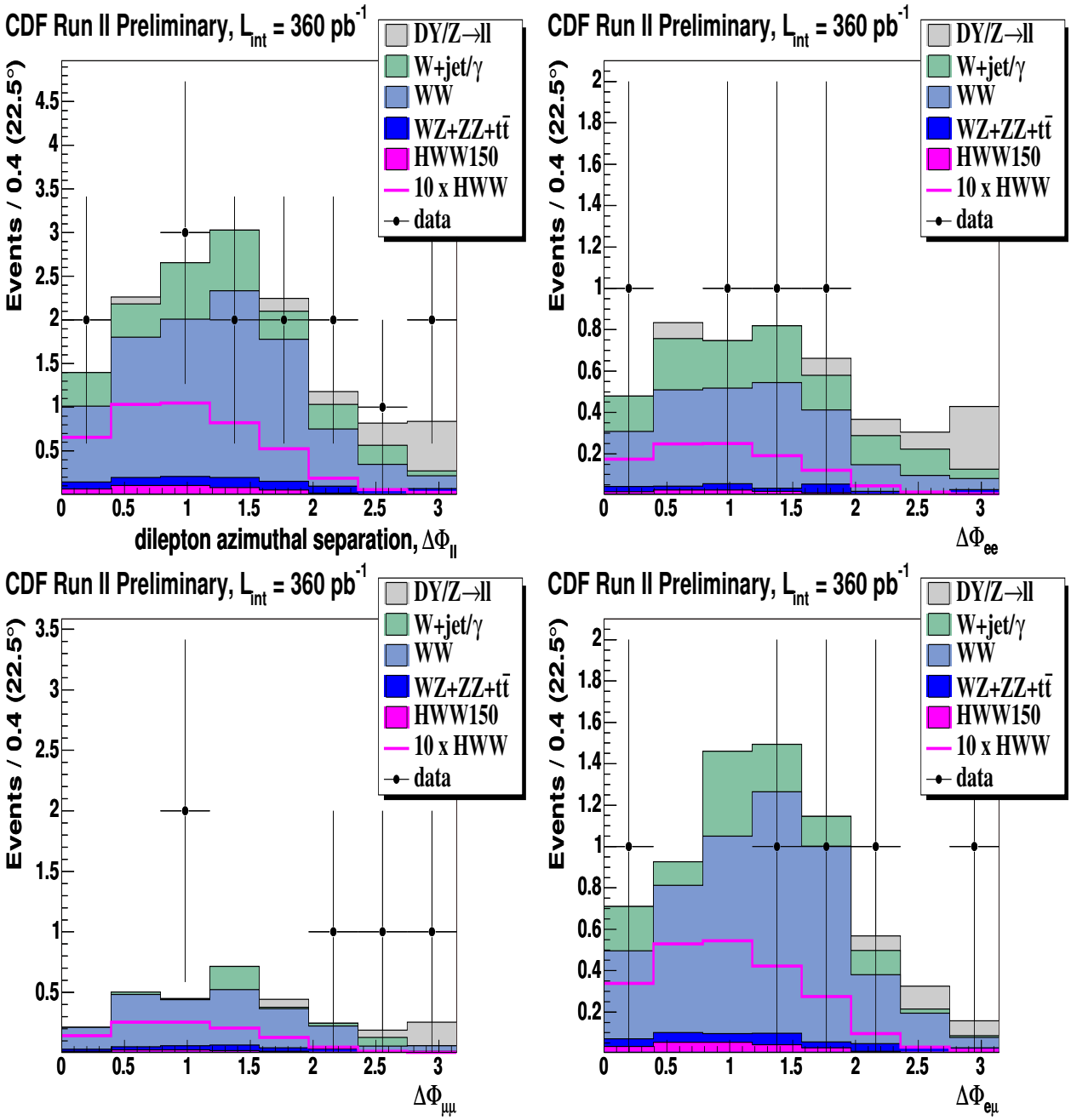

Figure 18: Azimuthal angular separation between the leptons, $\Delta\phi(\ell,\ell)$, from the decay of $H \to WW^* \to \ell\nu\ell\nu$. Distributions of data, HWW^* signal ($M_H = 150$ GeV) MC, WW MC and the sum of other considered background MC samples are shown. The MCs are normalized to the expectations for the integrated luminosity for analyzed data, about 360/pb. We use the upper-left $ee + e\mu + \mu\mu$ plot to fit for a limit on the cross-section of SM HWW production at Tevatron, at the Higgs mass of $M_H = 150$ GeV.

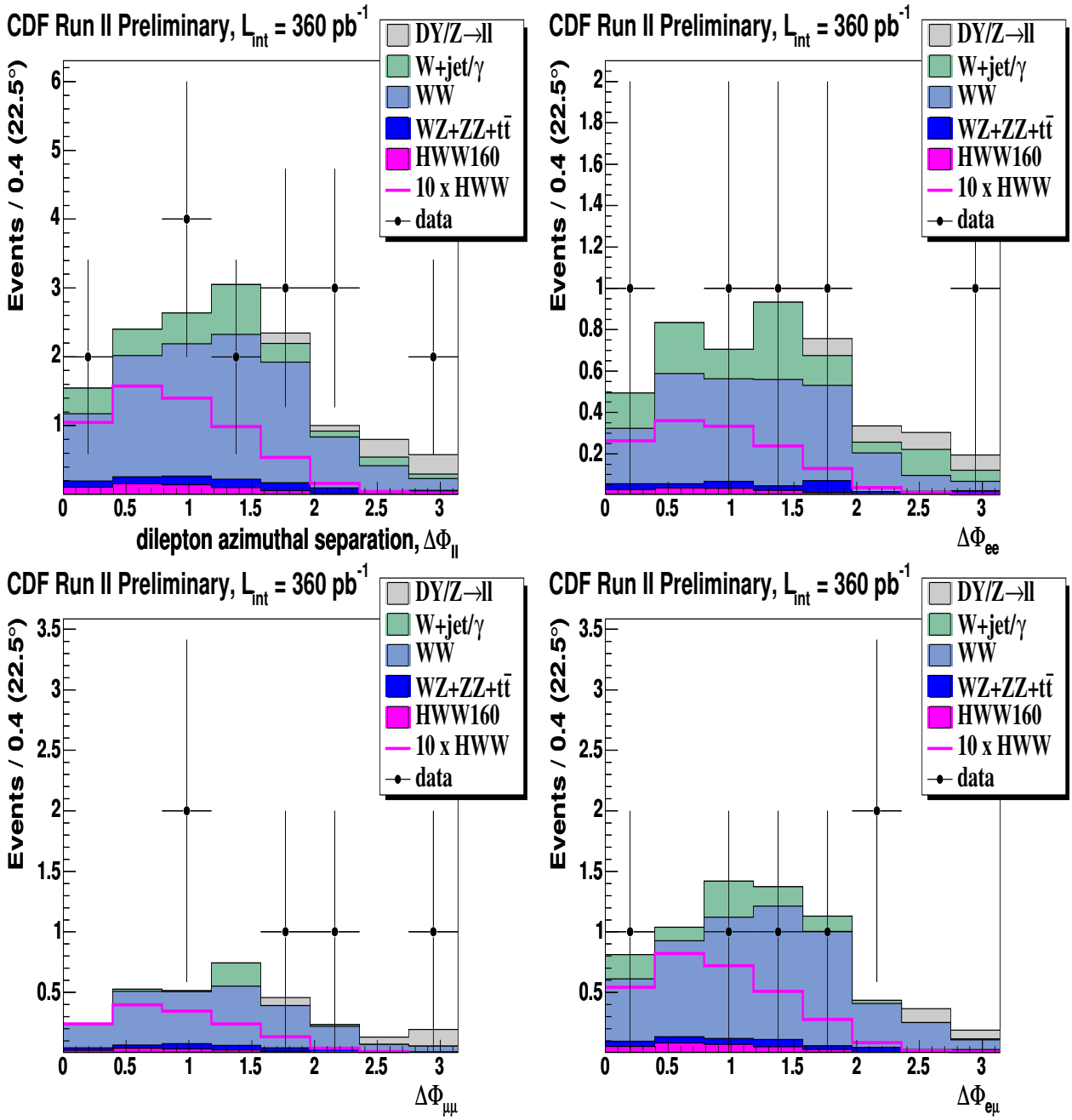

Figure 19: Azimuthal angular separation between the leptons, $\Delta\phi(\ell,\ell)$, from the decay of $H \to WW^* \to \ell\nu\ell\nu$. Distributions of data, HWW^* signal ($M_H = 160$ GeV) MC, WW MC and the sum of other considered background MC samples are shown. The MCs are normalized to the expectations for the integrated luminosity for analyzed data, about 360/pb. We use the upper-left $ee + e\mu + \mu\mu$ plot to fit for a limit on the cross-section of SM HWW production at Tevatron, at the Higgs mass of $M_H = 160$ GeV.

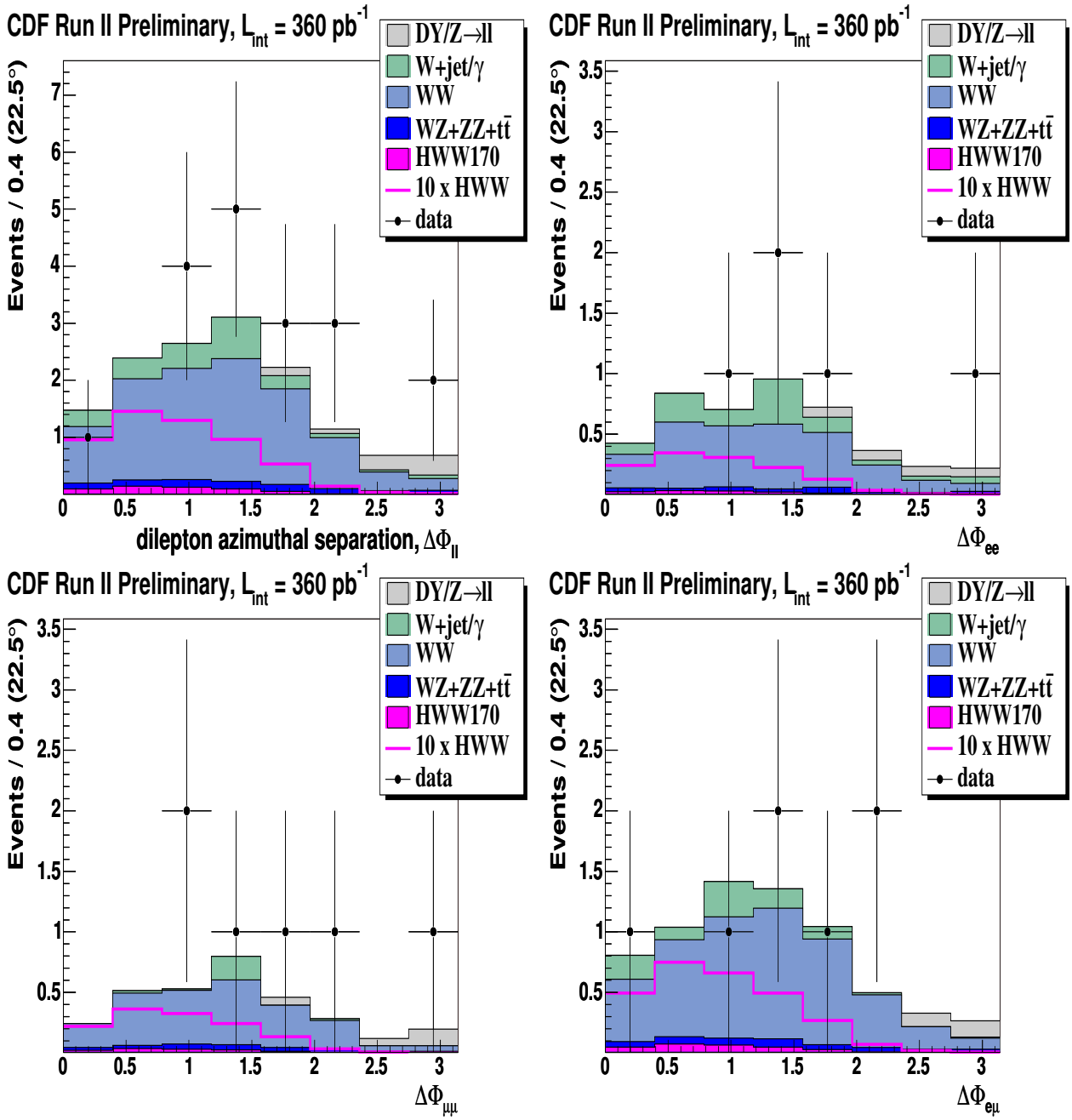

Figure 20: Azimuthal angular separation between the leptons, $\Delta\phi(\ell,\ell)$, from the decay of $H \to WW^* \to \ell\nu\ell\nu$. Distributions of data, HWW^* signal ($M_H = 170$ GeV) MC, WW MC and the sum of other considered background MC samples are shown. The MCs are normalized to the expectations for the integrated luminosity for analyzed data, about 360/pb. We use the upper-left $ee + e\mu + \mu\mu$ plot to fit for a limit on the cross-section of SM HWW production at Tevatron, at the Higgs mass of $M_H = 170$ GeV.

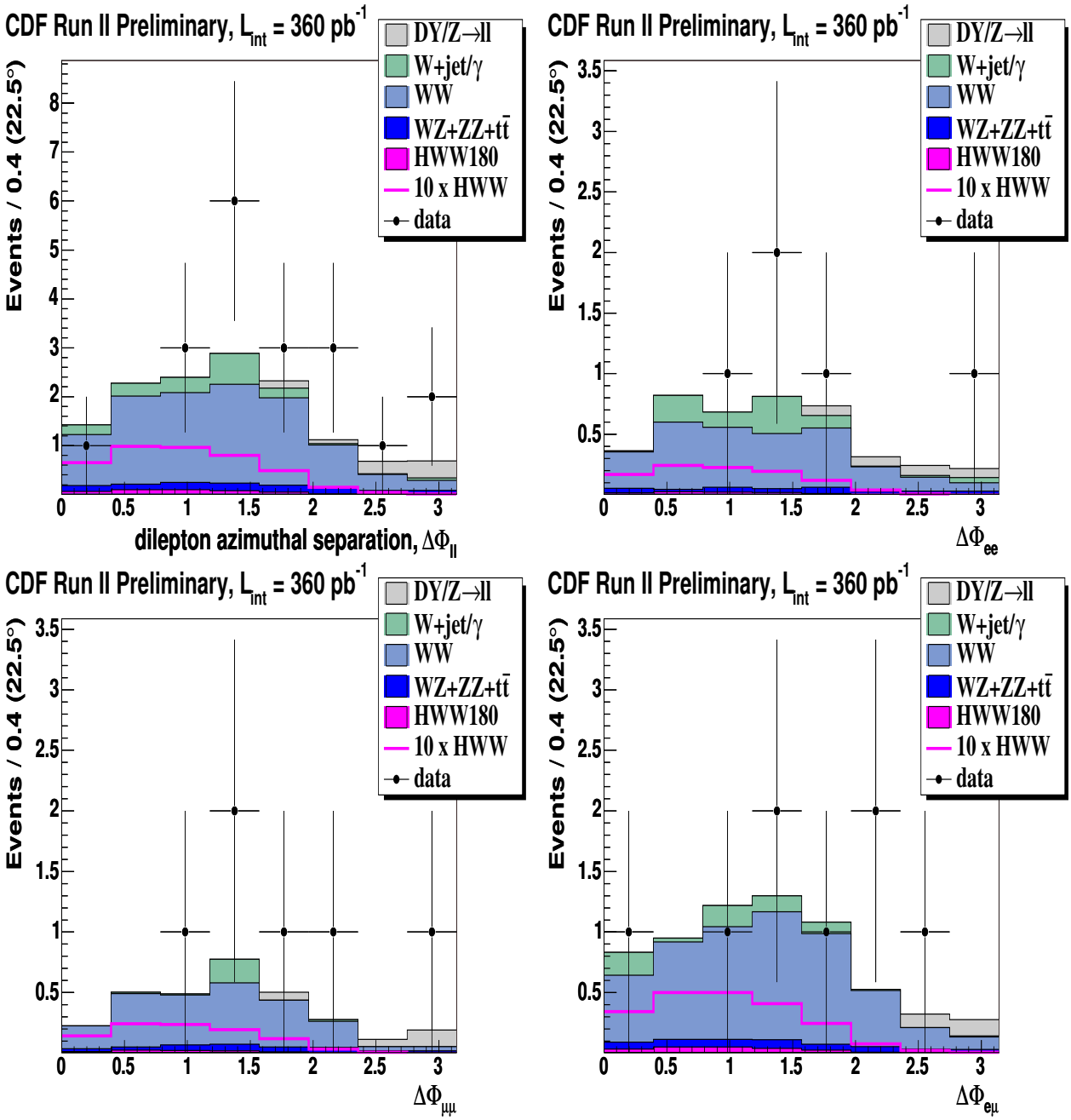

Figure 21: Azimuthal angular separation between the leptons, $\Delta\phi(\ell,\ell)$, from the decay of $H \to WW^* \to \ell\nu\ell\nu$. Distributions of data, HWW^* signal ($M_H = 180$ GeV) MC, WW MC and the sum of other considered background MC samples are shown. The MCs are normalized to the expectations for the integrated luminosity for analyzed data, about 360/pb. We use the upper-left $ee + e\mu + \mu\mu$ plot to fit for a limit on the cross-section of SM HWW production at Tevatron, at the Higgs mass of $M_H = 180$ GeV.

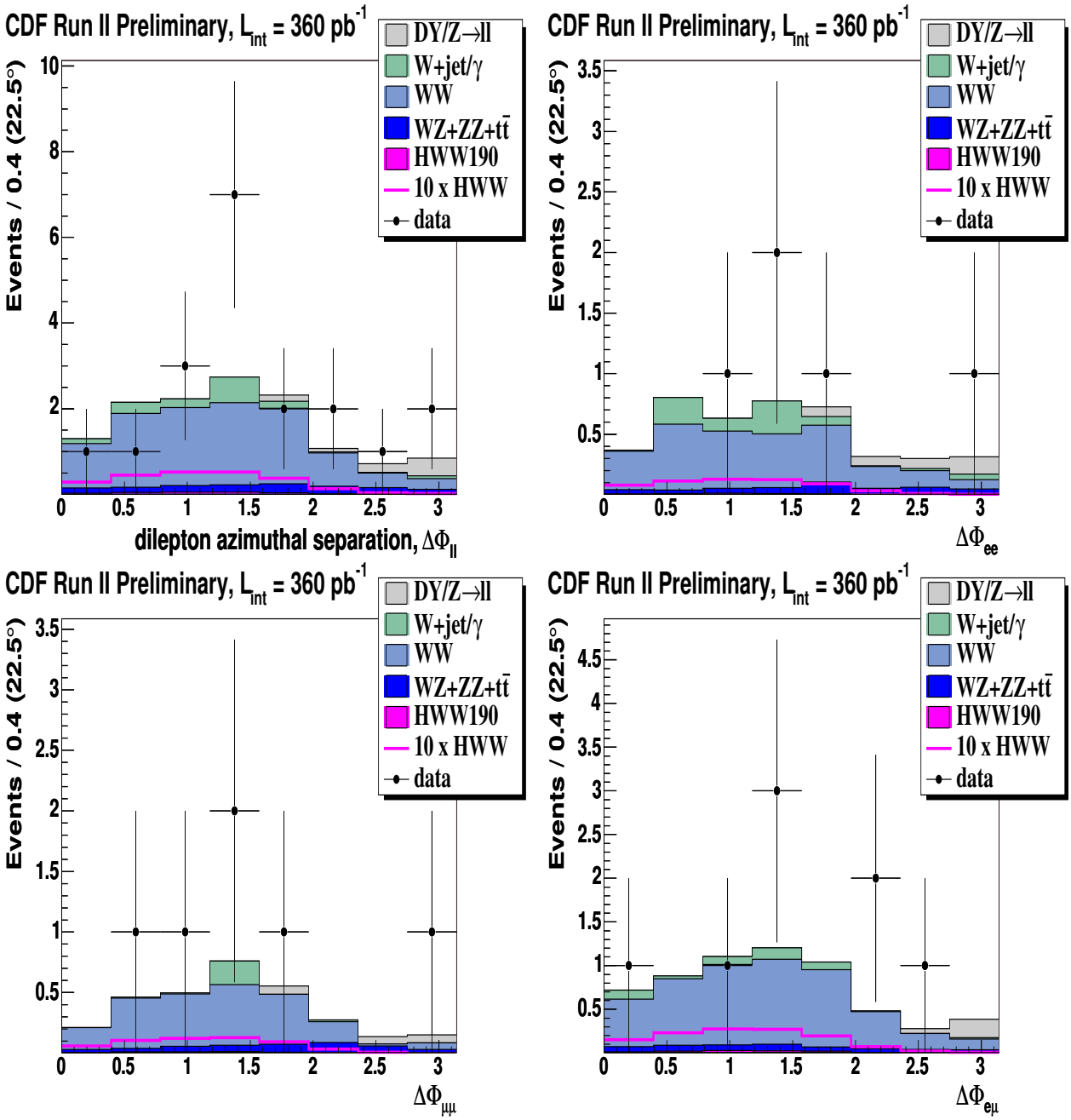

Figure 22: Azimuthal angular separation between the leptons, $\Delta\phi(\ell,\ell)$, from the decay of $H \to WW^* \to \ell\nu\ell\nu$. Distributions of data, HWW^* signal ($M_H = 190$ GeV) MC, WW MC and the sum of other considered background MC samples are shown. The MCs are normalized to the expectations for the integrated luminosity for analyzed data, about 360/pb. We use the upper-left $ee + e\mu + \mu\mu$ plot to fit for a limit on the cross-section of SM HWW production at Tevatron, at the Higgs mass of $M_H = 190$ GeV.

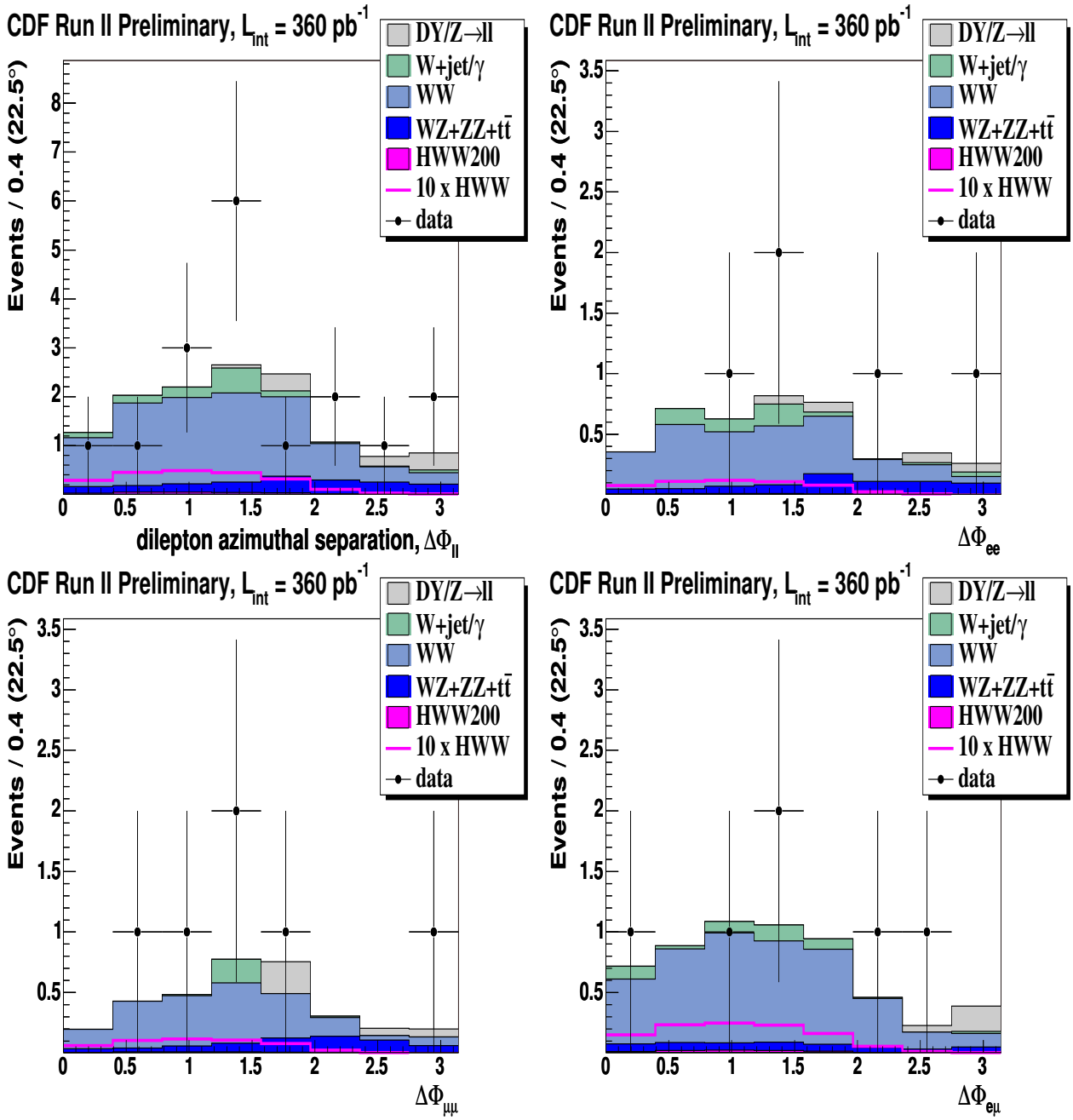

Figure 23: Azimuthal angular separation between the leptons, $\Delta\phi(\ell,\ell)$, from the decay of $H \to WW^* \to \ell\nu\ell\nu$. Distributions of data, HWW^* signal ($M_H = 200$ GeV) MC, WW MC and the sum of other considered background MC samples are shown. The MCs are normalized to the expectations for the integrated luminosity for analyzed data, about 360/pb. We use the upper-left $ee + e\mu + \mu\mu$ plot to fit for a limit on the cross-section of SM HWW production at Tevatron, at the Higgs mass of $M_H = 200$ GeV.

12.2 The Likelihood function and Posterior Density

A binned likelihood is used to compare the $\Delta\phi(\ell,\ell)$ spectrum in the data to a combination of expected distributions from the background processes and the $H \to WW^*$ signal, as a function of Higgs mass. The likelihood function is the usual product of Poisson probabilities over each bin, comparing the observed bin content to that expected.

A Bayesian procedure is used to extract cross section limits. For each Higgs mass, a posterior density is obtained by multiplying the likelihood function with prior densities for all the parameters in the likelihood: integrated luminosity, background normalizations, signal efficiency, and the product $\sigma'_H \equiv \sigma_H \times BR(H \to WW^*)$ of the signal production cross section σ_{H^0} by the branching ratio for $H \to WW^*$. With one exception, these priors are truncated Gaussian densities constraining a given parameter to its expected value within its uncertainty. The exception is σ'_H: since nothing is presumed known *a priori* about this, it is assigned a uniform prior. The posterior density is then integrated over all parameters except σ'_H, and a 95% credibility level (C.L.) upper limit on σ'_H is obtained by calculating the 95^{th} percentile of the resulting distribution. For now, we have assumed no correlations in the posterior density, between the systematic uncertainties of the signal and backgrounds. This assumption is not strictly correct, as there are correlations, but the effect is expected to be small, and we will revisit this assumption later.

12.3 Expected Limits from Pseudo-experiments

We obtain expected cross section limits from the average obtained from 1000 pseudo-experiments. The pseudo-experiments are generated for each Higgs mass as follows:

0) Assume zero signal

1) Use the mean and sigmas for WW, and "all other backgrounds". Gaussian fluctuate these means about their uncertainties to generate 2 new numbers.

2) Poisson fluctuate these numbers, and take the integer of them. This gives us a number of WW and "other" for a given pseudo-experiment.

3) Using these integers, randomly sample from the $\Delta\phi$ distributions for WW and "other" to generate the $\Delta\phi$ distribution for the pseudo-experiment.

4) Find the limit from the pseudo-experiment exactly as done for the data.

5) Repeat 1000 times.

6) The most likely 95% CL limit from the distribution of 1000 pseudo-experiments is our *expected limit.*

The distributions of limits from pseudo-experiments are given in figures 24 and 25. The resultant expected limits are given in Table 23 together with the limits obtained from the data.

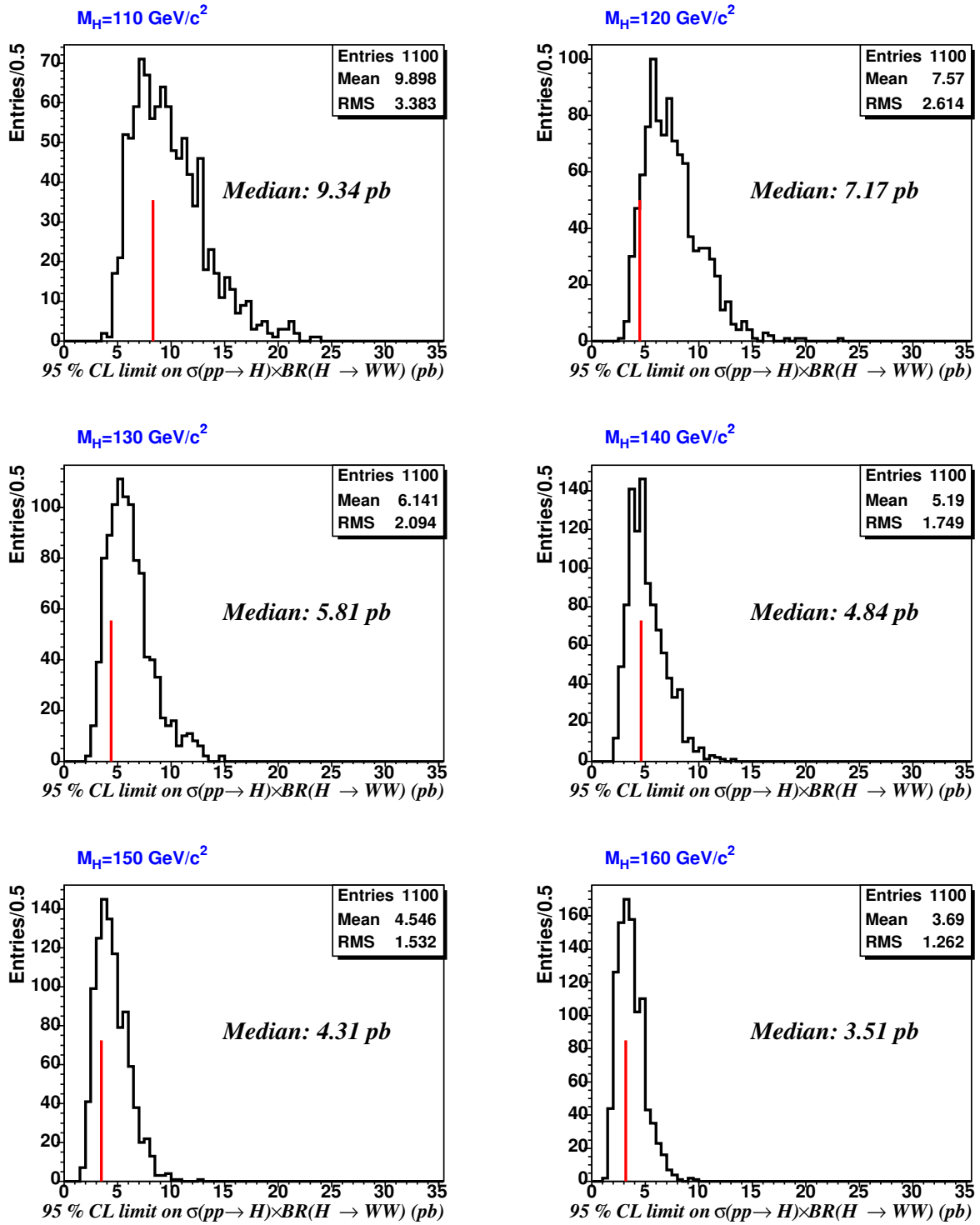

Figure 24: Expected limits obtained from pseudo-experiments drawn from $\Delta\phi(\ell,\ell)$ distributions, for Higgs masses from 110-160 GeV/c^2. The red line represents the 95% CL extracted from data.

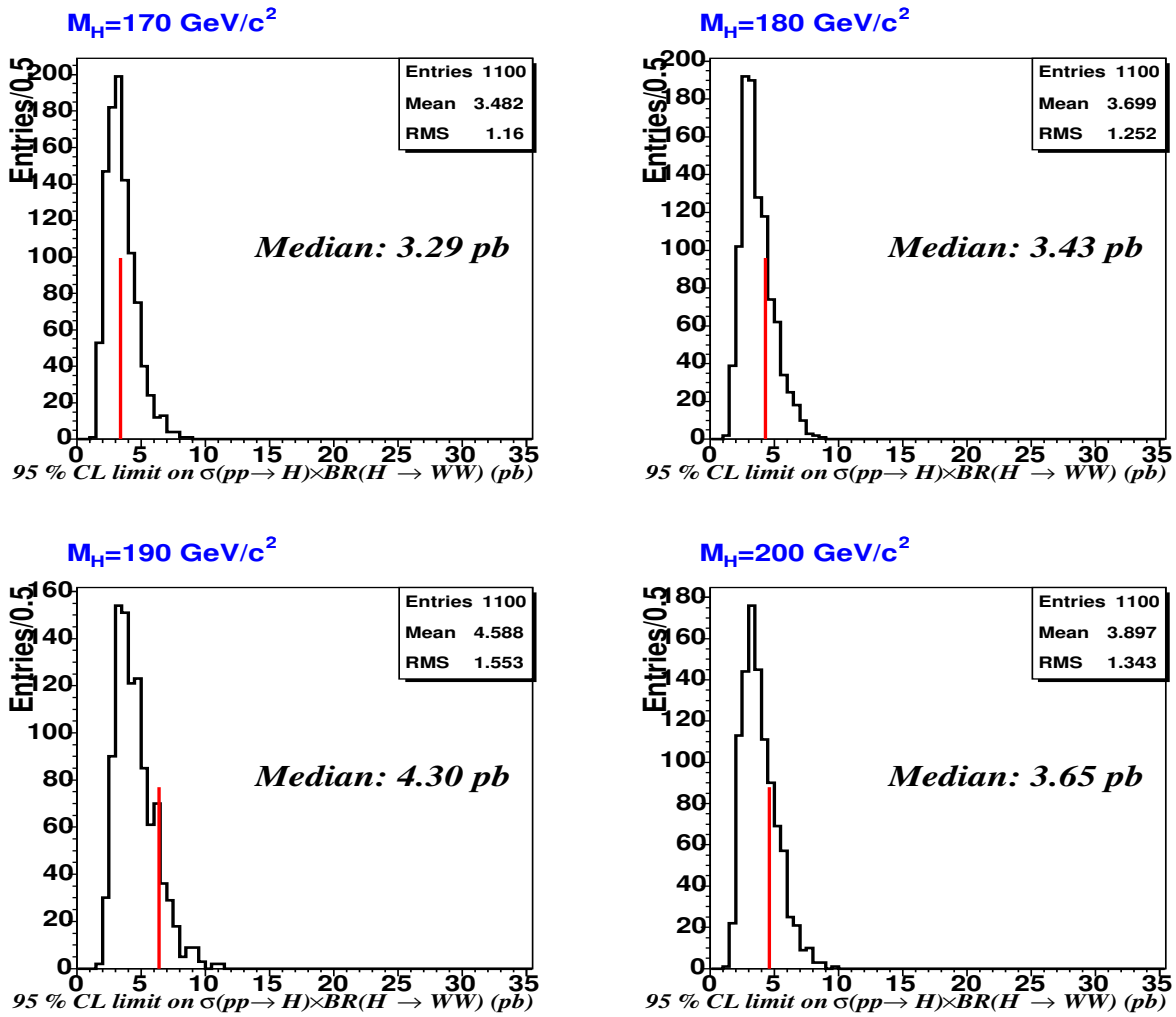

Figure 25: Expected limits obtained pseudo-experiments, drawn from $\Delta\phi(\ell,\ell)$ distributions, for Higgs masses from 170-200 GeV/c^2. The red line represents the 95% CL extracted from data.

12.4 Cross section Limits from the Data

The 95% CL cross section limits on $\sigma_H \times BR(H \to WW^*)$ are summarized in Table 23, and plotted in figures 26 and 27.

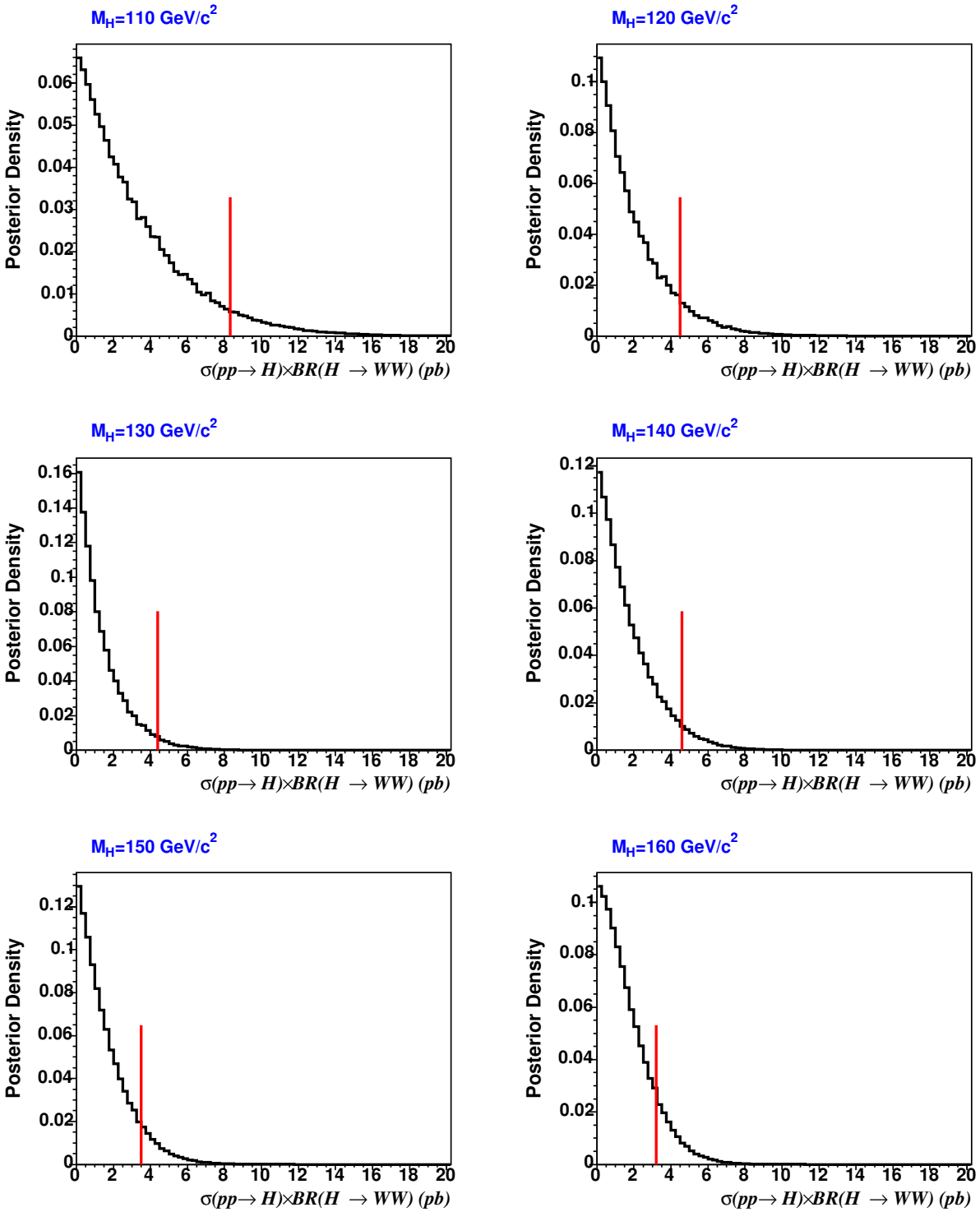

Figure 26: The likelihood functions obtained from $\Delta\phi(\ell,\ell)$ distributions, for Higgs masses from 110-160 GeV/c^2.

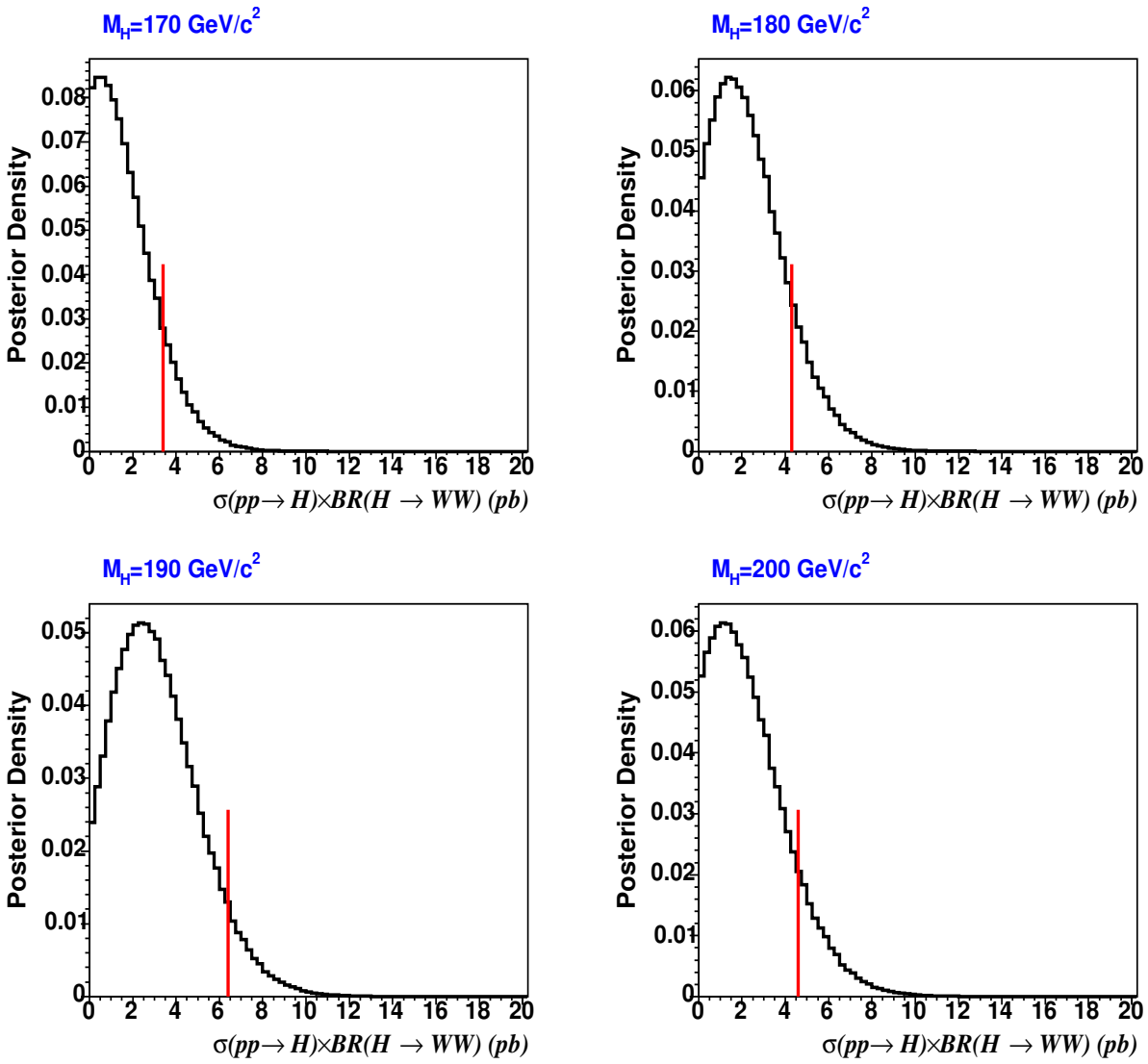

Figure 27: The likelihood functions obtained from $\Delta\phi(\ell,\ell)$ distributions, for Higgs masses from 170-200 GeV/c^2.

	M_H (GeV/c^2)									
95% CL Limit	110	120	130	140	150	160	170	180	190	200
$\Delta\phi$ (old) 4.11.1	-	-	-	17.8	9.4	5.6	5.6	6.4	-	-
$\Delta\phi$ (expected, new)	9.3	7.1	5.8	4.8	4.3	3.5	3.3	3.4	4.3	3.6
$\Delta\phi$ (new)	**8.3**	**4.5**	**4.4**	**4.6**	**3.5**	**3.2**	**3.4**	**4.3**	**6.4**	**4.6**

Table 23: 95% CL limits on $\sigma(gg \to H) \times BR(H \to WW^*)$ at $\sqrt{\hat{s}} = 1.96\,\text{TeV}$ for the different Higgs obtained using our old 20-20 selection from CDF-6958, for 200 /pb. The expected limits using the new selection are also shown, as discussed above. In all cases the limits correspond to $360\,\text{pb}^{-1}$.

13 Conclusions

We have studied the production of SM HWW to dilepton channels ($ee + e\mu + \mu\mu$) at Tevatron in 360/pb CDF Run II data. We do not see an excess over the SM expected background, so we proceed to set a 95% C.L. limit on the Standard-Model cross-section $\times$ branching ratio $\sigma \cdot \text{BR}_{\text{SM}}(p\bar{p} \to H \to WW^*)$ at center-of-mass energy $\sqrt{\hat{s}} = 1.96$ TeV, for Higgs masses between 110 - 200 GeV.

References

[1] J. Pumplin *et al.*-"New Generation of Parton Distributions with Uncertainties from Global QCD Analysis",hep-ph/0201195

[2] S. Sultansoy,"The "Golden Mode" at the Upgraded Tevatron?",hep-ex/0010037.

[3] S. Miller, "Pdf Acceptance Uncertainties for $t\bar{t}$ Cross Section", JPM March 19, 2004.

[4] David Dagenhart, "Measurement of the Z Production Cross Section", CDF-7865.

[5] Martin Griffiths, Beate Heinemann, Giulia Manca, "Central Electron ID Efficiencies at Medium Energy", CDF-7309.

[6] D.Bortoletto, A.Canepa, O.Gonzalez, E.Lytken, "Search for the associated production of chargino and neutralino in dimuon+lepton events", CDF-7714.

[7] C.Hill, J.Incandela, and C.Mills, "Electron Identification in Offline Release 5.3", CDF-7309.

[8] Tim Nelson, Rick Snider, David Stuart, "Forward Electron Tracking with the PhoenixMods Package", CDF-6278.

[9] Sunny S.Chuang, D.Carlsmith, Susana Cabrera, Mark Kruse, Dustin McGivern, David Waters, "Search for a SM Higgs Boson in the gg→H→WW* Dilepton Channel with 200/pb Run II Data at CDF", CDF-6958.

[10] Yoshio Ishizawa and Jason Nielsen, "Trigger Efficiencies for High Et Electrons", CDF-7401.

[11] Shan-Huei Chuang, Mark Kruse, Mircea Coca "Lepton Fake Estimate Using 314.2/pb CDF Run II Data", CDF-7497

[12] V.Martin, "High-Pt Muon ID Cuts and Efficiencies for use with 5.3.1 Data and 5.3.3 MC", CDF-7367.

[13] S.Cabrera, S.Carron, S.Chuang, J.Deng, A.Goshaw, Y.Huang, M.Kruse, D.McGivern, D.Waters, "WW Production in the Dilepton channel with 200/pb", CDF-6909

[14] S.Cabrera, J.Deng, A.Goshaw, C.Hays, Y.Huang, M.Kruse- Measurement of ZZ+ZW cross section using Run II data, CDF-6920

[15] Joint Physics Meeting High-Pt Lepton ID http://www-cdf.fnal.gov/internal/physics/joint_physics/index.html.

[16] Jet Energy and Resolution Group "Jet Energy Corrections Systematic Uncertainties" http://www-cdf.fnal.gov/internal/physics/top/jets/systematics.html.

[17] R.Barate *et al.*, ALEPH Collaboration", hep-ex/0306033 (Phys.Lett.B 565), 2003

[18] Tomura, Tomonobu, Top Mass at the Tevatron, HCP 2005, 4-9 July 2005

[19] M.Carena *et al.*, Report of the Tevatron Higgs Working Group, hep-ph/0010338

[20] D.Benjamin *et al.*, Measurement of the Wgamma and Zgamma Production Cross Sections using 200/pb of Run 2 Data, CDF-6601

[21] U.Baur, Berger El., Probing the WW gamma vertex at the Fermilab Tevatron Collider, Phys Rev D .41, 1476 (1990).

[22] B.Heinemann, A.Goshaw, M.Kirby, N.Tanimoto, H.Hayward - Measurement of Wgamma and Zgamma Production in $p\bar{p}$ collisions at sqrt(s)=1.96 TeV, CDF 7165

[23] M.Tecchio - Acceptance and background systematics for the Top Dilepton cross-section measurement, CDF 6590

A Comparison with the THWG's Prospects

Below we show a comparison of the THWG's prospects versus our current results. The interpretation of the results require a long discussion, which we will postpone for the moment.

Higgs Mass (GeV)	140	150	160	170	180	190
Total Background : Ours	13.07	14.00	13.78	13.83	13.37	13.15
THWG	15.84	10.80	1.58	0.86	1.37	2.70
$S/\sqrt{B}$ for 360/pb: Ours	0.09	0.12	0.16	0.15	0.11	0.07
THWG	0.23	0.31	0.43	0.42	0.30	0.19

Table 24: Comparison between the current status of our analysis and the THWG's prospect for the same integrated luminosity. The THWG's prospect are taken from Table 29 of the REPORT OF THE TEVATRON HIGGS WORKING GROUP [19] (originally at fb^{-1} scale) and interpolated to $\mathcal{L}_{\rm int} = 360$ pb^{-1}.

B Expected signal, backgrounds and data candidates per di-lepton channel

110 GeV	ee	$e\mu$	$\mu\mu$	ll
WW	0.893 ± 0.094	2.271 ± 0.238	0.674 ± 0.071	3.838 ± 0.403
WZ	0.033 ± 0.004	0.078 ± 0.010	0.034 ± 0.004	0.144 ± 0.019
ZZ	0.006 ± 0.001	0.007 ± 0.001	0.010 ± 0.002	0.023 ± 0.004
$t\bar{t}$	0.027 ± 0.003	0.027 ± 0.003	0.026 ± 0.003	0.080 ± 0.009
W γ	1.909 ± 0.140	0.929 ± 0.068	0.000 ± 0.000	2.837 ± 0.209
Drell-Yan $\ell\ell$	0.915 ± 0.229	0.805 ± 0.201	0.394 ± 0.099	2.114 ± 0.529
Fakes	0.564 ± 0.282	0.789 ± 0.395	0.241 ± 0.121	1.595 ± 0.797
Total Back	4.348 ± 0.401	4.905 ± 0.508	1.380 ± 0.171	10.632 ± 1.059
HWW	0.007 ± 0.000	0.014 ± 0.001	0.007 ± 0.000	0.028 ± 0.002
Data	3	3	2	8

Table 25: Summary of the signal and background expectations for a Higgs mass of 110 GeV, for 360 pb^{-1}. Also the observed number of events is shown. The error on luminosity it is not included.

120 GeV	ee	$e\mu$	$\mu\mu$	ll
WW	1.330 ± 0.140	2.995 ± 0.314	1.166 ± 0.122	5.491 ± 0.576
WZ	0.068 ± 0.009	0.112 ± 0.015	0.050 ± 0.006	0.230 ± 0.030
ZZ	0.006 ± 0.001	0.008 ± 0.001	0.011 ± 0.002	0.025 ± 0.005
$t\bar{t}$	0.036 ± 0.004	0.046 ± 0.005	0.036 ± 0.004	0.118 ± 0.013
W γ	1.972 ± 0.145	0.923 ± 0.068	0.000 ± 0.000	2.895 ± 0.213
Drell-Yan $\ell\ell$	0.695 ± 0.174	0.538 ± 0.134	0.402 ± 0.101	1.635 ± 0.409
Fakes	0.635 ± 0.318	0.572 ± 0.286	0.465 ± 0.232	1.672 ± 0.836
Total Back	4.743 ± 0.414	5.194 ± 0.451	2.129 ± 0.281	12.066 ± 1.116
HWW	0.025 ± 0.001	0.048 ± 0.003	0.022 ± 0.001	0.095 ± 0.006
Data	2	4	1	7

Table 26: Summary of the signal and background expectations for a Higgs mass of 120 GeV, for 360 pb^{-1}. Also the observed number of events is shown. The error on luminosity it is not included.

130 GeV	ee	$e\mu$	$\mu\mu$	ll
WW	1.689 ± 0.177	3.661 ± 0.384	1.477 ± 0.155	6.826 ± 0.717
WZ	0.074 ± 0.010	0.139 ± 0.018	0.072 ± 0.009	0.284 ± 0.037
ZZ	0.006 ± 0.001	0.010 ± 0.002	0.012 ± 0.002	0.029 ± 0.005
$t\bar{t}$	0.047 ± 0.005	0.060 ± 0.007	0.045 ± 0.005	0.152 ± 0.017
W γ	1.294 ± 0.095	0.923 ± 0.068	0.000 ± 0.000	2.217 ± 0.163
Drell-Yan $\ell\ell$	0.547 ± 0.137	0.312 ± 0.078	0.407 ± 0.102	1.265 ± 0.316
Fakes	0.682 ± 0.341	0.653 ± 0.326	0.445 ± 0.222	1.780 ± 0.890
Total Back	4.339 ± 0.419	5.758 ± 0.515	2.458 ± 0.290	12.554 ± 1.198
HWW	0.052 ± 0.003	0.105 ± 0.006	0.047 ± 0.003	0.205 ± 0.012
Data	2	6	1	9

Table 27: Summary of the signal and background expectations for a Higgs mass of 130 GeV, for 360 pb^{-1}. Also the observed number of events is shown. The error on luminosity it is not included.

140 GeV	ee	$e\mu$	$\mu\mu$	ll
WW	1.942 ± 0.204	4.220 ± 0.443	1.821 ± 0.191	7.983 ± 0.838
WZ	0.090 ± 0.012	0.163 ± 0.021	0.084 ± 0.011	0.338 ± 0.044
ZZ	0.010 ± 0.002	0.010 ± 0.002	0.012 ± 0.002	0.032 ± 0.006
$t\bar{t}$	0.063 ± 0.007	0.090 ± 0.010	0.058 ± 0.006	0.210 ± 0.023
W γ	1.127 ± 0.083	0.841 ± 0.062	0.000 ± 0.000	1.967 ± 0.145
Drell-Yan $\ell\ell$	0.311 ± 0.078	0.248 ± 0.062	0.456 ± 0.114	1.014 ± 0.254
Fakes	0.655 ± 0.328	0.595 ± 0.297	0.276 ± 0.138	1.526 ± 0.763
Total Back	4.199 ± 0.402	6.166 ± 0.541	2.707 ± 0.262	13.071 ± 1.172
HWW	0.081 ± 0.005	0.168 ± 0.010	0.078 ± 0.005	0.326 ± 0.020
Data	4	6	4	14

Table 28: Summary of the signal and background expectations for a Higgs mass of 140 GeV, for 360 pb^{-1}. Also the observed number of events is shown. The error on luminosity it is not included.

150 GeV	ee	$e\mu$	$\mu\mu$	ll
WW	2.326 ± 0.244	4.752 ± 0.499	2.053 ± 0.216	9.132 ± 0.959
WZ	0.106 ± 0.014	0.164 ± 0.021	0.102 ± 0.013	0.372 ± 0.048
ZZ	0.009 ± 0.002	0.010 ± 0.002	0.017 ± 0.003	0.036 ± 0.007
$t\bar{t}$	0.071 ± 0.008	0.127 ± 0.014	0.083 ± 0.009	0.281 ± 0.031
W γ	0.784 ± 0.058	0.693 ± 0.051	0.000 ± 0.000	1.477 ± 0.109
Drell-Yan $\ell\ell$	0.624 ± 0.156	0.253 ± 0.063	0.323 ± 0.081	1.200 ± 0.300
Fakes	0.617 ± 0.309	0.563 ± 0.281	0.327 ± 0.163	1.507 ± 0.754
Total Back	4.538 ± 0.428	6.562 ± 0.579	2.904 ± 0.283	14.005 ± 1.262
HWW	0.105 ± 0.006	0.225 ± 0.014	0.105 ± 0.006	0.436 ± 0.026
Data	4	5	5	14

Table 29: Summary of the signal and background expectations for a Higgs mass of 150 GeV, for 360 pb^{-1}. Also the observed number of events is shown. The error on luminosity it is not included.

160 GeV	ee	$e\mu$	$\mu\mu$	ll
WW	2.582 ± 0.271	5.017 ± 0.527	2.196 ± 0.231	9.794 ± 1.028
WZ	0.105 ± 0.014	0.161 ± 0.021	0.099 ± 0.013	0.365 ± 0.047
ZZ	0.012 ± 0.002	0.006 ± 0.001	0.018 ± 0.003	0.036 ± 0.007
$t\bar{t}$	0.098 ± 0.011	0.163 ± 0.018	0.088 ± 0.010	0.349 ± 0.038
W γ	0.691 ± 0.051	0.452 ± 0.033	0.000 ± 0.000	1.142 ± 0.084
Drell-Yan $\ell\ell$	0.315 ± 0.079	0.182 ± 0.046	0.266 ± 0.066	0.763 ± 0.191
Fakes	0.616 ± 0.308	0.482 ± 0.241	0.237 ± 0.118	1.334 ± 0.667
Total Back	4.418 ± 0.421	6.463 ± 0.583	2.903 ± 0.268	13.784 ± 1.245
HWW	0.138 ± 0.008	0.299 ± 0.018	0.141 ± 0.008	0.577 ± 0.035
Data	5	6	5	16

Table 30: Summary of the signal and background expectations for a Higgs mass of 160 GeV, for 360 pb^{-1}. Also the observed number of events is shown. The error on luminosity it is not included.

170 GeV	ee	$e\mu$	$\mu\mu$	ll
WW	2.708 ± 0.284	4.982 ± 0.523	2.277 ± 0.239	9.967 ± 1.046
WZ	0.105 ± 0.014	0.164 ± 0.021	0.110 ± 0.014	0.379 ± 0.049
ZZ	0.017 ± 0.003	0.008 ± 0.001	0.020 ± 0.004	0.044 ± 0.008
$t\bar{t}$	0.106 ± 0.012	0.195 ± 0.021	0.098 ± 0.011	0.399 ± 0.044
W γ	0.517 ± 0.038	0.452 ± 0.033	0.000 ± 0.000	0.969 ± 0.071
Drell-Yan $\ell\ell$	0.315 ± 0.079	0.246 ± 0.062	0.266 ± 0.066	0.827 ± 0.207
Fakes	0.572 ± 0.286	0.433 ± 0.217	0.237 ± 0.118	1.242 ± 0.621
Total Back	4.339 ± 0.413	6.479 ± 0.571	3.008 ± 0.276	13.826 ± 1.238
HWW	0.130 ± 0.008	0.277 ± 0.017	0.133 ± 0.008	0.541 ± 0.032
Data	5	7	6	18

Table 31: Summary of the signal and background expectations for a Higgs mass of 170 GeV, for 360 pb^{-1}. Also the observed number of events is shown. The error on luminosity it is not included.

180 GeV	ee	$e\mu$	$\mu\mu$	ll
WW	2.677 ± 0.281	4.995 ± 0.524	2.220 ± 0.233	9.892 ± 1.039
WZ	0.119 ± 0.015	0.179 ± 0.023	0.136 ± 0.018	0.433 ± 0.056
ZZ	0.026 ± 0.005	0.008 ± 0.001	0.028 ± 0.005	0.062 ± 0.012
$t\bar{t}$	0.124 ± 0.014	0.229 ± 0.025	0.107 ± 0.012	0.459 ± 0.050
W γ	0.436 ± 0.032	0.380 ± 0.028	0.000 ± 0.000	0.816 ± 0.060
Drell-Yan $\ell\ell$	0.315 ± 0.079	0.246 ± 0.062	0.266 ± 0.066	0.827 ± 0.207
Fakes	0.395 ± 0.197	0.263 ± 0.132	0.227 ± 0.113	0.884 ± 0.442
Total Back	4.091 ± 0.354	6.299 ± 0.546	2.983 ± 0.268	13.373 ± 1.152
HWW	0.100 ± 0.006	0.211 ± 0.013	0.098 ± 0.006	0.409 ± 0.025
Data	5	8	6	19

Table 32: Summary of the signal and background expectations for a Higgs mass of 180 GeV, for 360 pb^{-1}. Also the observed number of events is shown. The error on luminosity it is not included.

190 GeV	ee	$e\mu$	$\mu\mu$	ll
WW	2.639 ± 0.277	4.804 ± 0.504	2.180 ± 0.229	9.623 ± 1.010
WZ	0.193 ± 0.025	0.176 ± 0.023	0.208 ± 0.027	0.577 ± 0.075
ZZ	0.073 ± 0.014	0.008 ± 0.002	0.058 ± 0.011	0.139 ± 0.026
$t\bar{t}$	0.144 ± 0.016	0.247 ± 0.027	0.127 ± 0.014	0.518 ± 0.057
W γ	0.436 ± 0.032	0.218 ± 0.016	0.000 ± 0.000	0.654 ± 0.048
Drell-Yan $\ell\ell$	0.386 ± 0.097	0.263 ± 0.066	0.193 ± 0.048	0.843 ± 0.211
Fakes	0.312 ± 0.156	0.261 ± 0.130	0.227 ± 0.113	0.800 ± 0.400
Total Back	4.184 ± 0.336	5.977 ± 0.527	2.994 ± 0.262	13.154 ± 1.112
HWW	0.059 ± 0.004	0.123 ± 0.007	0.056 ± 0.003	0.238 ± 0.014
Data	5	8	6	19

Table 33: Summary of the signal and background expectations for a Higgs mass of 190 GeV, for 360 pb^{-1}. Also the observed number of events is shown. The error on luminosity it is not included.

200 GeV	ee	$e\mu$	$\mu\mu$	ll
WW	2.621 ± 0.275	4.484 ± 0.471	2.088 ± 0.219	9.193 ± 0.965
WZ	0.372 ± 0.048	0.161 ± 0.021	0.328 ± 0.043	0.860 ± 0.112
ZZ	0.167 ± 0.032	0.007 ± 0.001	0.128 ± 0.024	0.302 ± 0.057
$t\bar{t}$	0.151 ± 0.017	0.275 ± 0.030	0.150 ± 0.016	0.576 ± 0.063
W γ	0.259 ± 0.019	0.218 ± 0.016	0.000 ± 0.000	0.477 ± 0.035
Drell-Yan $\ell\ell$	0.305 ± 0.076	0.263 ± 0.066	0.390 ± 0.097	0.958 ± 0.239
Fakes	0.252 ± 0.126	0.253 ± 0.127	0.217 ± 0.108	0.722 ± 0.361
Total Back	4.128 ± 0.318	5.662 ± 0.494	3.299 ± 0.268	13.089 ± 1.068
HWW	0.053 ± 0.003	0.110 ± 0.007	0.051 ± 0.003	0.214 ± 0.013
Data	5	6	6	17

Table 34: Summary of the signal and background expectations for a Higgs mass of 200 GeV, for 360 pb^{-1}. Also the observed number of events is shown. The error on luminosity it is not included.

C Detailed acceptance tables

We present next the full tables of the number of data events after every selection cut, for all Higgs masses. Also we show the full tables for all backgrounds, for $M_H = 160$ GeV/c^2. For simplicity we introduce the notations: $M_u \equiv M_H/2 - 5$ GeV (the upper cut on $M_{\ell\ell}$.) and $H_T \equiv {p_T}^{\ell_1} + {p_T}^{\ell_2} + \not{E}_T$.

Table 35: data acceptance table, assuming $M_H^{\rm SM} = 130$ GeV

Category	Lepton ID	Lep1 Isol	Lep2 Isol	$M_{\ell\ell} > 16$	jet veto	opp sign	$\not\!\!E_t$	$\not\!\!E_t$ $\|\|$ $\Delta\phi$	$M_{\ell\ell} < M_H/2$	$p^1 p^2 \not\!\!E_t < M_H$
TCE-TCE	9493 0.10 ± 0.00	7991 84.18 ± 0.37	7288 91.20 ± 0.32	7195 98.72 ± 0.13	6969 96.86 ± 0.21	6959 99.86 ± 0.05	15 0.22 ± 0.06	9 60.00 ± 12.65	1 11.11 ± 10.48	1 100.00 ± 0.00
TCE-PHX	8804 0.09 ± 0.00	8275 93.99 ± 0.25	7922 95.73 ± 0.22	7920 99.97 ± 0.02	7729 97.59 ± 0.17	6837 88.46 ± 0.36	9 0.13 ± 0.04	7 77.78 ± 13.86	2 28.57 ± 17.07	1 50.00 ± 35.36
PHX-PHX	0 0.00 ± 0.00	0 0.00 ± 0.00	0 0.00 ± 0.00	0 0.00 ± 0.00	0 0.00 ± 0.00	0 0.00 ± 0.00	0 0.00 ± 0.00	0 0.00 ± 0.00	0 0.00 ± 0.00	0 0.00 ± 0.00
ee	18297 0.20 ± 0.00	16266 88.90 ± 0.23	15210 93.51 ± 0.19	15115 99.38 ± 0.06	14698 97.24 ± 0.13	13796 93.86 ± 0.20	24 0.17 ± 0.04	16 66.67 ± 9.62	3 18.75 ± 9.76	2 66.67 ± 27.22
TCE-CMUP	403 0.00 ± 0.00	86 21.34 ± 2.04	81 94.19 ± 2.52	79 97.53 ± 1.72	69 87.34 ± 3.74	68 98.55 ± 1.44	4 5.88 ± 2.85	4 100.00 ± 0.00	1 25.00 ± 21.65	1 100.00 ± 0.00
TCE-CMX	250 0.00 ± 0.00	48 19.20 ± 2.49	42 87.50 ± 4.77	42 100.00 ± 0.00	38 90.48 ± 4.53	37 97.37 ± 2.60	6 16.22 ± 6.06	6 100.00 ± 0.00	1 16.67 ± 15.21	1 100.00 ± 0.00
TCE-CMU	13 0.00 ± 0.00	8 61.54 ± 13.49	6 75.00 ± 15.31	6 100.00 ± 0.00	5 83.33 ± 15.21	5 100.00 ± 0.00	0 0.00 ± 0.00	0 0.00 ± 0.00	0 0.00 ± 0.00	0 0.00 ± 0.00
TCE-CMP	34 0.00 ± 0.00	12 35.29 ± 8.20	11 91.67 ± 7.98	11 100.00 ± 0.00	9 81.82 ± 11.63	9 100.00 ± 0.00	1 11.11 ± 10.48	1 100.00 ± 0.00	0 0.00 ± 0.00	0 0.00 ± 0.00
TCE-CMIO	419 0.00 ± 0.00	34 8.11 ± 1.33	31 91.18 ± 4.86	31 100.00 ± 0.00	29 93.55 ± 4.41	29 100.00 ± 0.00	6 20.69 ± 7.52	6 100.00 ± 0.00	2 33.33 ± 19.25	2 100.00 ± 0.00
PHX-CMUP	70 0.00 ± 0.00	22 31.43 ± 5.55	21 95.45 ± 4.44	21 100.00 ± 0.00	19 90.48 ± 6.41	10 52.63 ± 11.45	1 10.00 ± 9.49	1 100.00 ± 0.00	0 0.00 ± 0.00	0 0.00 ± 0.00
PHX-CMX	39 0.00 ± 0.00	17 43.59 ± 7.94	17 100.00 ± 0.00	17 100.00 ± 0.00	17 100.00 ± 0.00	11 64.71 ± 11.59	1 9.09 ± 8.67	0 0.00 ± 0.00	0 0.00 ± 0.00	0 0.00 ± 0.00
PHX-CMU	1 0.00 ± 0.00	0 0.00 ± 0.00	0 0.00 ± 0.00	0 0.00 ± 0.00	0 0.00 ± 0.00	0 0.00 ± 0.00	0 0.00 ± 0.00	0 0.00 ± 0.00	0 0.00 ± 0.00	0 0.00 ± 0.00
PHX-CMP	7 0.00 ± 0.00	2 28.57 ± 17.07	2 100.00 ± 0.00	2 100.00 ± 0.00	2 100.00 ± 0.00	2 100.00 ± 0.00	2 100.00 ± 0.00	2 100.00 ± 0.00	1 50.00 ± 35.36	1 100.00 ± 0.00
PHX-CMIO	42 0.00 ± 0.00	3 7.14 ± 3.97	3 100.00 ± 0.00	3 100.00 ± 0.00	2 66.67 ± 27.22	1 50.00 ± 35.36	1 100.00 ± 0.00	1 100.00 ± 0.00	1 100.00 ± 0.00	1 100.00 ± 0.00
$e\mu$	1278 0.01 ± 0.00	232 18.15 ± 1.08	214 92.24 ± 1.76	212 99.07 ± 0.66	190 89.62 ± 2.09	172 90.53 ± 2.12	22 12.79 ± 2.55	21 95.45 ± 4.44	6 28.57 ± 9.86	6 100.00 ± 0.00
CMUP-CMUP	2671 0.03 ± 0.00	2267 84.87 ± 0.69	2102 92.72 ± 0.55	2082 99.05 ± 0.21	2021 97.07 ± 0.37	2020 99.95 ± 0.05	3 0.15 ± 0.09	3 100.00 ± 0.00	1 33.33 ± 27.22	0 0.00 ± 0.00
CMUP-CMX	2507 0.03 ± 0.00	2286 91.18 ± 0.57	2247 98.29 ± 0.27	2234 99.42 ± 0.16	2158 96.60 ± 0.38	2157 99.95 ± 0.05	3 0.14 ± 0.08	3 100.00 ± 0.00	1 33.33 ± 27.22	0 0.00 ± 0.00
CMUP-CMU	831 0.01 ± 0.00	797 95.91 ± 0.69	785 98.49 ± 0.43	785 100.00 ± 0.00	762 97.07 ± 0.60	762 100.00 ± 0.00	0 0.00 ± 0.00	0 0.00 ± 0.00	0 0.00 ± 0.00	0 0.00 ± 0.00
CMUP-CMP	1132 0.01 ± 0.00	1047 92.49 ± 0.78	1012 96.66 ± 0.56	1011 99.90 ± 0.10	978 96.74 ± 0.56	978 100.00 ± 0.00	4 0.41 ± 0.20	2 50.00 ± 25.00	1 50.00 ± 35.36	0 0.00 ± 0.00
CMUP-CMIO	1956 0.02 ± 0.00	1677 85.74 ± 0.79	1614 96.24 ± 0.46	1592 98.64 ± 0.29	1533 96.29 ± 0.47	1533 100.00 ± 0.00	2 0.13 ± 0.09	2 100.00 ± 0.00	1 50.00 ± 35.36	1 100.00 ± 0.00
CMX-CMX	1114 0.01 ± 0.00	907 81.42 ± 1.17	796 87.76 ± 1.09	794 99.75 ± 0.18	774 97.48 ± 0.56	773 99.87 ± 0.13	0 0.00 ± 0.00	0 0.00 ± 0.00	0 0.00 ± 0.00	0 0.00 ± 0.00
CMX-CMU	474 0.01 ± 0.00	449 94.73 ± 1.03	436 97.10 ± 0.79	435 99.77 ± 0.23	428 98.39 ± 0.60	428 100.00 ± 0.00	0 0.00 ± 0.00	0 0.00 ± 0.00	0 0.00 ± 0.00	0 0.00 ± 0.00
CMX-CMP	524 0.01 ± 0.00	487 92.94 ± 1.12	480 98.56 ± 0.54	480 100.00 ± 0.00	465 96.88 ± 0.79	465 100.00 ± 0.00	0 0.00 ± 0.00	0 0.00 ± 0.00	0 0.00 ± 0.00	0 0.00 ± 0.00
CMX-CMIO	811 0.01 ± 0.00	685 84.46 ± 1.27	670 97.81 ± 0.56	666 99.40 ± 0.30	629 94.44 ± 0.89	629 100.00 ± 0.00	1 0.16 ± 0.16	1 100.00 ± 0.00	1 100.00 ± 0.00	0 0.00 ± 0.00
$\mu\mu$	12020 0.13 ± 0.00	10602 88.20 ± 0.29	10142 95.66 ± 0.20	10079 99.38 ± 0.08	9748 96.72 ± 0.18	9745 99.97 ± 0.02	13 0.13 ± 0.04	11 84.62 ± 10.01	5 45.45 ± 15.01	1 20.00 ± 17.89
total	31595 0.34 ± 0.00	27100 85.77 ± 0.20	25566 94.34 ± 0.14	25406 99.37 ± 0.05	24636 96.97 ± 0.11	23713 96.25 ± 0.12	59 0.25 ± 0.03	48 81.36 ± 5.07	14 29.17 ± 6.56	9 64.29 ± 12.81

Table 36: HWW acceptance table, assuming $M_H^{\rm SM} = 130$ GeV

Category	Lepton ID	Lep1 Isol	Lep2 Isol	$M_{\ell\ell} > 16$	jet veto	opp sign	$\not\!\!E_t$	$\not\!\!E_t$ $\|\|$ $\Delta\phi$	$M_{\ell\ell} < M_H/2$	$p^1 p^2 \not\!\!E_t < M_H$
TCE-TCE	18404	15291	13759	12603	11252	11242	8717	8455	7799	7398
	1.53 ± 0.01	83.09 ± 0.28	89.98 ± 0.24	91.60 ± 0.24	89.28 ± 0.28	99.91 ± 0.03	77.54 ± 0.39	96.99 ± 0.18	92.24 ± 0.29	94.86 ± 0.25
TCE-PHX	5804	5256	4956	4842	4385	4043	3234	3159	2774	2700
	0.48 ± 0.01	90.56 ± 0.38	94.29 ± 0.32	97.70 ± 0.21	90.56 ± 0.42	92.20 ± 0.40	79.99 ± 0.63	97.68 ± 0.26	87.81 ± 0.58	97.33 ± 0.31
PHX-PHX	0	0	0	0	0	0	0	0	0	0
	0.00 ± 0.00	0.00 ± 0.00	0.00 ± 0.00	0.00 ± 0.00	0.00 ± 0.00	0.00 ± 0.00	0.00 ± 0.00	0.00 ± 0.00	0.00 ± 0.00	0.00 ± 0.00
ee	24208	20547	18715	17445	15637	15285	11951	11614	10573	10098
	2.02 ± 0.01	84.88 ± 0.23	91.08 ± 0.20	93.21 ± 0.18	89.64 ± 0.23	97.75 ± 0.12	78.19 ± 0.33	97.18 ± 0.15	91.04 ± 0.27	95.51 ± 0.20
TCE-CMUP	23281	19489	18016	16388	14551	14546	11160	10836	10092	9599
	1.94 ± 0.01	83.71 ± 0.24	92.44 ± 0.19	90.96 ± 0.21	88.79 ± 0.25	99.97 ± 0.02	76.72 ± 0.35	97.10 ± 0.16	93.13 ± 0.24	95.11 ± 0.21
TCE-CMX	10050	8456	7822	7241	6507	6505	4974	4843	4469	4289
	0.84 ± 0.01	84.14 ± 0.36	92.50 ± 0.29	92.57 ± 0.30	89.86 ± 0.35	99.97 ± 0.02	76.46 ± 0.53	97.37 ± 0.23	92.28 ± 0.38	95.97 ± 0.29
TCE-CMU	2370	2032	1908	1823	1555	1555	1232	1193	1064	994
	0.20 ± 0.00	85.74 ± 0.72	93.90 ± 0.53	95.55 ± 0.47	85.30 ± 0.83	100.00 ± 0.00	79.23 ± 1.03	96.83 ± 0.50	89.19 ± 0.90	93.42 ± 0.76
TCE-CMP	3513	3017	2823	2677	2319	2319	1812	1754	1561	1460
	0.29 ± 0.00	85.88 ± 0.59	93.57 ± 0.45	94.83 ± 0.42	86.63 ± 0.66	100.00 ± 0.00	78.14 ± 0.86	96.80 ± 0.41	89.00 ± 0.75	93.53 ± 0.62
TCE-CMIO	6608	5511	5091	4677	4206	4204	3183	3089	2854	2741
	0.55 ± 0.01	83.40 ± 0.46	92.38 ± 0.36	91.87 ± 0.38	89.93 ± 0.44	99.95 ± 0.03	75.71 ± 0.66	97.05 ± 0.30	92.39 ± 0.48	96.04 ± 0.37
PHX-CMUP	2854	2632	2574	2571	2348	2149	1651	1616	1385	1365
	0.24 ± 0.00	92.22 ± 0.50	97.80 ± 0.29	99.88 ± 0.07	91.33 ± 0.56	91.52 ± 0.57	76.83 ± 0.91	97.88 ± 0.35	85.71 ± 0.87	98.56 ± 0.32
PHX-CMX	2215	2033	1989	1883	1704	1572	1257	1214	1088	1028
	0.18 ± 0.00	91.78 ± 0.58	97.84 ± 0.32	94.67 ± 0.50	90.49 ± 0.68	92.25 ± 0.65	79.96 ± 1.01	96.58 ± 0.51	89.62 ± 0.88	94.49 ± 0.69
PHX-CMU	402	384	381	380	344	310	272	265	222	221
	0.03 ± 0.00	95.52 ± 1.03	99.22 ± 0.45	99.74 ± 0.26	90.53 ± 1.50	90.12 ± 1.61	87.74 ± 1.86	97.43 ± 0.96	83.77 ± 2.26	99.55 ± 0.45
PHX-CMP	414	395	391	391	352	334	283	278	230	228
	0.03 ± 0.00	95.41 ± 1.03	98.99 ± 0.50	100.00 ± 0.00	90.03 ± 1.52	94.89 ± 1.17	84.73 ± 1.97	98.23 ± 0.78	82.73 ± 2.27	99.13 ± 0.61
PHX-CMIO	1551	1426	1386	1347	1226	1120	959	935	839	810
	0.13 ± 0.00	91.94 ± 0.69	97.19 ± 0.44	97.19 ± 0.44	91.02 ± 0.78	91.35 ± 0.80	85.62 ± 1.05	97.50 ± 0.50	89.73 ± 0.99	96.54 ± 0.63
$e\mu$	53258	45375	42381	39378	35112	34614	26783	26023	23804	22735
	4.44 ± 0.02	85.20 ± 0.15	93.40 ± 0.12	92.91 ± 0.12	89.17 ± 0.16	98.58 ± 0.06	77.38 ± 0.22	97.16 ± 0.10	91.47 ± 0.17	95.51 ± 0.13
CMUP-CMUP	7414	6406	5785	5149	4577	4577	3417	3317	3081	2930
	0.62 ± 0.01	86.40 ± 0.40	90.31 ± 0.37	89.01 ± 0.41	88.89 ± 0.44	100.00 ± 0.00	74.66 ± 0.64	97.07 ± 0.29	92.89 ± 0.45	95.10 ± 0.39
CMUP-CMX	6008	5426	5164	4876	4328	4328	3265	3180	2949	2879
	0.50 ± 0.01	90.31 ± 0.38	95.17 ± 0.29	94.42 ± 0.32	88.76 ± 0.45	100.00 ± 0.00	75.44 ± 0.65	97.40 ± 0.28	92.74 ± 0.46	97.63 ± 0.28
CMUP-CMU	1559	1418	1319	1263	1091	1091	855	832	742	699
	0.13 ± 0.00	90.96 ± 0.73	93.02 ± 0.68	95.75 ± 0.56	86.38 ± 0.97	100.00 ± 0.00	78.37 ± 1.25	97.31 ± 0.55	89.18 ± 1.08	94.20 ± 0.86
CMUP-CMP	2386	2137	1927	1792	1547	1547	1201	1171	1028	963
	0.20 ± 0.00	89.56 ± 0.63	90.17 ± 0.64	92.99 ± 0.58	86.33 ± 0.81	100.00 ± 0.00	77.63 ± 1.06	97.50 ± 0.45	87.79 ± 0.96	93.68 ± 0.76
CMUP-CMIO	4349	3793	3572	3250	2921	2921	2129	2074	1944	1880
	0.36 ± 0.01	87.22 ± 0.51	94.17 ± 0.38	90.99 ± 0.48	89.88 ± 0.53	100.00 ± 0.00	72.89 ± 0.82	97.42 ± 0.34	93.73 ± 0.53	96.71 ± 0.40
CMX-CMX	1484	1226	1044	931	842	842	597	573	519	492
	0.12 ± 0.00	82.61 ± 0.98	85.15 ± 1.02	89.18 ± 0.96	90.44 ± 0.96	100.00 ± 0.00	70.90 ± 1.57	95.98 ± 0.80	90.58 ± 1.22	94.80 ± 0.97
CMX-CMU	538	481	435	397	342	342	264	255	217	210
	0.04 ± 0.00	89.41 ± 1.33	90.44 ± 1.34	91.26 ± 1.35	86.15 ± 1.73	100.00 ± 0.00	77.19 ± 2.27	96.59 ± 1.12	85.10 ± 2.23	96.77 ± 1.20
CMX-CMP	794	735	694	678	589	589	467	453	387	375
	0.07 ± 0.00	92.57 ± 0.93	94.42 ± 0.85	97.69 ± 0.57	86.87 ± 1.30	100.00 ± 0.00	79.29 ± 1.67	97.00 ± 0.79	85.43 ± 1.66	96.90 ± 0.88
CMX-CMIO	1539	1340	1250	1162	1036	1036	741	721	662	642
	0.13 ± 0.00	87.07 ± 0.86	93.28 ± 0.68	92.96 ± 0.72	89.16 ± 0.91	100.00 ± 0.00	71.53 ± 1.40	97.30 ± 0.60	91.82 ± 1.02	96.98 ± 0.67
$\mu\mu$	26071	22962	21190	19498	17273	17273	12936	12576	11529	11070
	2.17 ± 0.01	88.07 ± 0.20	92.28 ± 0.18	92.02 ± 0.19	88.59 ± 0.23	100.00 ± 0.00	74.89 ± 0.33	97.22 ± 0.14	91.67 ± 0.25	96.02 ± 0.18
total	103537	88884	82286	76321	68022	67172	51670	50213	45906	43903
	8.63 ± 0.03	85.85 ± 0.11	92.58 ± 0.09	92.75 ± 0.09	89.13 ± 0.11	98.75 ± 0.04	76.92 ± 0.16	97.18 ± 0.07	91.42 ± 0.12	95.64 ± 0.10

Table 37: data acceptance table, assuming $M_H^{\rm SM} = 140$ GeV

Category	Lepton ID	Lep1 Isol	Lep2 Isol	$M_{\ell\ell} > 16$	jet veto	opp sign	$\not\!\!E_t$	$\not\!\!E_t$ || $\Delta\phi$	$M_{\ell\ell} < M_H/2$	$p^1 p^2 \not\!\!E_t < M_H$
TCE-TCE	9493	7991	7288	7195	6969	6959	12	8	2	1
	0.10 ± 0.00	84.18 ± 0.37	91.20 ± 0.32	98.72 ± 0.13	96.86 ± 0.21	99.86 ± 0.05	0.17 ± 0.05	66.67 ± 13.61	25.00 ± 15.31	50.00 ± 35.36
TCE-PHX	8804	8275	7922	7920	7729	6837	8	7	4	3
	0.09 ± 0.00	93.99 ± 0.25	95.73 ± 0.22	99.97 ± 0.02	97.59 ± 0.17	88.46 ± 0.36	0.12 ± 0.04	87.50 ± 11.69	57.14 ± 18.70	75.00 ± 21.65
PHX-PHX	0	0	0	0	0	0	0	0	0	0
	0.00 ± 0.00	0.00 ± 0.00	0.00 ± 0.00	0.00 ± 0.00	0.00 ± 0.00	0.00 ± 0.00	0.00 ± 0.00	0.00 ± 0.00	0.00 ± 0.00	0.00 ± 0.00
ee	18297	16266	15210	15115	14698	13796	20	15	6	4
	0.20 ± 0.00	88.90 ± 0.23	93.51 ± 0.19	99.38 ± 0.06	97.24 ± 0.13	93.86 ± 0.20	0.14 ± 0.03	75.00 ± 9.68	40.00 ± 12.65	66.67 ± 19.25
TCE-CMUP	403	86	81	79	69	68	4	4	2	1
	0.00 ± 0.00	21.34 ± 2.04	94.19 ± 2.52	97.53 ± 1.72	87.34 ± 3.74	98.55 ± 1.44	5.88 ± 2.85	100.00 ± 0.00	50.00 ± 25.00	50.00 ± 35.36
TCE-CMX	250	48	42	42	38	37	5	5	2	2
	0.00 ± 0.00	19.20 ± 2.49	87.50 ± 4.77	100.00 ± 0.00	90.48 ± 4.53	97.37 ± 2.60	13.51 ± 5.62	100.00 ± 0.00	40.00 ± 21.91	100.00 ± 0.00
TCE-CMU	13	8	6	6	5	5	0	0	0	0
	0.00 ± 0.00	61.54 ± 13.49	75.00 ± 15.31	100.00 ± 0.00	83.33 ± 15.21	100.00 ± 0.00	0.00 ± 0.00	0.00 ± 0.00	0.00 ± 0.00	0.00 ± 0.00
TCE-CMP	34	12	11	11	9	9	1	1	0	0
	0.00 ± 0.00	35.29 ± 8.20	91.67 ± 7.98	100.00 ± 0.00	81.82 ± 11.63	100.00 ± 0.00	11.11 ± 10.48	100.00 ± 0.00	0.00 ± 0.00	0.00 ± 0.00
TCE-CMIO	419	34	31	31	29	29	4	4	2	1
	0.00 ± 0.00	8.11 ± 1.33	91.18 ± 4.86	100.00 ± 0.00	93.55 ± 4.41	100.00 ± 0.00	13.79 ± 6.40	100.00 ± 0.00	50.00 ± 25.00	50.00 ± 35.36
PHX-CMUP	70	22	21	21	19	10	1	1	0	0
	0.00 ± 0.00	31.43 ± 5.55	95.45 ± 4.44	100.00 ± 0.00	90.48 ± 6.41	52.63 ± 11.45	10.00 ± 9.49	100.00 ± 0.00	0.00 ± 0.00	0.00 ± 0.00
PHX-CMX	39	17	17	17	17	11	1	0	0	0
	0.00 ± 0.00	43.59 ± 7.94	100.00 ± 0.00	100.00 ± 0.00	100.00 ± 0.00	64.71 ± 11.59	9.09 ± 8.67	0.00 ± 0.00	0.00 ± 0.00	0.00 ± 0.00
PHX-CMU	1	0	0	0	0	0	0	0	0	0
	0.00 ± 0.00	0.00 ± 0.00	0.00 ± 0.00	0.00 ± 0.00	0.00 ± 0.00	0.00 ± 0.00	0.00 ± 0.00	0.00 ± 0.00	0.00 ± 0.00	0.00 ± 0.00
PHX-CMP	7	2	2	2	2	2	2	2	1	1
	0.00 ± 0.00	28.57 ± 17.07	100.00 ± 0.00	100.00 ± 0.00	100.00 ± 0.00	100.00 ± 0.00	100.00 ± 0.00	100.00 ± 0.00	50.00 ± 35.36	100.00 ± 0.00
PHX-CMIO	42	3	3	3	2	1	1	1	1	1
	0.00 ± 0.00	7.14 ± 3.97	100.00 ± 0.00	100.00 ± 0.00	66.67 ± 27.22	50.00 ± 35.36	100.00 ± 0.00	100.00 ± 0.00	100.00 ± 0.00	100.00 ± 0.00
$e\mu$	1278	232	214	212	190	172	19	18	8	6
	0.01 ± 0.00	18.15 ± 1.08	92.24 ± 1.76	99.07 ± 0.66	89.62 ± 2.09	90.53 ± 2.12	11.05 ± 2.39	94.74 ± 5.12	44.44 ± 11.71	75.00 ± 15.31
CMUP-CMUP	2671	2267	2102	2082	2021	2020	3	3	2	2
	0.03 ± 0.00	84.87 ± 0.69	92.72 ± 0.55	99.05 ± 0.21	97.07 ± 0.37	99.95 ± 0.05	0.15 ± 0.09	100.00 ± 0.00	66.67 ± 27.22	100.00 ± 0.00
CMUP-CMX	2507	2286	2247	2234	2158	2157	3	3	2	1
	0.03 ± 0.00	91.18 ± 0.57	98.29 ± 0.27	99.42 ± 0.16	96.60 ± 0.38	99.95 ± 0.05	0.14 ± 0.08	100.00 ± 0.00	66.67 ± 27.22	50.00 ± 35.36
CMUP-CMU	831	797	785	785	762	762	0	0	0	0
	0.01 ± 0.00	95.91 ± 0.69	98.49 ± 0.43	100.00 ± 0.00	97.07 ± 0.60	100.00 ± 0.00	0.00 ± 0.00	0.00 ± 0.00	0.00 ± 0.00	0.00 ± 0.00
CMUP-CMP	1132	1047	1012	1011	978	978	3	1	1	0
	0.01 ± 0.00	92.49 ± 0.78	96.66 ± 0.56	99.90 ± 0.10	96.74 ± 0.56	100.00 ± 0.00	0.31 ± 0.18	33.33 ± 27.22	100.00 ± 0.00	0.00 ± 0.00
CMUP-CMIO	1956	1677	1614	1592	1533	1533	2	2	1	1
	0.02 ± 0.00	85.74 ± 0.79	96.24 ± 0.46	98.64 ± 0.29	96.29 ± 0.47	100.00 ± 0.00	0.13 ± 0.09	100.00 ± 0.00	50.00 ± 35.36	100.00 ± 0.00
CMX-CMX	1114	907	796	794	774	773	0	0	0	0
	0.01 ± 0.00	81.42 ± 1.17	87.76 ± 1.09	99.75 ± 0.18	97.48 ± 0.56	99.87 ± 0.13	0.00 ± 0.00	0.00 ± 0.00	0.00 ± 0.00	0.00 ± 0.00
CMX-CMU	474	449	436	435	428	428	0	0	0	0
	0.01 ± 0.00	94.73 ± 1.03	97.10 ± 0.79	99.77 ± 0.23	98.39 ± 0.60	100.00 ± 0.00	0.00 ± 0.00	0.00 ± 0.00	0.00 ± 0.00	0.00 ± 0.00
CMX-CMP	524	487	480	480	465	465	0	0	0	0
	0.01 ± 0.00	92.94 ± 1.12	98.56 ± 0.54	100.00 ± 0.00	96.88 ± 0.79	100.00 ± 0.00	0.00 ± 0.00	0.00 ± 0.00	0.00 ± 0.00	0.00 ± 0.00
CMX-CMIO	811	685	670	666	629	629	1	1	1	0
	0.01 ± 0.00	84.46 ± 1.27	97.81 ± 0.56	99.40 ± 0.30	94.44 ± 0.89	100.00 ± 0.00	0.16 ± 0.16	100.00 ± 0.00	100.00 ± 0.00	0.00 ± 0.00
$\mu\mu$	12020	10602	10142	10079	9748	9745	12	10	7	4
	0.13 ± 0.00	88.20 ± 0.29	95.66 ± 0.20	99.38 ± 0.08	96.72 ± 0.18	99.97 ± 0.02	0.12 ± 0.04	83.33 ± 10.76	70.00 ± 14.49	57.14 ± 18.70
total	31595	27100	25566	25406	24636	23713	51	43	21	14
	0.34 ± 0.00	85.77 ± 0.20	94.34 ± 0.14	99.37 ± 0.05	96.97 ± 0.11	96.25 ± 0.12	0.22 ± 0.03	84.31 ± 5.09	48.84 ± 7.62	66.67 ± 10.29

Table 38: data acceptance table, assuming $M_H^{\rm SM} = 150$ GeV

Category	Lepton ID	Lep1 Isol	Lep2 Isol	$M_{\ell\ell} > 16$	jet veto	opp sign	$\not\!\!E_t$	$\not\!\!E_t$ || $\Delta\phi$	$M_{\ell\ell} < M_H/2$	$p^1 p^2 \not\!\!E_t < M_H$
TCE-TCE	9493	7991	7288	7195	6969	6959	9	7	3	2
	0.10 ± 0.00	84.18 ± 0.37	91.20 ± 0.32	98.72 ± 0.13	96.86 ± 0.21	99.86 ± 0.05	0.13 ± 0.04	77.78 ± 13.86	42.86 ± 18.70	66.67 ± 27.22
TCE-PHX	8804	8275	7922	7920	7729	6837	5	5	3	2
	0.09 ± 0.00	93.99 ± 0.25	95.73 ± 0.22	99.97 ± 0.02	97.59 ± 0.17	88.46 ± 0.36	0.07 ± 0.03	100.00 ± 0.00	60.00 ± 21.91	66.67 ± 27.22
PHX-PHX	0	0	0	0	0	0	0	0	0	0
	0.00 ± 0.00	0.00 ± 0.00	0.00 ± 0.00	0.00 ± 0.00	0.00 ± 0.00	0.00 ± 0.00	0.00 ± 0.00	0.00 ± 0.00	0.00 ± 0.00	0.00 ± 0.00
ee	18297	16266	15210	15115	14698	13796	14	12	6	4
	0.20 ± 0.00	88.90 ± 0.23	93.51 ± 0.19	99.38 ± 0.06	97.24 ± 0.13	93.86 ± 0.20	0.10 ± 0.03	85.71 ± 9.35	50.00 ± 14.43	66.67 ± 19.25
TCE-CMUP	403	86	81	79	69	68	3	3	1	0
	0.00 ± 0.00	21.34 ± 2.04	94.19 ± 2.52	97.53 ± 1.72	87.34 ± 3.74	98.55 ± 1.44	4.41 ± 2.49	100.00 ± 0.00	33.33 ± 27.22	0.00 ± 0.00
TCE-CMX	250	48	42	42	38	37	4	4	2	2
	0.00 ± 0.00	19.20 ± 2.49	87.50 ± 4.77	100.00 ± 0.00	90.48 ± 4.53	97.37 ± 2.60	10.81 ± 5.10	100.00 ± 0.00	50.00 ± 25.00	100.00 ± 0.00
TCE-CMU	13	8	6	6	5	5	0	0	0	0
	0.00 ± 0.00	61.54 ± 13.49	75.00 ± 15.31	100.00 ± 0.00	83.33 ± 15.21	100.00 ± 0.00	0.00 ± 0.00	0.00 ± 0.00	0.00 ± 0.00	0.00 ± 0.00
TCE-CMP	34	12	11	11	9	9	1	1	0	0
	0.00 ± 0.00	35.29 ± 8.20	91.67 ± 7.98	100.00 ± 0.00	81.82 ± 11.63	100.00 ± 0.00	11.11 ± 10.48	100.00 ± 0.00	0.00 ± 0.00	0.00 ± 0.00
TCE-CMIO	419	34	31	31	29	29	4	4	3	1
	0.00 ± 0.00	8.11 ± 1.33	91.18 ± 4.86	100.00 ± 0.00	93.55 ± 4.41	100.00 ± 0.00	13.79 ± 6.40	100.00 ± 0.00	75.00 ± 21.65	33.33 ± 27.22
PHX-CMUP	70	22	21	21	19	10	1	1	0	0
	0.00 ± 0.00	31.43 ± 5.55	95.45 ± 4.44	100.00 ± 0.00	90.48 ± 6.41	52.63 ± 11.45	10.00 ± 9.49	100.00 ± 0.00	0.00 ± 0.00	0.00 ± 0.00
PHX-CMX	39	17	17	17	17	11	1	0	0	0
	0.00 ± 0.00	43.59 ± 7.94	100.00 ± 0.00	100.00 ± 0.00	100.00 ± 0.00	64.71 ± 11.59	9.09 ± 8.67	0.00 ± 0.00	0.00 ± 0.00	0.00 ± 0.00
PHX-CMU	1	0	0	0	0	0	0	0	0	0
	0.00 ± 0.00	0.00 ± 0.00	0.00 ± 0.00	0.00 ± 0.00	0.00 ± 0.00	0.00 ± 0.00	0.00 ± 0.00	0.00 ± 0.00	0.00 ± 0.00	0.00 ± 0.00
PHX-CMP	7	2	2	2	2	2	2	2	1	1
	0.00 ± 0.00	28.57 ± 17.07	100.00 ± 0.00	100.00 ± 0.00	100.00 ± 0.00	100.00 ± 0.00	100.00 ± 0.00	100.00 ± 0.00	50.00 ± 35.36	100.00 ± 0.00
PHX-CMIO	42	3	3	3	2	1	1	1	1	1
	0.00 ± 0.00	7.14 ± 3.97	100.00 ± 0.00	100.00 ± 0.00	66.67 ± 27.22	50.00 ± 35.36	100.00 ± 0.00	100.00 ± 0.00	100.00 ± 0.00	100.00 ± 0.00
$e\mu$	1278	232	214	212	190	172	17	16	8	5
	0.01 ± 0.00	18.15 ± 1.08	92.24 ± 1.76	99.07 ± 0.66	89.62 ± 2.09	90.53 ± 2.12	9.88 ± 2.28	94.12 ± 5.71	50.00 ± 12.50	62.50 ± 17.12
CMUP-CMUP	2671	2267	2102	2082	2021	2020	3	3	2	2
	0.03 ± 0.00	84.87 ± 0.69	92.72 ± 0.55	99.05 ± 0.21	97.07 ± 0.37	99.95 ± 0.05	0.15 ± 0.09	100.00 ± 0.00	66.67 ± 27.22	100.00 ± 0.00
CMUP-CMX	2507	2286	2247	2234	2158	2157	3	3	3	2
	0.03 ± 0.00	91.18 ± 0.57	98.29 ± 0.27	99.42 ± 0.16	96.60 ± 0.38	99.95 ± 0.05	0.14 ± 0.08	100.00 ± 0.00	100.00 ± 0.00	66.67 ± 27.22
CMUP-CMU	831	797	785	785	762	762	0	0	0	0
	0.01 ± 0.00	95.91 ± 0.69	98.49 ± 0.43	100.00 ± 0.00	97.07 ± 0.60	100.00 ± 0.00	0.00 ± 0.00	0.00 ± 0.00	0.00 ± 0.00	0.00 ± 0.00
CMUP-CMP	1132	1047	1012	1011	978	978	3	1	1	0
	0.01 ± 0.00	92.49 ± 0.78	96.66 ± 0.56	99.90 ± 0.10	96.74 ± 0.56	100.00 ± 0.00	0.31 ± 0.18	33.33 ± 27.22	100.00 ± 0.00	0.00 ± 0.00
CMUP-CMIO	1956	1677	1614	1592	1533	1533	2	2	1	1
	0.02 ± 0.00	85.74 ± 0.79	96.24 ± 0.46	98.64 ± 0.29	96.29 ± 0.47	100.00 ± 0.00	0.13 ± 0.09	100.00 ± 0.00	50.00 ± 35.36	100.00 ± 0.00
CMX-CMX	1114	907	796	794	774	773	0	0	0	0
	0.01 ± 0.00	81.42 ± 1.17	87.76 ± 1.09	99.75 ± 0.18	97.48 ± 0.56	99.87 ± 0.13	0.00 ± 0.00	0.00 ± 0.00	0.00 ± 0.00	0.00 ± 0.00
CMX-CMU	474	449	436	435	428	428	0	0	0	0
	0.01 ± 0.00	94.73 ± 1.03	97.10 ± 0.79	99.77 ± 0.23	98.39 ± 0.60	100.00 ± 0.00	0.00 ± 0.00	0.00 ± 0.00	0.00 ± 0.00	0.00 ± 0.00
CMX-CMP	524	487	480	480	465	465	0	0	0	0
	0.01 ± 0.00	92.94 ± 1.12	98.56 ± 0.54	100.00 ± 0.00	96.88 ± 0.79	100.00 ± 0.00	0.00 ± 0.00	0.00 ± 0.00	0.00 ± 0.00	0.00 ± 0.00
CMX-CMIO	811	685	670	666	629	629	1	1	1	0
	0.01 ± 0.00	84.46 ± 1.27	97.81 ± 0.56	99.40 ± 0.30	94.44 ± 0.89	100.00 ± 0.00	0.16 ± 0.16	100.00 ± 0.00	100.00 ± 0.00	0.00 ± 0.00
$\mu\mu$	12020	10602	10142	10079	9748	9745	12	10	8	5
	0.13 ± 0.00	88.20 ± 0.29	95.66 ± 0.20	99.38 ± 0.08	96.72 ± 0.18	99.97 ± 0.02	0.12 ± 0.04	83.33 ± 10.76	80.00 ± 12.65	62.50 ± 17.12
total	31595	27100	25566	25406	24636	23713	43	38	22	14
	0.34 ± 0.00	85.77 ± 0.20	94.34 ± 0.14	99.37 ± 0.05	96.97 ± 0.11	96.25 ± 0.12	0.18 ± 0.03	88.37 ± 4.89	57.89 ± 8.01	63.64 ± 10.26

Table 39: data acceptance table, assuming $M_H^{\rm SM} = 160$ GeV

Category	Lepton ID	Lep1 Isol	Lep2 Isol	$M_{\ell\ell} > 16$	jet veto	opp sign	$\not\!\!E_t$	$\not\!\!E_t$ $\|\|$ $\Delta\phi$	$M_{\ell\ell} < M_H/2$	$p^1 p^2 \not\!\!E_t < M_H$
TCE-TCE	9493 0.10 ± 0.00	7991 84.18 ± 0.37	7288 91.20 ± 0.32	7195 98.72 ± 0.13	6969 96.86 ± 0.21	6959 99.86 ± 0.05	7 0.10 ± 0.04	5 71.43 ± 17.07	3 60.00 ± 21.91	3 100.00 ± 0.00
TCE-PHX	8804 0.09 ± 0.00	8275 93.99 ± 0.25	7922 95.73 ± 0.22	7920 99.97 ± 0.02	7729 97.59 ± 0.17	6837 88.46 ± 0.36	5 0.07 ± 0.03	5 100.00 ± 0.00	3 60.00 ± 21.91	2 66.67 ± 27.22
PHX-PHX	0 0.00 ± 0.00	0 0.00 ± 0.00	0 0.00 ± 0.00	0 0.00 ± 0.00	0 0.00 ± 0.00	0 0.00 ± 0.00	0 0.00 ± 0.00	0 0.00 ± 0.00	0 0.00 ± 0.00	0 0.00 ± 0.00
ee	18297 0.20 ± 0.00	16266 88.90 ± 0.23	15210 93.51 ± 0.19	15115 99.38 ± 0.06	14698 97.24 ± 0.13	13796 93.86 ± 0.20	12 0.09 ± 0.03	10 83.33 ± 10.76	6 60.00 ± 15.49	5 83.33 ± 15.21
TCE-CMUP	403 0.00 ± 0.00	86 21.34 ± 2.04	81 94.19 ± 2.52	79 97.53 ± 1.72	69 87.34 ± 3.74	68 98.55 ± 1.44	3 4.41 ± 2.49	3 100.00 ± 0.00	2 66.67 ± 27.22	1 50.00 ± 35.36
TCE-CMX	250 0.00 ± 0.00	48 19.20 ± 2.49	42 87.50 ± 4.77	42 100.00 ± 0.00	38 90.48 ± 4.53	37 97.37 ± 2.60	4 10.81 ± 5.10	4 100.00 ± 0.00	2 50.00 ± 25.00	2 100.00 ± 0.00
TCE-CMU	13 0.00 ± 0.00	8 61.54 ± 13.49	6 75.00 ± 15.31	6 100.00 ± 0.00	5 83.33 ± 15.21	5 100.00 ± 0.00	0 0.00 ± 0.00	0 0.00 ± 0.00	0 0.00 ± 0.00	0 0.00 ± 0.00
TCE-CMP	34 0.00 ± 0.00	12 35.29 ± 8.20	11 91.67 ± 7.98	11 100.00 ± 0.00	9 81.82 ± 11.63	9 100.00 ± 0.00	1 11.11 ± 10.48	1 100.00 ± 0.00	0 0.00 ± 0.00	0 0.00 ± 0.00
TCE-CMIO	419 0.00 ± 0.00	34 8.11 ± 1.33	31 91.18 ± 4.86	31 100.00 ± 0.00	29 93.55 ± 4.41	29 100.00 ± 0.00	3 10.34 ± 5.66	3 100.00 ± 0.00	2 66.67 ± 27.22	1 50.00 ± 35.36
PHX-CMUP	70 0.00 ± 0.00	22 31.43 ± 5.55	21 95.45 ± 4.44	21 100.00 ± 0.00	19 90.48 ± 6.41	10 52.63 ± 11.45	1 10.00 ± 9.49	1 100.00 ± 0.00	0 0.00 ± 0.00	0 0.00 ± 0.00
PHX-CMX	39 0.00 ± 0.00	17 43.59 ± 7.94	17 100.00 ± 0.00	17 100.00 ± 0.00	17 100.00 ± 0.00	11 64.71 ± 11.59	0 0.00 ± 0.00	0 0.00 ± 0.00	0 0.00 ± 0.00	0 0.00 ± 0.00
PHX-CMU	1 0.00 ± 0.00	0 0.00 ± 0.00	0 0.00 ± 0.00	0 0.00 ± 0.00	0 0.00 ± 0.00	0 0.00 ± 0.00	0 0.00 ± 0.00	0 0.00 ± 0.00	0 0.00 ± 0.00	0 0.00 ± 0.00
PHX-CMP	7 0.00 ± 0.00	2 28.57 ± 17.07	2 100.00 ± 0.00	2 100.00 ± 0.00	2 100.00 ± 0.00	2 100.00 ± 0.00	2 100.00 ± 0.00	2 100.00 ± 0.00	1 50.00 ± 35.36	1 100.00 ± 0.00
PHX-CMIO	42 0.00 ± 0.00	3 7.14 ± 3.97	3 100.00 ± 0.00	3 100.00 ± 0.00	2 66.67 ± 27.22	1 50.00 ± 35.36	1 100.00 ± 0.00	1 100.00 ± 0.00	1 100.00 ± 0.00	1 100.00 ± 0.00
$e\mu$	1278 0.01 ± 0.00	232 18.15 ± 1.08	214 92.24 ± 1.76	212 99.07 ± 0.66	190 89.62 ± 2.09	172 90.53 ± 2.12	15 8.72 ± 2.15	15 100.00 ± 0.00	8 53.33 ± 12.88	6 75.00 ± 15.31
CMUP-CMUP	2671 0.03 ± 0.00	2267 84.87 ± 0.69	2102 92.72 ± 0.55	2082 99.05 ± 0.21	2021 97.07 ± 0.37	2020 99.95 ± 0.05	3 0.15 ± 0.09	3 100.00 ± 0.00	3 100.00 ± 0.00	3 100.00 ± 0.00
CMUP-CMX	2507 0.03 ± 0.00	2286 91.18 ± 0.57	2247 98.29 ± 0.27	2234 99.42 ± 0.16	2158 96.60 ± 0.38	2157 99.95 ± 0.05	2 0.09 ± 0.07	2 100.00 ± 0.00	2 100.00 ± 0.00	1 50.00 ± 35.36
CMUP-CMU	831 0.01 ± 0.00	797 95.91 ± 0.69	785 98.49 ± 0.43	785 100.00 ± 0.00	762 97.07 ± 0.60	762 100.00 ± 0.00	0 0.00 ± 0.00	0 0.00 ± 0.00	0 0.00 ± 0.00	0 0.00 ± 0.00
CMUP-CMP	1132 0.01 ± 0.00	1047 92.49 ± 0.78	1012 96.66 ± 0.56	1011 99.90 ± 0.10	978 96.74 ± 0.56	978 100.00 ± 0.00	2 0.20 ± 0.14	1 50.00 ± 35.36	1 100.00 ± 0.00	0 0.00 ± 0.00
CMUP-CMIO	1956 0.02 ± 0.00	1677 85.74 ± 0.79	1614 96.24 ± 0.46	1592 98.64 ± 0.29	1533 96.29 ± 0.47	1533 100.00 ± 0.00	2 0.13 ± 0.09	2 100.00 ± 0.00	1 50.00 ± 35.36	1 100.00 ± 0.00
CMX-CMX	1114 0.01 ± 0.00	907 81.42 ± 1.17	796 87.76 ± 1.09	794 99.75 ± 0.18	774 97.48 ± 0.56	773 99.87 ± 0.13	0 0.00 ± 0.00	0 0.00 ± 0.00	0 0.00 ± 0.00	0 0.00 ± 0.00
CMX-CMU	474 0.01 ± 0.00	449 94.73 ± 1.03	436 97.10 ± 0.79	435 99.77 ± 0.23	428 98.39 ± 0.60	428 100.00 ± 0.00	0 0.00 ± 0.00	0 0.00 ± 0.00	0 0.00 ± 0.00	0 0.00 ± 0.00
CMX-CMP	524 0.01 ± 0.00	487 92.94 ± 1.12	480 98.56 ± 0.54	480 100.00 ± 0.00	465 96.88 ± 0.79	465 100.00 ± 0.00	0 0.00 ± 0.00	0 0.00 ± 0.00	0 0.00 ± 0.00	0 0.00 ± 0.00
CMX-CMIO	811 0.01 ± 0.00	685 84.46 ± 1.27	670 97.81 ± 0.56	666 99.40 ± 0.30	629 94.44 ± 0.89	629 100.00 ± 0.00	1 0.16 ± 0.16	1 100.00 ± 0.00	1 100.00 ± 0.00	0 0.00 ± 0.00
$\mu\mu$	12020 0.13 ± 0.00	10602 88.20 ± 0.29	10142 95.66 ± 0.20	10079 99.38 ± 0.08	9748 96.72 ± 0.18	9745 99.97 ± 0.02	10 0.10 ± 0.03	9 90.00 ± 9.49	8 88.89 ± 10.48	5 62.50 ± 17.12
total	31595 0.34 ± 0.00	27100 85.77 ± 0.20	25566 94.34 ± 0.14	25406 99.37 ± 0.05	24636 96.97 ± 0.11	23713 96.25 ± 0.12	37 0.16 ± 0.03	34 91.89 ± 4.49	22 64.71 ± 8.20	16 72.73 ± 9.50

Table 40: HWW dilepton MC acceptance table, assuming $M_H^{SM} = 160$ GeV

Category	Lepton ID	Lep1 Isol	Lep2 Isol	$M_{\ell\ell} > 16$	jet veto	opp sign	$\not\!\!E_t$	$\not\!\!E_t$ $\|\|$ $\Delta\phi$	$M_{\ell\ell} < M_H/2$	$p^1 p^2 \not\!\!E_t < M_H$
TCE-TCE	22638	18669	16786	15987	14051	14048	11235	11117	10871	10362
	2.02 ± 0.01	82.47 ± 0.25	89.91 ± 0.22	95.24 ± 0.16	87.89 ± 0.26	99.98 ± 0.01	79.98 ± 0.34	98.95 ± 0.10	97.79 ± 0.14	95.32 ± 0.20
TCE-PHX	8087	7379	6971	6875	6146	5664	4602	4553	4314	4238
	0.72 ± 0.01	91.25 ± 0.31	94.47 ± 0.27	98.62 ± 0.14	89.40 ± 0.37	92.16 ± 0.34	81.25 ± 0.52	98.94 ± 0.15	94.75 ± 0.33	98.24 ± 0.20
PHX-PHX	0	0	0	0	0	0	0	0	0	0
	0.00 ± 0.00	0.00 ± 0.00	0.00 ± 0.00	0.00 ± 0.00	0.00 ± 0.00	0.00 ± 0.00	0.00 ± 0.00	0.00 ± 0.00	0.00 ± 0.00	0.00 ± 0.00
ee	30725	26048	23757	22862	20197	19712	15837	15670	15185	14600
	2.75 ± 0.02	84.78 ± 0.20	91.20 ± 0.18	96.23 ± 0.12	88.34 ± 0.21	97.60 ± 0.11	80.34 ± 0.28	98.95 ± 0.08	96.90 ± 0.14	96.15 ± 0.16
TCE-CMUP	28827	23920	22349	21200	18622	18619	14768	14619	14269	13667
	2.58 ± 0.01	82.98 ± 0.22	93.43 ± 0.16	94.86 ± 0.15	87.84 ± 0.22	99.98 ± 0.01	79.32 ± 0.30	98.99 ± 0.08	97.61 ± 0.13	95.78 ± 0.17
TCE-CMX	12306	10338	9680	9296	8220	8217	6504	6446	6276	6061
	1.10 ± 0.01	84.01 ± 0.33	93.64 ± 0.24	96.03 ± 0.20	88.43 ± 0.33	99.96 ± 0.02	79.15 ± 0.45	99.11 ± 0.12	97.36 ± 0.20	96.57 ± 0.23
TCE-CMU	4722	3935	3703	3594	3162	3162	2630	2598	2526	2413
	0.42 ± 0.01	83.33 ± 0.54	94.10 ± 0.38	97.06 ± 0.28	87.98 ± 0.54	100.00 ± 0.00	83.18 ± 0.67	98.78 ± 0.21	97.23 ± 0.32	95.53 ± 0.41
TCE-CMP	6796	5736	5408	5236	4629	4629	3899	3860	3770	3598
	0.61 ± 0.01	84.40 ± 0.44	94.28 ± 0.31	96.82 ± 0.24	88.41 ± 0.44	100.00 ± 0.00	84.23 ± 0.54	99.00 ± 0.16	97.67 ± 0.24	95.44 ± 0.34
TCE-CMIO	7719	6351	5931	5638	4955	4955	3867	3805	3722	3600
	0.69 ± 0.01	82.28 ± 0.43	93.39 ± 0.31	95.06 ± 0.28	87.89 ± 0.43	100.00 ± 0.00	78.04 ± 0.59	98.40 ± 0.20	97.82 ± 0.24	96.72 ± 0.29
PHX-CMUP	3776	3538	3478	3477	3140	2902	2403	2372	2225	2212
	0.34 ± 0.01	93.70 ± 0.40	98.30 ± 0.22	99.97 ± 0.03	90.31 ± 0.50	92.42 ± 0.47	82.80 ± 0.70	98.71 ± 0.23	93.80 ± 0.50	99.42 ± 0.16
PHX-CMX	3175	2918	2871	2794	2486	2253	1837	1812	1752	1701
	0.28 ± 0.01	91.91 ± 0.48	98.39 ± 0.23	97.32 ± 0.30	88.98 ± 0.59	90.63 ± 0.58	81.54 ± 0.82	98.64 ± 0.27	96.69 ± 0.42	97.09 ± 0.40
PHX-CMU	865	822	815	813	723	670	583	580	550	541
	0.08 ± 0.00	95.03 ± 0.74	99.15 ± 0.32	99.75 ± 0.17	88.93 ± 1.10	92.67 ± 0.97	87.01 ± 1.30	99.49 ± 0.30	94.83 ± 0.92	98.36 ± 0.54
PHX-CMP	863	810	805	805	724	672	591	582	542	542
	0.08 ± 0.00	93.86 ± 0.82	99.38 ± 0.28	100.00 ± 0.00	89.94 ± 1.06	92.82 ± 0.96	87.95 ± 1.26	98.48 ± 0.50	93.13 ± 1.05	100.00 ± 0.00
PHX-CMIO	1741	1606	1580	1551	1383	1277	1074	1060	1004	983
	0.16 ± 0.00	92.25 ± 0.64	98.38 ± 0.31	98.16 ± 0.34	89.17 ± 0.79	92.34 ± 0.72	84.10 ± 1.02	98.70 ± 0.35	94.72 ± 0.69	97.91 ± 0.45
$e\mu$	70790	59974	56620	54404	48044	47356	38156	37734	36636	35318
	6.33 ± 0.02	84.72 ± 0.14	94.41 ± 0.09	96.09 ± 0.08	88.31 ± 0.14	98.57 ± 0.05	80.57 ± 0.18	98.89 ± 0.05	97.09 ± 0.09	96.40 ± 0.10
CMUP-CMUP	9553	8390	7380	6932	6035	6035	4744	4691	4583	4389
	0.85 ± 0.01	87.83 ± 0.33	87.96 ± 0.36	93.93 ± 0.28	87.06 ± 0.40	100.00 ± 0.00	78.61 ± 0.53	98.88 ± 0.15	97.70 ± 0.22	95.77 ± 0.30
CMUP-CMX	7410	6765	6467	6262	5533	5533	4432	4379	4266	4181
	0.66 ± 0.01	91.30 ± 0.33	95.59 ± 0.25	96.83 ± 0.22	88.36 ± 0.41	100.00 ± 0.00	80.10 ± 0.54	98.80 ± 0.16	97.42 ± 0.24	98.01 ± 0.21
CMUP-CMU	3022	2750	2538	2475	2150	2150	1743	1729	1688	1636
	0.27 ± 0.00	91.00 ± 0.52	92.29 ± 0.51	97.52 ± 0.31	86.87 ± 0.68	100.00 ± 0.00	81.07 ± 0.84	99.20 ± 0.21	97.63 ± 0.37	96.92 ± 0.42
CMUP-CMP	4826	4382	3796	3649	3201	3201	2626	2599	2547	2453
	0.43 ± 0.01	90.80 ± 0.42	86.63 ± 0.51	96.13 ± 0.31	87.72 ± 0.54	100.00 ± 0.00	82.04 ± 0.68	98.97 ± 0.20	98.00 ± 0.27	96.31 ± 0.37
CMUP-CMIO	4973	4429	4129	3917	3455	3455	2696	2667	2608	2529
	0.44 ± 0.01	89.06 ± 0.44	93.23 ± 0.38	94.87 ± 0.34	88.21 ± 0.52	100.00 ± 0.00	78.03 ± 0.70	98.92 ± 0.20	97.79 ± 0.28	96.97 ± 0.34
CMX-CMX	1738	1498	1177	1104	980	980	727	719	699	675
	0.16 ± 0.00	86.19 ± 0.83	78.57 ± 1.06	93.80 ± 0.70	88.77 ± 0.95	100.00 ± 0.00	74.18 ± 1.40	98.90 ± 0.39	97.22 ± 0.61	96.57 ± 0.69
CMX-CMU	979	882	783	743	675	675	553	547	529	510
	0.09 ± 0.00	90.09 ± 0.95	88.78 ± 1.06	94.89 ± 0.79	90.85 ± 1.06	100.00 ± 0.00	81.93 ± 1.48	98.92 ± 0.44	96.71 ± 0.76	96.41 ± 0.81
CMX-CMP	1443	1359	1308	1293	1118	1118	928	920	900	881
	0.13 ± 0.00	94.18 ± 0.62	96.25 ± 0.52	98.85 ± 0.29	86.47 ± 0.95	100.00 ± 0.00	83.01 ± 1.12	99.14 ± 0.30	97.83 ± 0.48	97.89 ± 0.48
CMX-CMIO	1619	1459	1321	1270	1119	1119	834	826	795	772
	0.14 ± 0.00	90.12 ± 0.74	90.54 ± 0.77	96.14 ± 0.53	88.11 ± 0.91	100.00 ± 0.00	74.53 ± 1.30	99.04 ± 0.34	96.25 ± 0.66	97.11 ± 0.59
$\mu\mu$	35563	31914	28899	27645	24266	24266	19283	19077	18615	18026
	3.18 ± 0.02	89.74 ± 0.16	90.55 ± 0.16	95.66 ± 0.12	87.78 ± 0.20	100.00 ± 0.00	79.47 ± 0.26	98.93 ± 0.07	97.58 ± 0.11	96.84 ± 0.13
total	137078	117936	109276	104911	92507	91334	73276	72481	70436	67944
	12.25 ± 0.03	86.04 ± 0.09	92.66 ± 0.08	96.01 ± 0.06	88.18 ± 0.10	98.73 ± 0.04	80.23 ± 0.13	98.92 ± 0.04	97.18 ± 0.06	96.46 ± 0.07

Table 41: WW MC acceptance table, assuming $M_H^{\rm SM} = 160$ GeV

Category	Lepton ID	Lep1 Isol	Lep2 Isol	$M_{\ell\ell} > 16$	jet veto	opp sign	$\not\!\!E_t$	$\not\!\!E_t$ $\|\|$ $\Delta\phi$	$M_{\ell\ell} < M_H/2$	$p^1 p^2 \not\!\!E_t < M_H$
TCE-TCE	764	662	597	586	548	548	273	270	166	150
	0.18 ± 0.01	86.65 ± 1.23	90.18 ± 1.16	98.16 ± 0.55	93.52 ± 1.02	100.00 ± 0.00	49.82 ± 2.14	98.90 ± 0.63	61.48 ± 2.96	90.36 ± 2.29
TCE-PHX	524	478	460	458	428	376	198	194	92	85
	0.12 ± 0.01	91.22 ± 1.24	96.23 ± 0.87	99.57 ± 0.31	93.45 ± 1.16	87.85 ± 1.58	52.66 ± 2.57	97.98 ± 1.00	47.42 ± 3.59	92.39 ± 2.76
PHX-PHX	0	0	0	0	0	0	0	0	0	0
	0.00 ± 0.00	0.00 ± 0.00	0.00 ± 0.00	0.00 ± 0.00	0.00 ± 0.00	0.00 ± 0.00	0.00 ± 0.00	0.00 ± 0.00	0.00 ± 0.00	0.00 ± 0.00
ee	1288	1140	1057	1044	976	924	471	464	258	235
	0.31 ± 0.01	88.51 ± 0.89	92.72 ± 0.77	98.77 ± 0.34	93.49 ± 0.76	94.67 ± 0.72	50.97 ± 1.64	98.51 ± 0.56	55.60 ± 2.31	91.09 ± 1.77
TCE-CMUP	821	732	682	663	632	632	302	295	193	170
	0.20 ± 0.01	89.16 ± 1.09	93.17 ± 0.93	97.21 ± 0.63	95.32 ± 0.82	100.00 ± 0.00	47.78 ± 1.99	97.68 ± 0.87	65.42 ± 2.77	88.08 ± 2.33
TCE-CMX	450	395	373	365	338	338	169	164	108	100
	0.11 ± 0.01	87.78 ± 1.54	94.43 ± 1.15	97.86 ± 0.75	92.60 ± 1.37	100.00 ± 0.00	50.00 ± 2.72	97.04 ± 1.30	65.85 ± 3.70	92.59 ± 2.52
TCE-CMU	140	129	124	121	114	114	60	60	36	33
	0.03 ± 0.00	92.14 ± 2.27	96.12 ± 1.70	97.58 ± 1.38	94.21 ± 2.12	100.00 ± 0.00	52.63 ± 4.68	100.00 ± 0.00	60.00 ± 6.32	91.67 ± 4.61
TCE-CMP	190	171	158	157	151	151	74	72	42	36
	0.05 ± 0.00	90.00 ± 2.18	92.40 ± 2.03	99.37 ± 0.63	96.18 ± 1.53	100.00 ± 0.00	49.01 ± 4.07	97.30 ± 1.89	58.33 ± 5.81	85.71 ± 5.40
TCE-CMIO	280	247	236	228	216	216	114	113	62	57
	0.07 ± 0.00	88.21 ± 1.93	95.55 ± 1.31	96.61 ± 1.18	94.74 ± 1.48	100.00 ± 0.00	52.78 ± 3.40	99.12 ± 0.87	54.87 ± 4.68	91.94 ± 3.46
PHX-CMUP	279	257	252	252	237	215	113	112	57	54
	0.07 ± 0.00	92.11 ± 1.61	98.05 ± 0.86	100.00 ± 0.00	94.05 ± 1.49	90.72 ± 1.88	52.56 ± 3.41	99.12 ± 0.88	50.89 ± 4.72	94.74 ± 2.96
PHX-CMX	161	138	134	133	127	110	47	47	22	22
	0.04 ± 0.00	85.71 ± 2.76	97.10 ± 1.43	99.25 ± 0.74	95.49 ± 1.80	86.61 ± 3.02	42.73 ± 4.72	100.00 ± 0.00	46.81 ± 7.28	100.00 ± 0.00
PHX-CMU	32	31	31	31	28	25	15	15	7	7
	0.01 ± 0.00	96.88 ± 3.08	100.00 ± 0.00	100.00 ± 0.00	90.32 ± 5.31	89.29 ± 5.85	60.00 ± 9.80	100.00 ± 0.00	46.67 ± 12.88	100.00 ± 0.00
PHX-CMP	50	44	44	44	43	41	32	30	7	6
	0.01 ± 0.00	88.00 ± 4.60	100.00 ± 0.00	100.00 ± 0.00	97.73 ± 2.25	95.35 ± 3.21	78.05 ± 6.46	93.75 ± 4.28	23.33 ± 7.72	85.71 ± 13.23
PHX-CMIO	114	95	90	90	86	72	48	47	24	23
	0.03 ± 0.00	83.33 ± 3.49	94.74 ± 2.29	100.00 ± 0.00	95.56 ± 2.17	83.72 ± 3.98	66.67 ± 5.56	97.92 ± 2.06	51.06 ± 7.29	95.83 ± 4.08
$e\mu$	2517	2239	2124	2084	1972	1914	974	955	558	508
	0.60 ± 0.01	88.96 ± 0.62	94.86 ± 0.47	98.12 ± 0.29	94.63 ± 0.49	97.06 ± 0.38	50.89 ± 1.14	98.05 ± 0.44	58.43 ± 1.59	91.04 ± 1.21
CMUP-CMUP	259	238	230	221	210	210	103	102	66	60
	0.06 ± 0.00	91.89 ± 1.70	96.64 ± 1.17	96.09 ± 1.28	95.02 ± 1.46	100.00 ± 0.00	49.05 ± 3.45	99.03 ± 0.97	64.71 ± 4.73	90.91 ± 3.54
CMUP-CMX	284	263	258	253	236	236	121	116	72	68
	0.07 ± 0.00	92.61 ± 1.55	98.10 ± 0.84	98.06 ± 0.86	93.28 ± 1.57	100.00 ± 0.00	51.27 ± 3.25	95.87 ± 1.81	62.07 ± 4.51	94.44 ± 2.70
CMUP-CMU	70	66	64	62	61	61	34	34	23	18
	0.02 ± 0.00	94.29 ± 2.77	96.97 ± 2.11	96.88 ± 2.17	98.39 ± 1.60	100.00 ± 0.00	55.74 ± 6.36	100.00 ± 0.00	67.65 ± 8.02	78.26 ± 8.60
CMUP-CMP	136	132	125	124	118	118	57	56	41	36
	0.03 ± 0.00	97.06 ± 1.45	94.70 ± 1.95	99.20 ± 0.80	95.16 ± 1.93	100.00 ± 0.00	48.31 ± 4.60	98.25 ± 1.74	73.21 ± 5.92	87.80 ± 5.11
CMUP-CMIO	145	127	124	122	112	112	51	51	32	30
	0.03 ± 0.00	87.59 ± 2.74	97.64 ± 1.35	98.39 ± 1.13	91.80 ± 2.48	100.00 ± 0.00	45.54 ± 4.71	100.00 ± 0.00	62.75 ± 6.77	93.75 ± 4.28
CMX-CMX	64	54	52	52	52	52	22	22	9	8
	0.02 ± 0.00	84.38 ± 4.54	96.30 ± 2.57	100.00 ± 0.00	100.00 ± 0.00	100.00 ± 0.00	42.31 ± 6.85	100.00 ± 0.00	40.91 ± 10.48	88.89 ± 10.48
CMX-CMU	25	22	21	21	21	21	9	9	6	6
	0.01 ± 0.00	88.00 ± 6.50	95.45 ± 4.44	100.00 ± 0.00	100.00 ± 0.00	100.00 ± 0.00	42.86 ± 10.80	100.00 ± 0.00	66.67 ± 15.71	100.00 ± 0.00
CMX-CMP	55	53	52	52	50	50	16	16	7	6
	0.01 ± 0.00	96.36 ± 2.52	98.11 ± 1.87	100.00 ± 0.00	96.15 ± 2.67	100.00 ± 0.00	32.00 ± 6.60	100.00 ± 0.00	43.75 ± 12.40	85.71 ± 13.23
CMX-CMIO	53	47	45	44	42	42	18	18	9	8
	0.01 ± 0.00	88.68 ± 4.35	95.74 ± 2.94	97.78 ± 2.20	95.45 ± 3.14	100.00 ± 0.00	42.86 ± 7.64	100.00 ± 0.00	50.00 ± 11.79	88.89 ± 10.48
$\mu\mu$	1091	1002	971	951	902	902	431	424	265	240
	0.26 ± 0.01	91.84 ± 0.83	96.91 ± 0.55	97.94 ± 0.46	94.85 ± 0.72	100.00 ± 0.00	47.78 ± 1.66	98.38 ± 0.61	62.50 ± 2.35	90.57 ± 1.80
total	4896	4381	4152	4079	3850	3740	1876	1843	1081	983
	1.17 ± 0.02	89.48 ± 0.44	94.77 ± 0.34	98.24 ± 0.20	94.39 ± 0.36	97.14 ± 0.27	50.16 ± 0.82	98.24 ± 0.30	58.65 ± 1.15	90.93 ± 0.87

Table 42: WZ MC acceptance table, assuming $M_H^{\rm SM} = 160$ GeV

Category	Lepton ID	Lep1 Isol	Lep2 Isol	$M_{\ell\ell} > 16$	jet veto	opp sign	$\not\!\!E_t$	$\not\!\!E_t$ || $\Delta\phi$	$M_{\ell\ell} < M_H/2$	$p^1 p^2 \not\!\!E_t < M_H$
TCE-TCE	1411	1225	1112	1110	531	476	143	136	20	19
	0.35 ± 0.01	86.82 ± 0.90	90.78 ± 0.83	99.82 ± 0.13	47.84 ± 1.50	89.64 ± 1.32	30.04 ± 2.10	95.10 ± 1.80	14.71 ± 3.04	95.00 ± 4.87
TCE-PHX	1274	1178	1127	1126	526	442	114	110	14	13
	0.31 ± 0.01	92.46 ± 0.74	95.67 ± 0.59	99.91 ± 0.09	46.71 ± 1.49	84.03 ± 1.60	25.79 ± 2.08	96.49 ± 1.72	12.73 ± 3.18	92.86 ± 6.88
PHX-PHX	0	0	0	0	0	0	0	0	0	0
	0.00 ± 0.00	0.00 ± 0.00	0.00 ± 0.00	0.00 ± 0.00	0.00 ± 0.00	0.00 ± 0.00	0.00 ± 0.00	0.00 ± 0.00	0.00 ± 0.00	0.00 ± 0.00
ee	2685	2403	2239	2236	1057	918	257	246	34	32
	0.66 ± 0.01	89.50 ± 0.59	93.18 ± 0.51	99.87 ± 0.08	47.27 ± 1.06	86.85 ± 1.04	28.00 ± 1.48	95.72 ± 1.26	13.82 ± 2.20	94.12 ± 4.04
TCE-CMUP	273	227	215	204	161	88	44	43	25	22
	0.07 ± 0.00	83.15 ± 2.27	94.71 ± 1.49	94.88 ± 1.50	78.92 ± 2.86	54.66 ± 3.92	50.00 ± 5.33	97.73 ± 2.25	58.14 ± 7.52	88.00 ± 6.50
TCE-CMX	154	131	120	117	85	47	27	24	16	15
	0.04 ± 0.00	85.06 ± 2.87	91.60 ± 2.42	97.50 ± 1.43	72.65 ± 4.12	55.29 ± 5.39	57.45 ± 7.21	88.89 ± 6.05	66.67 ± 9.62	93.75 ± 6.05
TCE-CMU	33	28	28	28	17	10	8	7	2	2
	0.01 ± 0.00	84.85 ± 6.24	100.00 ± 0.00	100.00 ± 0.00	60.71 ± 9.23	58.82 ± 11.94	80.00 ± 12.65	87.50 ± 11.69	28.57 ± 17.07	100.00 ± 0.00
TCE-CMP	43	40	37	37	25	13	5	5	2	1
	0.01 ± 0.00	93.02 ± 3.88	92.50 ± 4.16	100.00 ± 0.00	67.57 ± 7.70	52.00 ± 9.99	38.46 ± 13.49	100.00 ± 0.00	40.00 ± 21.91	50.00 ± 35.36
TCE-CMIO	96	72	70	65	44	19	10	10	4	4
	0.02 ± 0.00	75.00 ± 4.42	97.22 ± 1.94	92.86 ± 3.08	67.69 ± 5.80	43.18 ± 7.47	52.63 ± 11.45	100.00 ± 0.00	40.00 ± 15.49	100.00 ± 0.00
PHX-CMUP	120	107	105	105	80	34	19	17	4	4
	0.03 ± 0.00	89.17 ± 2.84	98.13 ± 1.31	100.00 ± 0.00	76.19 ± 4.16	42.50 ± 5.53	55.88 ± 8.52	89.47 ± 7.04	23.53 ± 10.29	100.00 ± 0.00
PHX-CMX	58	52	52	52	38	22	11	11	2	2
	0.01 ± 0.00	89.66 ± 4.00	100.00 ± 0.00	100.00 ± 0.00	73.08 ± 6.15	57.89 ± 8.01	50.00 ± 10.66	100.00 ± 0.00	18.18 ± 11.63	100.00 ± 0.00
PHX-CMU	12	12	12	12	10	5	3	3	1	1
	0.00 ± 0.00	100.00 ± 0.00	100.00 ± 0.00	100.00 ± 0.00	83.33 ± 10.76	50.00 ± 15.81	60.00 ± 21.91	100.00 ± 0.00	33.33 ± 27.22	100.00 ± 0.00
PHX-CMP	19	17	17	17	12	5	3	3	1	1
	0.00 ± 0.00	89.47 ± 7.04	100.00 ± 0.00	100.00 ± 0.00	70.59 ± 11.05	41.67 ± 14.23	60.00 ± 21.91	100.00 ± 0.00	33.33 ± 27.22	100.00 ± 0.00
PHX-CMIO	40	32	30	30	22	16	9	9	2	2
	0.01 ± 0.00	80.00 ± 6.32	93.75 ± 4.28	100.00 ± 0.00	73.33 ± 8.07	72.73 ± 9.50	56.25 ± 12.40	100.00 ± 0.00	22.22 ± 13.86	100.00 ± 0.00
$e\mu$	848	718	686	667	494	259	139	132	59	54
	0.21 ± 0.01	84.67 ± 1.24	95.54 ± 0.77	97.23 ± 0.63	74.06 ± 1.70	52.43 ± 2.25	53.67 ± 3.10	94.96 ± 1.85	44.70 ± 4.33	91.53 ± 3.63
CMUP-CMUP	468	409	404	403	221	198	62	56	9	6
	0.11 ± 0.01	87.39 ± 1.53	98.78 ± 0.54	99.75 ± 0.25	54.84 ± 2.48	89.59 ± 2.05	31.31 ± 3.30	90.32 ± 3.75	16.07 ± 4.91	66.67 ± 15.71
CMUP-CMX	493	433	420	419	203	178	52	49	16	10
	0.12 ± 0.01	87.83 ± 1.47	97.00 ± 0.82	99.76 ± 0.24	48.45 ± 2.44	87.68 ± 2.31	29.21 ± 3.41	94.23 ± 3.23	32.65 ± 6.70	62.50 ± 12.10
CMUP-CMU	194	177	173	173	98	92	32	30	3	2
	0.05 ± 0.00	91.24 ± 2.03	97.74 ± 1.12	100.00 ± 0.00	56.65 ± 3.77	93.88 ± 2.42	34.78 ± 4.97	93.75 ± 4.28	10.00 ± 5.48	66.67 ± 27.22
CMUP-CMP	272	244	240	239	124	111	29	28	3	2
	0.07 ± 0.00	89.71 ± 1.84	98.36 ± 0.81	99.58 ± 0.42	51.88 ± 3.23	89.52 ± 2.75	26.13 ± 4.17	96.55 ± 3.39	10.71 ± 5.85	66.67 ± 27.22
CMUP-CMIO	303	254	245	244	131	118	31	31	4	4
	0.07 ± 0.00	83.83 ± 2.12	96.46 ± 1.16	99.59 ± 0.41	53.69 ± 3.19	90.08 ± 2.61	26.27 ± 4.05	100.00 ± 0.00	12.90 ± 6.02	100.00 ± 0.00
CMX-CMX	115	101	98	98	44	39	14	10	3	3
	0.03 ± 0.00	87.83 ± 3.05	97.03 ± 1.69	100.00 ± 0.00	44.90 ± 5.02	88.64 ± 4.78	35.90 ± 7.68	71.43 ± 12.07	30.00 ± 14.49	100.00 ± 0.00
CMX-CMU	77	71	71	71	42	37	10	10	3	3
	0.02 ± 0.00	92.21 ± 3.05	100.00 ± 0.00	100.00 ± 0.00	59.15 ± 5.83	88.10 ± 5.00	27.03 ± 7.30	100.00 ± 0.00	30.00 ± 14.49	100.00 ± 0.00
CMX-CMP	103	98	96	95	48	43	14	13	2	2
	0.03 ± 0.00	95.15 ± 2.12	97.96 ± 1.43	98.96 ± 1.04	50.53 ± 5.13	89.58 ± 4.41	32.56 ± 7.15	92.86 ± 6.88	15.38 ± 10.01	100.00 ± 0.00
CMX-CMIO	136	114	111	111	60	56	21	20	4	3
	0.03 ± 0.00	83.82 ± 3.16	97.37 ± 1.50	100.00 ± 0.00	54.05 ± 4.73	93.33 ± 3.22	37.50 ± 6.47	95.24 ± 4.65	20.00 ± 8.94	75.00 ± 21.65
$\mu\mu$	2161	1901	1858	1853	971	872	265	247	47	35
	0.53 ± 0.01	87.97 ± 0.70	97.74 ± 0.34	99.73 ± 0.12	52.40 ± 1.16	89.80 ± 0.97	30.39 ± 1.56	93.21 ± 1.55	19.03 ± 2.50	74.47 ± 6.36
total	5694	5022	4783	4756	2522	2049	661	625	140	121
	1.40 ± 0.02	88.20 ± 0.43	95.24 ± 0.30	99.44 ± 0.11	53.03 ± 0.72	81.25 ± 0.78	32.26 ± 1.03	94.55 ± 0.88	22.40 ± 1.67	86.43 ± 2.89

Table 43: $t\bar{t}$ MC acceptance table, assuming $M_H^{\rm SM} = 160$ GeV

Category	Lepton ID	Lep1 Isol	Lep2 Isol	$M_{\ell\ell} > 16$	jet veto	opp sign	$\not\!\!E_t$	$\not\!\!E_t$ || $\Delta\phi$	$M_{\ell\ell} < M_H/2$	$p^1 p^2 \not\!\!E_t < M_H$
TCE-TCE	3188	2153	1924	1905	195	195	137	132	53	36
	0.28 ± 0.00	67.53 ± 0.83	89.36 ± 0.66	99.01 ± 0.23	10.24 ± 0.69	100.00 ± 0.00	70.26 ± 3.27	96.35 ± 1.60	40.15 ± 4.27	67.92 ± 6.41
TCE-PHX	1237	981	926	924	82	75	51	49	12	8
	0.11 ± 0.00	79.30 ± 1.15	94.39 ± 0.73	99.78 ± 0.15	8.87 ± 0.94	91.46 ± 3.09	68.00 ± 5.39	96.08 ± 2.72	24.49 ± 6.14	66.67 ± 13.61
PHX-PHX	0	0	0	0	0	0	0	0	0	0
	0.00 ± 0.00	0.00 ± 0.00	0.00 ± 0.00	0.00 ± 0.00	0.00 ± 0.00	0.00 ± 0.00	0.00 ± 0.00	0.00 ± 0.00	0.00 ± 0.00	0.00 ± 0.00
ee	4425	3134	2850	2829	277	270	188	181	65	44
	0.39 ± 0.01	70.82 ± 0.68	90.94 ± 0.51	99.26 ± 0.16	9.79 ± 0.56	97.47 ± 0.94	69.63 ± 2.80	96.28 ± 1.38	35.91 ± 3.57	67.69 ± 5.80
TCE-CMUP	4200	2607	2422	2394	215	215	150	144	55	34
	0.37 ± 0.01	62.07 ± 0.75	92.90 ± 0.50	98.84 ± 0.22	8.98 ± 0.58	100.00 ± 0.00	69.77 ± 3.13	96.00 ± 1.60	38.19 ± 4.05	61.82 ± 6.55
TCE-CMX	1863	1148	1059	1045	108	108	66	63	24	15
	0.16 ± 0.00	61.62 ± 1.13	92.25 ± 0.79	98.68 ± 0.35	10.33 ± 0.94	100.00 ± 0.00	61.11 ± 4.69	95.45 ± 2.56	38.10 ± 6.12	62.50 ± 9.88
TCE-CMU	589	457	421	420	38	38	25	23	7	2
	0.05 ± 0.00	77.59 ± 1.72	92.12 ± 1.26	99.76 ± 0.24	9.05 ± 1.40	100.00 ± 0.00	65.79 ± 7.70	92.00 ± 5.43	30.43 ± 9.59	28.57 ± 17.07
TCE-CMP	839	636	588	586	53	53	39	38	11	9
	0.07 ± 0.00	75.80 ± 1.48	92.45 ± 1.05	99.66 ± 0.24	9.04 ± 1.18	100.00 ± 0.00	73.58 ± 6.06	97.44 ± 2.53	28.95 ± 7.36	81.82 ± 11.63
TCE-CMIO	1364	756	691	682	67	67	40	39	17	9
	0.12 ± 0.00	55.43 ± 1.35	91.40 ± 1.02	98.70 ± 0.43	9.82 ± 1.14	100.00 ± 0.00	59.70 ± 5.99	97.50 ± 2.47	43.59 ± 7.94	52.94 ± 12.11
PHX-CMUP	876	615	600	600	41	37	23	23	7	7
	0.08 ± 0.00	70.21 ± 1.55	97.56 ± 0.62	100.00 ± 0.00	6.83 ± 1.03	90.24 ± 4.63	62.16 ± 7.97	100.00 ± 0.00	30.43 ± 9.59	100.00 ± 0.00
PHX-CMX	385	283	273	273	27	23	21	21	5	2
	0.03 ± 0.00	73.51 ± 2.25	96.47 ± 1.10	100.00 ± 0.00	9.89 ± 1.81	85.19 ± 6.84	91.30 ± 5.88	100.00 ± 0.00	23.81 ± 9.29	40.00 ± 21.91
PHX-CMU	137	114	112	112	12	10	7	7	1	1
	0.01 ± 0.00	83.21 ± 3.19	98.25 ± 1.23	100.00 ± 0.00	10.71 ± 2.92	83.33 ± 10.76	70.00 ± 14.49	100.00 ± 0.00	14.29 ± 13.23	100.00 ± 0.00
PHX-CMP	193	158	156	156	12	10	8	8	1	1
	0.02 ± 0.00	81.87 ± 2.77	98.73 ± 0.89	100.00 ± 0.00	7.69 ± 2.13	83.33 ± 10.76	80.00 ± 12.65	100.00 ± 0.00	12.50 ± 11.69	100.00 ± 0.00
PHX-CMIO	292	180	173	173	12	11	9	9	4	3
	0.03 ± 0.00	61.64 ± 2.85	96.11 ± 1.44	100.00 ± 0.00	6.94 ± 1.93	91.67 ± 7.98	81.82 ± 11.63	100.00 ± 0.00	44.44 ± 16.56	75.00 ± 21.65
$e\mu$	10738	6954	6495	6441	585	572	388	375	132	83
	0.94 ± 0.01	64.76 ± 0.46	93.40 ± 0.30	99.17 ± 0.11	9.08 ± 0.36	97.78 ± 0.61	67.83 ± 1.95	96.65 ± 0.91	35.20 ± 2.47	62.88 ± 4.21
CMUP-CMUP	1405	869	826	810	101	101	64	60	24	16
	0.12 ± 0.00	61.85 ± 1.30	95.05 ± 0.74	98.06 ± 0.48	12.47 ± 1.16	100.00 ± 0.00	63.37 ± 4.79	93.75 ± 3.03	40.00 ± 6.32	66.67 ± 9.62
CMUP-CMX	1236	732	704	696	73	73	54	53	21	14
	0.11 ± 0.00	59.22 ± 1.40	96.17 ± 0.71	98.86 ± 0.40	10.49 ± 1.16	100.00 ± 0.00	73.97 ± 5.14	98.15 ± 1.83	39.62 ± 6.72	66.67 ± 10.29
CMUP-CMU	372	293	281	279	34	34	28	28	8	4
	0.03 ± 0.00	78.76 ± 2.12	95.90 ± 1.16	99.29 ± 0.50	12.19 ± 1.96	100.00 ± 0.00	82.35 ± 6.54	100.00 ± 0.00	28.57 ± 8.54	50.00 ± 17.68
CMUP-CMP	544	383	364	359	28	28	20	19	3	2
	0.05 ± 0.00	70.40 ± 1.96	95.04 ± 1.11	98.63 ± 0.61	7.80 ± 1.42	100.00 ± 0.00	71.43 ± 8.54	95.00 ± 4.87	15.79 ± 8.37	66.67 ± 27.22
CMUP-CMIO	876	459	439	429	43	43	35	34	8	6
	0.08 ± 0.00	52.40 ± 1.69	95.64 ± 0.95	97.72 ± 0.71	10.02 ± 1.45	100.00 ± 0.00	81.40 ± 5.93	97.14 ± 2.82	23.53 ± 7.27	75.00 ± 15.31
CMX-CMX	236	130	116	114	6	6	3	3	1	1
	0.02 ± 0.00	55.08 ± 3.24	89.23 ± 2.72	98.28 ± 1.21	5.26 ± 2.09	100.00 ± 0.00	50.00 ± 20.41	100.00 ± 0.00	33.33 ± 27.22	100.00 ± 0.00
CMX-CMU	131	97	96	96	13	13	10	10	4	3
	0.01 ± 0.00	74.05 ± 3.83	98.97 ± 1.03	100.00 ± 0.00	13.54 ± 3.49	100.00 ± 0.00	76.92 ± 11.69	100.00 ± 0.00	40.00 ± 15.49	75.00 ± 21.65
CMX-CMP	190	152	150	150	9	9	4	4	2	2
	0.02 ± 0.00	80.00 ± 2.90	98.68 ± 0.92	100.00 ± 0.00	6.00 ± 1.94	100.00 ± 0.00	44.44 ± 16.56	100.00 ± 0.00	50.00 ± 25.00	100.00 ± 0.00
CMX-CMIO	324	172	164	162	18	18	11	11	4	1
	0.03 ± 0.00	53.09 ± 2.77	95.35 ± 1.61	98.78 ± 0.86	11.11 ± 2.47	100.00 ± 0.00	61.11 ± 11.49	100.00 ± 0.00	36.36 ± 14.50	25.00 ± 21.65
$\mu\mu$	5314	3287	3140	3095	325	325	229	222	75	49
	0.47 ± 0.01	61.86 ± 0.67	95.53 ± 0.36	98.57 ± 0.21	10.50 ± 0.55	100.00 ± 0.00	70.46 ± 2.53	96.94 ± 1.14	33.78 ± 3.17	65.33 ± 5.50
total	20477	13375	12485	12365	1187	1167	805	778	272	176
	1.79 ± 0.01	65.32 ± 0.33	93.35 ± 0.22	99.04 ± 0.09	9.60 ± 0.26	98.32 ± 0.37	68.98 ± 1.35	96.65 ± 0.63	34.96 ± 1.71	64.71 ± 2.90

Table 44: Drell-Yan MC acceptance table, assuming $M_H^{\rm SM} = 160$ GeV/c^2.

Category	Lepton ID	Lep1 Isol	Lep2 Isol	$M_{\ell\ell} > 16$	jet veto	opp sign	$\not\!\!E_t$	$\not\!\!E_t$ $\|\|$ $\Delta\phi$	$M_{\ell\ell} < M_H/2$	$p^1 p^2 \not\!\!E_t < M_H$
TCE-TCE	101043	94505	86362	86128	83755	83727	33	12	4	4
	3.19 ± 0.01	93.53 ± 0.08	91.38 ± 0.09	99.73 ± 0.02	97.24 ± 0.06	99.97 ± 0.01	0.04 ± 0.01	36.36 ± 8.37	33.33 ± 13.61	100.00 ± 0.00
TCE-PHX	122697	117671	112416	112409	109859	98338	15	6	0	0
	3.88 ± 0.01	95.90 ± 0.06	95.53 ± 0.06	99.99 ± 0.00	97.73 ± 0.04	89.51 ± 0.09	0.02 ± 0.00	40.00 ± 12.65	0.00 ± 0.00	0.00 ± 0.00
PHX-PHX	0	0	0	0	0	0	0	0	0	0
	0.00 ± 0.00	0.00 ± 0.00	0.00 ± 0.00	0.00 ± 0.00	0.00 ± 0.00	0.00 ± 0.00	0.00 ± 0.00	0.00 ± 0.00	0.00 ± 0.00	0.00 ± 0.00
ee	223740	212176	198778	198537	193614	182065	48	18	4	4
	7.07 ± 0.01	94.83 ± 0.05	93.69 ± 0.05	99.88 ± 0.01	97.52 ± 0.03	94.04 ± 0.05	0.03 ± 0.00	37.50 ± 6.99	22.22 ± 9.80	100.00 ± 0.00
TCE-CMUP	1050	924	831	827	805	802	8	1	0	0
	0.03 ± 0.00	88.00 ± 1.00	89.94 ± 0.99	99.52 ± 0.24	97.34 ± 0.56	99.63 ± 0.21	1.00 ± 0.35	12.50 ± 11.69	0.00 ± 0.00	0.00 ± 0.00
TCE-CMX	521	464	434	434	421	419	8	3	2	1
	0.02 ± 0.00	89.06 ± 1.37	93.53 ± 1.14	100.00 ± 0.00	97.00 ± 0.82	99.52 ± 0.34	1.91 ± 0.67	37.50 ± 17.12	66.67 ± 27.22	50.00 ± 35.36
TCE-CMU	74	69	62	62	60	60	1	1	0	0
	0.00 ± 0.00	93.24 ± 2.92	89.86 ± 3.63	100.00 ± 0.00	96.77 ± 2.24	100.00 ± 0.00	1.67 ± 1.65	100.00 ± 0.00	0.00 ± 0.00	0.00 ± 0.00
TCE-CMP	120	115	104	104	102	102	3	2	0	0
	0.00 ± 0.00	95.83 ± 1.82	90.43 ± 2.74	100.00 ± 0.00	98.08 ± 1.35	100.00 ± 0.00	2.94 ± 1.67	66.67 ± 27.22	0.00 ± 0.00	0.00 ± 0.00
TCE-CMIO	352	301	271	270	262	260	3	1	0	0
	0.01 ± 0.00	85.51 ± 1.88	90.03 ± 1.73	99.63 ± 0.37	97.04 ± 1.03	99.24 ± 0.54	1.15 ± 0.66	33.33 ± 27.22	0.00 ± 0.00	0.00 ± 0.00
PHX-CMUP	193	176	173	173	155	125	1	0	0	0
	0.01 ± 0.00	91.19 ± 2.04	98.30 ± 0.98	100.00 ± 0.00	89.60 ± 2.32	80.65 ± 3.17	0.80 ± 0.80	0.00 ± 0.00	0.00 ± 0.00	0.00 ± 0.00
PHX-CMX	146	138	136	134	126	95	3	2	2	2
	0.00 ± 0.00	94.52 ± 1.88	98.55 ± 1.02	98.53 ± 1.03	94.03 ± 2.05	75.40 ± 3.84	3.16 ± 1.79	66.67 ± 27.22	100.00 ± 0.00	100.00 ± 0.00
PHX-CMU	6	4	4	4	3	1	1	0	0	0
	0.00 ± 0.00	66.67 ± 19.25	100.00 ± 0.00	100.00 ± 0.00	75.00 ± 21.65	33.33 ± 27.22	100.00 ± 0.00	0.00 ± 0.00	0.00 ± 0.00	0.00 ± 0.00
PHX-CMP	3	2	2	2	1	1	0	0	0	0
	0.00 ± 0.00	66.67 ± 27.22	100.00 ± 0.00	100.00 ± 0.00	50.00 ± 35.36	100.00 ± 0.00	0.00 ± 0.00	0.00 ± 0.00	0.00 ± 0.00	0.00 ± 0.00
PHX-CMIO	20	15	15	14	11	8	0	0	0	0
	0.00 ± 0.00	75.00 ± 9.68	100.00 ± 0.00	93.33 ± 6.44	78.57 ± 10.97	72.73 ± 13.43	0.00 ± 0.00	0.00 ± 0.00	0.00 ± 0.00	0.00 ± 0.00
$e\mu$	2485	2208	2032	2024	1946	1873	28	10	4	3
	0.08 ± 0.00	88.85 ± 0.63	92.03 ± 0.58	99.61 ± 0.14	96.15 ± 0.43	96.25 ± 0.43	1.49 ± 0.28	35.71 ± 9.06	40.00 ± 15.49	75.00 ± 21.65
CMUP-CMUP	32737	31023	30558	30464	29587	29587	8	5	1	1
	1.03 ± 0.01	94.76 ± 0.12	98.50 ± 0.07	99.69 ± 0.03	97.12 ± 0.10	100.00 ± 0.00	0.03 ± 0.01	62.50 ± 17.12	20.00 ± 17.89	100.00 ± 0.00
CMUP-CMX	35973	34076	33560	33479	32494	32494	10	4	1	1
	1.14 ± 0.01	94.73 ± 0.12	98.49 ± 0.07	99.76 ± 0.03	97.06 ± 0.09	100.00 ± 0.00	0.03 ± 0.01	40.00 ± 15.49	25.00 ± 21.65	100.00 ± 0.00
CMUP-CMU	13023	12442	12297	12290	11908	11908	1	0	0	0
	0.41 ± 0.00	95.54 ± 0.18	98.83 ± 0.10	99.94 ± 0.02	96.89 ± 0.16	100.00 ± 0.00	0.01 ± 0.01	0.00 ± 0.00	0.00 ± 0.00	0.00 ± 0.00
CMUP-CMP	17209	16435	16194	16189	15743	15743	3	1	1	1
	0.54 ± 0.00	95.50 ± 0.16	98.53 ± 0.09	99.97 ± 0.01	97.25 ± 0.13	100.00 ± 0.00	0.02 ± 0.01	33.33 ± 27.22	100.00 ± 0.00	100.00 ± 0.00
CMUP-CMIO	20886	19738	19394	19329	18774	18774	5	3	0	0
	0.66 ± 0.00	94.50 ± 0.16	98.26 ± 0.09	99.66 ± 0.04	97.13 ± 0.12	100.00 ± 0.00	0.03 ± 0.01	60.00 ± 21.91	0.00 ± 0.00	0.00 ± 0.00
CMX-CMX	11045	10457	10249	10227	9981	9981	1	1	0	0
	0.35 ± 0.00	94.68 ± 0.21	98.01 ± 0.14	99.79 ± 0.05	97.59 ± 0.15	100.00 ± 0.00	0.01 ± 0.01	100.00 ± 0.00	0.00 ± 0.00	0.00 ± 0.00
CMX-CMU	6796	6504	6406	6404	6269	6269	1	1	0	0
	0.21 ± 0.00	95.70 ± 0.25	98.49 ± 0.15	99.97 ± 0.02	97.89 ± 0.18	100.00 ± 0.00	0.02 ± 0.02	100.00 ± 0.00	0.00 ± 0.00	0.00 ± 0.00
CMX-CMP	7808	7452	7347	7344	7153	7153	1	1	0	0
	0.25 ± 0.00	95.44 ± 0.24	98.59 ± 0.14	99.96 ± 0.02	97.40 ± 0.19	100.00 ± 0.00	0.01 ± 0.01	100.00 ± 0.00	0.00 ± 0.00	0.00 ± 0.00
CMX-CMIO	8930	8445	8282	8256	7986	7986	2	1	1	1
	0.28 ± 0.00	94.57 ± 0.24	98.07 ± 0.15	99.69 ± 0.06	96.73 ± 0.20	100.00 ± 0.00	0.03 ± 0.02	50.00 ± 35.36	100.00 ± 0.00	100.00 ± 0.00
$\mu\mu$	154407	146572	144287	143982	139895	139895	32	17	4	4
	4.88 ± 0.01	94.93 ± 0.06	98.44 ± 0.03	99.79 ± 0.01	97.16 ± 0.04	100.00 ± 0.00	0.02 ± 0.00	53.12 ± 8.82	23.53 ± 10.29	100.00 ± 0.00
total	380632	360956	345097	344543	335455	323833	108	45	12	11
	12.03 ± 0.02	94.83 ± 0.04	95.61 ± 0.03	99.84 ± 0.01	97.36 ± 0.03	96.54 ± 0.03	0.03 ± 0.00	41.67 ± 4.74	26.67 ± 6.59	91.67 ± 7.98

Table 45: ZZ MC acceptance table, assuming $M_H^{\rm SM} = 160$ GeV

Category	Lepton ID	Lep1 Isol	Lep2 Isol	$M_{\ell\ell} > 16$	jet veto	opp sign	$\not\!\!E_t$	$\not\!\!E_t$ $\|\|$ $\Delta\phi$	$M_{\ell\ell} < M_H/2$	$p^1 p^2 \not\!\!E_t < M_H$
TCE-TCE	1730	1459	1294	1265	667	659	153	150	8	5
	0.44 ± 0.01	84.34 ± 0.87	88.69 ± 0.83	97.76 ± 0.41	52.73 ± 1.40	98.80 ± 0.42	23.22 ± 1.64	98.04 ± 1.12	5.33 ± 1.83	62.50 ± 17.12
TCE-PHX	1231	1123	1067	1067	623	551	101	100	5	4
	0.31 ± 0.01	91.23 ± 0.81	95.01 ± 0.65	100.00 ± 0.00	58.39 ± 1.51	88.44 ± 1.28	18.33 ± 1.65	99.01 ± 0.99	5.00 ± 2.18	80.00 ± 17.89
PHX-PHX	0	0	0	0	0	0	0	0	0	0
	0.00 ± 0.00	0.00 ± 0.00	0.00 ± 0.00	0.00 ± 0.00	0.00 ± 0.00	0.00 ± 0.00	0.00 ± 0.00	0.00 ± 0.00	0.00 ± 0.00	0.00 ± 0.00
ee	2961	2582	2361	2332	1290	1210	254	250	13	9
	0.75 ± 0.01	87.20 ± 0.61	91.44 ± 0.55	98.77 ± 0.23	55.32 ± 1.03	93.80 ± 0.67	20.99 ± 1.17	98.43 ± 0.78	5.20 ± 1.40	69.23 ± 12.80
TCE-CMUP	96	76	70	70	37	18	3	3	1	1
	0.02 ± 0.00	79.17 ± 4.14	92.11 ± 3.09	100.00 ± 0.00	52.86 ± 5.97	48.65 ± 8.22	16.67 ± 8.78	100.00 ± 0.00	33.33 ± 27.22	100.00 ± 0.00
TCE-CMX	51	38	32	32	21	12	2	2	1	1
	0.01 ± 0.00	74.51 ± 6.10	84.21 ± 5.92	100.00 ± 0.00	65.62 ± 8.40	57.14 ± 10.80	16.67 ± 10.76	100.00 ± 0.00	50.00 ± 35.36	100.00 ± 0.00
TCE-CMU	11	8	8	8	4	2	0	0	0	0
	0.00 ± 0.00	72.73 ± 13.43	100.00 ± 0.00	100.00 ± 0.00	50.00 ± 17.68	50.00 ± 25.00	0.00 ± 0.00	0.00 ± 0.00	0.00 ± 0.00	0.00 ± 0.00
TCE-CMP	13	7	7	6	5	4	1	1	1	1
	0.00 ± 0.00	53.85 ± 13.83	100.00 ± 0.00	85.71 ± 13.23	83.33 ± 15.21	80.00 ± 17.89	25.00 ± 21.65	100.00 ± 0.00	100.00 ± 0.00	100.00 ± 0.00
TCE-CMIO	39	19	14	14	10	4	1	1	1	0
	0.01 ± 0.00	48.72 ± 8.00	73.68 ± 10.10	100.00 ± 0.00	71.43 ± 12.07	40.00 ± 15.49	25.00 ± 21.65	100.00 ± 0.00	100.00 ± 0.00	0.00 ± 0.00
PHX-CMUP	22	20	18	18	8	3	0	0	0	0
	0.01 ± 0.00	90.91 ± 6.13	90.00 ± 6.71	100.00 ± 0.00	44.44 ± 11.71	37.50 ± 17.12	0.00 ± 0.00	0.00 ± 0.00	0.00 ± 0.00	0.00 ± 0.00
PHX-CMX	11	10	9	9	6	3	3	3	2	2
	0.00 ± 0.00	90.91 ± 8.67	90.00 ± 9.49	100.00 ± 0.00	66.67 ± 15.71	50.00 ± 20.41	100.00 ± 0.00	100.00 ± 0.00	66.67 ± 27.22	100.00 ± 0.00
PHX-CMU	4	3	3	3	3	1	1	1	1	1
	0.00 ± 0.00	75.00 ± 21.65	100.00 ± 0.00	100.00 ± 0.00	100.00 ± 0.00	33.33 ± 27.22	100.00 ± 0.00	100.00 ± 0.00	100.00 ± 0.00	100.00 ± 0.00
PHX-CMP	3	1	1	1	1	1	0	0	0	0
	0.00 ± 0.00	33.33 ± 27.22	100.00 ± 0.00	100.00 ± 0.00	100.00 ± 0.00	100.00 ± 0.00	0.00 ± 0.00	0.00 ± 0.00	0.00 ± 0.00	0.00 ± 0.00
PHX-CMIO	3	2	2	2	2	1	0	0	0	0
	0.00 ± 0.00	66.67 ± 27.22	100.00 ± 0.00	100.00 ± 0.00	100.00 ± 0.00	50.00 ± 35.36	0.00 ± 0.00	0.00 ± 0.00	0.00 ± 0.00	0.00 ± 0.00
$e\mu$	253	184	164	163	97	49	11	11	7	6
	0.06 ± 0.00	72.73 ± 2.80	89.13 ± 2.29	99.39 ± 0.61	59.51 ± 3.84	50.52 ± 5.08	22.45 ± 5.96	100.00 ± 0.00	63.64 ± 14.50	85.71 ± 13.23
CMUP-CMUP	647	528	486	469	242	234	52	51	4	3
	0.16 ± 0.01	81.61 ± 1.52	92.05 ± 1.18	96.50 ± 0.83	51.60 ± 2.31	96.69 ± 1.15	22.22 ± 2.72	98.08 ± 1.90	7.84 ± 3.76	75.00 ± 21.65
CMUP-CMX	528	462	449	442	241	240	59	58	4	3
	0.13 ± 0.01	87.50 ± 1.44	97.19 ± 0.77	98.44 ± 0.58	54.52 ± 2.37	99.59 ± 0.41	24.58 ± 2.78	98.31 ± 1.68	6.90 ± 3.33	75.00 ± 21.65
CMUP-CMU	220	195	187	186	102	97	22	22	1	1
	0.06 ± 0.00	88.64 ± 2.14	95.90 ± 1.42	99.47 ± 0.53	54.84 ± 3.65	95.10 ± 2.14	22.68 ± 4.25	100.00 ± 0.00	4.55 ± 4.44	100.00 ± 0.00
CMUP-CMP	322	285	269	267	138	134	36	36	1	1
	0.08 ± 0.00	88.51 ± 1.78	94.39 ± 1.36	99.26 ± 0.52	51.69 ± 3.06	97.10 ± 1.43	26.87 ± 3.83	100.00 ± 0.00	2.78 ± 2.74	100.00 ± 0.00
CMUP-CMIO	391	344	319	313	161	160	32	30	5	4
	0.10 ± 0.00	87.98 ± 1.64	92.73 ± 1.40	98.12 ± 0.76	51.44 ± 2.82	99.38 ± 0.62	20.00 ± 3.16	93.75 ± 4.28	16.67 ± 6.80	80.00 ± 17.89
CMX-CMX	177	151	118	116	67	64	12	12	1	1
	0.04 ± 0.00	85.31 ± 2.66	78.15 ± 3.36	98.31 ± 1.19	57.76 ± 4.59	95.52 ± 2.53	18.75 ± 4.88	100.00 ± 0.00	8.33 ± 7.98	100.00 ± 0.00
CMX-CMU	92	83	82	81	45	44	9	9	1	0
	0.02 ± 0.00	90.22 ± 3.10	98.80 ± 1.20	98.78 ± 1.21	55.56 ± 5.52	97.78 ± 2.20	20.45 ± 6.08	100.00 ± 0.00	11.11 ± 10.48	0.00 ± 0.00
CMX-CMP	118	108	105	104	58	56	15	14	1	0
	0.03 ± 0.00	91.53 ± 2.56	97.22 ± 1.58	99.05 ± 0.95	55.77 ± 4.87	96.55 ± 2.40	26.79 ± 5.92	93.33 ± 6.44	7.14 ± 6.88	0.00 ± 0.00
CMX-CMIO	152	126	121	120	66	66	24	23	4	3
	0.04 ± 0.00	82.89 ± 3.05	96.03 ± 1.74	99.17 ± 0.82	55.00 ± 4.54	100.00 ± 0.00	36.36 ± 5.92	95.83 ± 4.08	17.39 ± 7.90	75.00 ± 21.65
$\mu\mu$	2647	2282	2136	2098	1120	1095	261	255	22	16
	0.67 ± 0.01	86.21 ± 0.67	93.60 ± 0.51	98.22 ± 0.29	53.38 ± 1.09	97.77 ± 0.44	23.84 ± 1.29	97.70 ± 0.93	8.63 ± 1.76	72.73 ± 9.50
total	5861	5048	4661	4593	2507	2354	526	516	42	31
	1.48 ± 0.02	86.13 ± 0.45	92.33 ± 0.37	98.54 ± 0.18	54.58 ± 0.73	93.90 ± 0.48	22.34 ± 0.86	98.10 ± 0.60	8.14 ± 1.20	73.81 ± 6.78

Table 46: $W\gamma$ MC acceptance table, assuming $M_H^{\rm SM} = 160$ GeV

Category	Lepton ID	Lep1 Isol	Lep2 Isol	$M_{\ell\ell} > 16$	jet veto	opp sign	$\not\!\!E_t$	$\not\!\!E_t$ || $\Delta\phi$	$M_{\ell\ell} < M_H/2$	$p^1 p^2 \not\!\!E_t < M_H$
TCE-TCE	88	47	38	25	25	15	3	3	3	3
	0.02 ± 0.00	53.41 ± 5.32	80.85 ± 5.74	65.79 ± 7.70	100.00 ± 0.00	60.00 ± 9.80	20.00 ± 10.33	100.00 ± 0.00	100.00 ± 0.00	100.00 ± 0.00
TCE-PHX	88	76	69	60	58	36	7	7	5	5
	0.02 ± 0.00	86.36 ± 3.66	90.79 ± 3.32	86.96 ± 4.05	96.67 ± 2.32	62.07 ± 6.37	19.44 ± 6.60	100.00 ± 0.00	71.43 ± 17.07	100.00 ± 0.00
PHX-PHX	0	0	0	0	0	0	0	0	0	0
	0.00 ± 0.00	0.00 ± 0.00	0.00 ± 0.00	0.00 ± 0.00	0.00 ± 0.00	0.00 ± 0.00	0.00 ± 0.00	0.00 ± 0.00	0.00 ± 0.00	0.00 ± 0.00
ee	176	123	107	85	83	51	10	10	8	8
	0.05 ± 0.00	69.89 ± 3.46	86.99 ± 3.03	79.44 ± 3.91	97.65 ± 1.64	61.45 ± 5.34	19.61 ± 5.56	100.00 ± 0.00	80.00 ± 12.65	100.00 ± 0.00
TCE-CMUP	70	31	26	15	15	9	2	2	2	2
	0.02 ± 0.00	44.29 ± 5.94	83.87 ± 6.61	57.69 ± 9.69	100.00 ± 0.00	60.00 ± 12.65	22.22 ± 13.86	100.00 ± 0.00	100.00 ± 0.00	100.00 ± 0.00
TCE-CMX	37	15	9	8	8	2	0	0	0	0
	0.01 ± 0.00	40.54 ± 8.07	60.00 ± 12.65	88.89 ± 10.48	100.00 ± 0.00	25.00 ± 15.31	0.00 ± 0.00	0.00 ± 0.00	0.00 ± 0.00	0.00 ± 0.00
TCE-CMU	4	4	4	4	4	1	1	1	0	0
	0.00 ± 0.00	100.00 ± 0.00	100.00 ± 0.00	100.00 ± 0.00	100.00 ± 0.00	25.00 ± 21.65	100.00 ± 0.00	100.00 ± 0.00	0.00 ± 0.00	0.00 ± 0.00
TCE-CMP	2	2	1	0	0	0	0	0	0	0
	0.00 ± 0.00	100.00 ± 0.00	50.00 ± 35.36	0.00 ± 0.00	0.00 ± 0.00	0.00 ± 0.00	0.00 ± 0.00	0.00 ± 0.00	0.00 ± 0.00	0.00 ± 0.00
TCE-CMIO	14	8	5	4	4	2	0	0	0	0
	0.00 ± 0.00	57.14 ± 13.23	62.50 ± 17.12	80.00 ± 17.89	100.00 ± 0.00	50.00 ± 25.00	0.00 ± 0.00	0.00 ± 0.00	0.00 ± 0.00	0.00 ± 0.00
PHX-CMUP	28	26	26	25	24	10	6	6	3	2
	0.01 ± 0.00	92.86 ± 4.87	100.00 ± 0.00	96.15 ± 3.77	96.00 ± 3.92	41.67 ± 10.06	60.00 ± 15.49	100.00 ± 0.00	50.00 ± 20.41	66.67 ± 27.22
PHX-CMX	26	23	22	17	16	8	1	1	1	1
	0.01 ± 0.00	88.46 ± 6.27	95.65 ± 4.25	77.27 ± 8.93	94.12 ± 5.71	50.00 ± 12.50	12.50 ± 11.69	100.00 ± 0.00	100.00 ± 0.00	100.00 ± 0.00
PHX-CMU	6	6	6	6	6	4	0	0	0	0
	0.00 ± 0.00	100.00 ± 0.00	100.00 ± 0.00	100.00 ± 0.00	100.00 ± 0.00	66.67 ± 19.25	0.00 ± 0.00	0.00 ± 0.00	0.00 ± 0.00	0.00 ± 0.00
PHX-CMP	7	7	7	7	6	4	2	2	1	1
	0.00 ± 0.00	100.00 ± 0.00	100.00 ± 0.00	100.00 ± 0.00	85.71 ± 13.23	66.67 ± 19.25	50.00 ± 25.00	100.00 ± 0.00	50.00 ± 35.36	100.00 ± 0.00
PHX-CMIO	13	10	9	8	8	2	0	0	0	0
	0.00 ± 0.00	76.92 ± 11.69	90.00 ± 9.49	88.89 ± 10.48	100.00 ± 0.00	25.00 ± 15.31	0.00 ± 0.00	0.00 ± 0.00	0.00 ± 0.00	0.00 ± 0.00
$e\mu$	207	132	115	94	91	42	12	12	7	6
	0.06 ± 0.00	63.77 ± 3.34	87.12 ± 2.92	81.74 ± 3.60	96.81 ± 1.81	46.15 ± 5.23	28.57 ± 6.97	100.00 ± 0.00	58.33 ± 14.23	85.71 ± 13.23
CMUP-CMUP	0	0	0	0	0	0	0	0	0	0
	0.00 ± 0.00	0.00 ± 0.00	0.00 ± 0.00	0.00 ± 0.00	0.00 ± 0.00	0.00 ± 0.00	0.00 ± 0.00	0.00 ± 0.00	0.00 ± 0.00	0.00 ± 0.00
CMUP-CMX	0	0	0	0	0	0	0	0	0	0
	0.00 ± 0.00	0.00 ± 0.00	0.00 ± 0.00	0.00 ± 0.00	0.00 ± 0.00	0.00 ± 0.00	0.00 ± 0.00	0.00 ± 0.00	0.00 ± 0.00	0.00 ± 0.00
CMUP-CMU	0	0	0	0	0	0	0	0	0	0
	0.00 ± 0.00	0.00 ± 0.00	0.00 ± 0.00	0.00 ± 0.00	0.00 ± 0.00	0.00 ± 0.00	0.00 ± 0.00	0.00 ± 0.00	0.00 ± 0.00	0.00 ± 0.00
CMUP-CMP	0	0	0	0	0	0	0	0	0	0
	0.00 ± 0.00	0.00 ± 0.00	0.00 ± 0.00	0.00 ± 0.00	0.00 ± 0.00	0.00 ± 0.00	0.00 ± 0.00	0.00 ± 0.00	0.00 ± 0.00	0.00 ± 0.00
CMUP-CMIO	2	0	0	0	0	0	0	0	0	0
	0.00 ± 0.00	0.00 ± 0.00	0.00 ± 0.00	0.00 ± 0.00	0.00 ± 0.00	0.00 ± 0.00	0.00 ± 0.00	0.00 ± 0.00	0.00 ± 0.00	0.00 ± 0.00
CMX-CMX	0	0	0	0	0	0	0	0	0	0
	0.00 ± 0.00	0.00 ± 0.00	0.00 ± 0.00	0.00 ± 0.00	0.00 ± 0.00	0.00 ± 0.00	0.00 ± 0.00	0.00 ± 0.00	0.00 ± 0.00	0.00 ± 0.00
CMX-CMU	0	0	0	0	0	0	0	0	0	0
	0.00 ± 0.00	0.00 ± 0.00	0.00 ± 0.00	0.00 ± 0.00	0.00 ± 0.00	0.00 ± 0.00	0.00 ± 0.00	0.00 ± 0.00	0.00 ± 0.00	0.00 ± 0.00
CMX-CMP	0	0	0	0	0	0	0	0	0	0
	0.00 ± 0.00	0.00 ± 0.00	0.00 ± 0.00	0.00 ± 0.00	0.00 ± 0.00	0.00 ± 0.00	0.00 ± 0.00	0.00 ± 0.00	0.00 ± 0.00	0.00 ± 0.00
CMX-CMIO	0	0	0	0	0	0	0	0	0	0
	0.00 ± 0.00	0.00 ± 0.00	0.00 ± 0.00	0.00 ± 0.00	0.00 ± 0.00	0.00 ± 0.00	0.00 ± 0.00	0.00 ± 0.00	0.00 ± 0.00	0.00 ± 0.00
$\mu\mu$	2	0	0	0	0	0	0	0	0	0
	0.00 ± 0.00	0.00 ± 0.00	0.00 ± 0.00	0.00 ± 0.00	0.00 ± 0.00	0.00 ± 0.00	0.00 ± 0.00	0.00 ± 0.00	0.00 ± 0.00	0.00 ± 0.00
total	385	255	222	179	174	93	22	22	15	14
	0.10 ± 0.01	66.23 ± 2.41	87.06 ± 2.10	80.63 ± 2.65	97.21 ± 1.23	53.45 ± 3.78	23.66 ± 4.41	100.00 ± 0.00	68.18 ± 9.93	93.33 ± 6.44

Table 47: fakesacceptance table, assuming $M_H^{\rm SM} = 160$ GeV

Category	Lepton ID	Lep1 Isol	Lep2 Isol	$M_{\ell\ell} > 16$	jet veto	opp sign	$\not\!\!E_t$	$\not\!\!E_t$ || $\Delta\phi$	$M_{\ell\ell} < M_H/2$	$p^1 p^2 \not\!\!E_t < M_H$
TCE-TCE	9735	7937	7278	7191	6856	6523	94	69	54	54
	0.10 ± 0.00	81.53 ± 0.39	91.70 ± 0.31	98.80 ± 0.13	95.34 ± 0.25	95.14 ± 0.26	1.44 ± 0.15	73.40 ± 4.56	78.26 ± 4.97	100.00 ± 0.00
TCE-PHX	8301	6792	6415	6406	6139	2352	35	31	20	20
	0.09 ± 0.00	81.82 ± 0.42	94.45 ± 0.28	99.86 ± 0.05	95.83 ± 0.25	38.31 ± 0.62	1.49 ± 0.25	88.57 ± 5.38	64.52 ± 8.59	100.00 ± 0.00
PHX-PHX	0	0	0	0	0	0	0	0	0	0
	0.00 ± 0.00	0.00 ± 0.00	0.00 ± 0.00	0.00 ± 0.00	0.00 ± 0.00	0.00 ± 0.00	0.00 ± 0.00	0.00 ± 0.00	0.00 ± 0.00	0.00 ± 0.00
ee	18036	14729	13693	13597	12995	8875	129	100	74	74
	0.19 ± 0.00	81.66 ± 0.29	92.97 ± 0.21	99.30 ± 0.07	95.57 ± 0.18	68.30 ± 0.41	1.45 ± 0.13	77.52 ± 3.68	74.00 ± 4.39	100.00 ± 0.00
TCE-CMUP	818	383	345	328	298	216	25	25	20	16
	0.01 ± 0.00	46.82 ± 1.74	90.08 ± 1.53	95.07 ± 1.17	90.85 ± 1.59	72.48 ± 2.59	11.57 ± 2.18	100.00 ± 0.00	80.00 ± 8.00	80.00 ± 8.94
TCE-CMX	534	201	181	174	164	109	18	17	12	12
	0.01 ± 0.00	37.64 ± 2.10	90.05 ± 2.11	96.13 ± 1.43	94.25 ± 1.76	66.46 ± 3.69	16.51 ± 3.56	94.44 ± 5.40	70.59 ± 11.05	100.00 ± 0.00
TCE-CMU	19	11	7	7	5	4	2	2	2	2
	0.00 ± 0.00	57.89 ± 11.33	63.64 ± 14.50	100.00 ± 0.00	71.43 ± 17.07	80.00 ± 17.89	50.00 ± 25.00	100.00 ± 0.00	100.00 ± 0.00	100.00 ± 0.00
TCE-CMP	9	7	5	5	3	3	0	0	0	0
	0.00 ± 0.00	77.78 ± 13.86	71.43 ± 17.07	100.00 ± 0.00	60.00 ± 21.91	100.00 ± 0.00	0.00 ± 0.00	0.00 ± 0.00	0.00 ± 0.00	0.00 ± 0.00
TCE-CMIO	1093	820	747	736	474	436	10	9	6	6
	0.01 ± 0.00	75.02 ± 1.31	91.10 ± 0.99	98.53 ± 0.44	64.40 ± 1.76	91.98 ± 1.25	2.29 ± 0.72	90.00 ± 9.49	66.67 ± 15.71	100.00 ± 0.00
PHX-CMUP	599	216	194	194	175	7	0	0	0	0
	0.01 ± 0.00	36.06 ± 1.96	89.81 ± 2.06	100.00 ± 0.00	90.21 ± 2.13	4.00 ± 1.48	0.00 ± 0.00	0.00 ± 0.00	0.00 ± 0.00	0.00 ± 0.00
PHX-CMX	300	106	97	92	85	3	2	2	1	1
	0.00 ± 0.00	35.33 ± 2.76	91.51 ± 2.71	94.85 ± 2.25	92.39 ± 2.76	3.53 ± 2.00	66.67 ± 27.22	100.00 ± 0.00	50.00 ± 35.36	100.00 ± 0.00
PHX-CMU	10	5	5	5	3	0	0	0	0	0
	0.00 ± 0.00	50.00 ± 15.81	100.00 ± 0.00	100.00 ± 0.00	60.00 ± 21.91	0.00 ± 0.00	0.00 ± 0.00	0.00 ± 0.00	0.00 ± 0.00	0.00 ± 0.00
PHX-CMP	39	7	5	5	5	0	0	0	0	0
	0.00 ± 0.00	17.95 ± 6.15	71.43 ± 17.07	100.00 ± 0.00	100.00 ± 0.00	0.00 ± 0.00	0.00 ± 0.00	0.00 ± 0.00	0.00 ± 0.00	0.00 ± 0.00
PHX-CMIO	323	204	199	192	125	14	4	4	1	1
	0.00 ± 0.00	63.16 ± 2.68	97.55 ± 1.08	96.48 ± 1.31	65.10 ± 3.44	11.20 ± 2.82	28.57 ± 12.07	100.00 ± 0.00	25.00 ± 21.65	100.00 ± 0.00
$e\mu$	3744	1960	1785	1738	1337	792	61	59	42	38
	0.04 ± 0.00	52.35 ± 0.82	91.07 ± 0.64	97.37 ± 0.38	76.93 ± 1.01	59.24 ± 1.34	7.70 ± 0.95	96.72 ± 2.28	71.19 ± 5.90	90.48 ± 4.53
CMUP-CMUP	651	607	542	535	483	481	0	0	0	0
	0.01 ± 0.00	93.24 ± 0.98	89.29 ± 1.26	98.71 ± 0.48	90.28 ± 1.28	99.59 ± 0.29	0.00 ± 0.00	0.00 ± 0.00	0.00 ± 0.00	0.00 ± 0.00
CMUP-CMX	421	399	398	397	362	362	0	0	0	0
	0.00 ± 0.00	94.77 ± 1.08	99.75 ± 0.25	99.75 ± 0.25	91.18 ± 1.42	100.00 ± 0.00	0.00 ± 0.00	0.00 ± 0.00	0.00 ± 0.00	0.00 ± 0.00
CMUP-CMU	110	102	102	102	98	98	0	0	0	0
	0.00 ± 0.00	92.73 ± 2.48	100.00 ± 0.00	100.00 ± 0.00	96.08 ± 1.92	100.00 ± 0.00	0.00 ± 0.00	0.00 ± 0.00	0.00 ± 0.00	0.00 ± 0.00
CMUP-CMP	108	100	99	99	91	90	1	1	1	1
	0.00 ± 0.00	92.59 ± 2.52	99.00 ± 0.99	100.00 ± 0.00	91.92 ± 2.74	98.90 ± 1.09	1.11 ± 1.10	100.00 ± 0.00	100.00 ± 0.00	100.00 ± 0.00
CMUP-CMIO	393	307	296	286	254	231	8	8	5	4
	0.00 ± 0.00	78.12 ± 2.09	96.42 ± 1.06	96.62 ± 1.05	88.81 ± 1.86	90.94 ± 1.80	3.46 ± 1.20	100.00 ± 0.00	62.50 ± 17.12	80.00 ± 17.89
CMX-CMX	120	97	76	73	67	67	0	0	0	0
	0.00 ± 0.00	80.83 ± 3.59	78.35 ± 4.18	96.05 ± 2.23	91.78 ± 3.21	100.00 ± 0.00	0.00 ± 0.00	0.00 ± 0.00	0.00 ± 0.00	0.00 ± 0.00
CMX-CMU	50	46	45	45	40	40	0	0	0	0
	0.00 ± 0.00	92.00 ± 3.84	97.83 ± 2.15	100.00 ± 0.00	88.89 ± 4.68	100.00 ± 0.00	0.00 ± 0.00	0.00 ± 0.00	0.00 ± 0.00	0.00 ± 0.00
CMX-CMP	41	40	40	40	35	35	0	0	0	0
	0.00 ± 0.00	97.56 ± 2.41	100.00 ± 0.00	100.00 ± 0.00	87.50 ± 5.23	100.00 ± 0.00	0.00 ± 0.00	0.00 ± 0.00	0.00 ± 0.00	0.00 ± 0.00
CMX-CMIO	158	121	116	113	98	84	0	0	0	0
	0.00 ± 0.00	76.58 ± 3.37	95.87 ± 1.81	97.41 ± 1.47	86.73 ± 3.19	85.71 ± 3.53	0.00 ± 0.00	0.00 ± 0.00	0.00 ± 0.00	0.00 ± 0.00
$\mu\mu$	2052	1819	1714	1690	1528	1488	9	9	6	5
	0.02 ± 0.00	88.65 ± 0.70	94.23 ± 0.55	98.60 ± 0.28	90.41 ± 0.72	97.38 ± 0.41	0.60 ± 0.20	100.00 ± 0.00	66.67 ± 15.71	83.33 ± 15.21
total	23832	18508	17192	17025	15860	11155	199	168	122	117
	0.25 ± 0.00	77.66 ± 0.27	92.89 ± 0.19	99.03 ± 0.07	93.16 ± 0.19	70.33 ± 0.36	1.78 ± 0.13	84.42 ± 2.57	72.62 ± 3.44	95.90 ± 1.79

Table 48: data acceptance table, assuming $M_H^{\rm SM} = 170$ GeV

Category	Lepton ID	Lep1 Isol	Lep2 Isol	$M_{\ell\ell} > 16$	jet veto	opp sign	$\not\!\!E_t$	$\not\!\!E_t$ $\|\|$ $\Delta\phi$	$M_{\ell\ell} < M_H/2$	$p^1 p^2 \not\!\!E_t < M_H$
TCE-TCE	9493	7991	7288	7195	6969	6959	6	4	2	2
	0.10 ± 0.00	84.18 ± 0.37	91.20 ± 0.32	98.72 ± 0.13	96.86 ± 0.21	99.86 ± 0.05	0.09 ± 0.04	66.67 ± 19.25	50.00 ± 25.00	100.00 ± 0.00
TCE-PHX	8804	8275	7922	7920	7729	6837	4	4	3	3
	0.09 ± 0.00	93.99 ± 0.25	95.73 ± 0.22	99.97 ± 0.02	97.59 ± 0.17	88.46 ± 0.36	0.06 ± 0.03	100.00 ± 0.00	75.00 ± 21.65	100.00 ± 0.00
PHX-PHX	0	0	0	0	0	0	0	0	0	0
	0.00 ± 0.00	0.00 ± 0.00	0.00 ± 0.00	0.00 ± 0.00	0.00 ± 0.00	0.00 ± 0.00	0.00 ± 0.00	0.00 ± 0.00	0.00 ± 0.00	0.00 ± 0.00
ee	18297	16266	15210	15115	14698	13796	10	8	5	5
	0.20 ± 0.00	88.90 ± 0.23	93.51 ± 0.19	99.38 ± 0.06	97.24 ± 0.13	93.86 ± 0.20	0.07 ± 0.02	80.00 ± 12.65	62.50 ± 17.12	100.00 ± 0.00
TCE-CMUP	403	86	81	79	69	68	3	3	2	2
	0.00 ± 0.00	21.34 ± 2.04	94.19 ± 2.52	97.53 ± 1.72	87.34 ± 3.74	98.55 ± 1.44	4.41 ± 2.49	100.00 ± 0.00	66.67 ± 27.22	100.00 ± 0.00
TCE-CMX	250	48	42	42	38	37	4	4	2	2
	0.00 ± 0.00	19.20 ± 2.49	87.50 ± 4.77	100.00 ± 0.00	90.48 ± 4.53	97.37 ± 2.60	10.81 ± 5.10	100.00 ± 0.00	50.00 ± 25.00	100.00 ± 0.00
TCE-CMU	13	8	6	6	5	5	0	0	0	0
	0.00 ± 0.00	61.54 ± 13.49	75.00 ± 15.31	100.00 ± 0.00	83.33 ± 15.21	100.00 ± 0.00	0.00 ± 0.00	0.00 ± 0.00	0.00 ± 0.00	0.00 ± 0.00
TCE-CMP	34	12	11	11	9	9	1	1	0	0
	0.00 ± 0.00	35.29 ± 8.20	91.67 ± 7.98	100.00 ± 0.00	81.82 ± 11.63	100.00 ± 0.00	11.11 ± 10.48	100.00 ± 0.00	0.00 ± 0.00	0.00 ± 0.00
TCE-CMIO	419	34	31	31	29	29	3	3	2	1
	0.00 ± 0.00	8.11 ± 1.33	91.18 ± 4.86	100.00 ± 0.00	93.55 ± 4.41	100.00 ± 0.00	10.34 ± 5.66	100.00 ± 0.00	66.67 ± 27.22	50.00 ± 35.36
PHX-CMUP	70	22	21	21	19	10	1	1	0	0
	0.00 ± 0.00	31.43 ± 5.55	95.45 ± 4.44	100.00 ± 0.00	90.48 ± 6.41	52.63 ± 11.45	10.00 ± 9.49	100.00 ± 0.00	0.00 ± 0.00	0.00 ± 0.00
PHX-CMX	39	17	17	17	17	11	0	0	0	0
	0.00 ± 0.00	43.59 ± 7.94	100.00 ± 0.00	100.00 ± 0.00	100.00 ± 0.00	64.71 ± 11.59	0.00 ± 0.00	0.00 ± 0.00	0.00 ± 0.00	0.00 ± 0.00
PHX-CMU	1	0	0	0	0	0	0	0	0	0
	0.00 ± 0.00	0.00 ± 0.00	0.00 ± 0.00	0.00 ± 0.00	0.00 ± 0.00	0.00 ± 0.00	0.00 ± 0.00	0.00 ± 0.00	0.00 ± 0.00	0.00 ± 0.00
PHX-CMP	7	2	2	2	2	2	2	2	1	1
	0.00 ± 0.00	28.57 ± 17.07	100.00 ± 0.00	100.00 ± 0.00	100.00 ± 0.00	100.00 ± 0.00	100.00 ± 0.00	100.00 ± 0.00	50.00 ± 35.36	100.00 ± 0.00
PHX-CMIO	42	3	3	3	2	1	1	1	1	1
	0.00 ± 0.00	7.14 ± 3.97	100.00 ± 0.00	100.00 ± 0.00	66.67 ± 27.22	50.00 ± 35.36	100.00 ± 0.00	100.00 ± 0.00	100.00 ± 0.00	100.00 ± 0.00
$e\mu$	1278	232	214	212	190	172	15	15	8	7
	0.01 ± 0.00	18.15 ± 1.08	92.24 ± 1.76	99.07 ± 0.66	89.62 ± 2.09	90.53 ± 2.12	8.72 ± 2.15	100.00 ± 0.00	53.33 ± 12.88	87.50 ± 11.69
CMUP-CMUP	2671	2267	2102	2082	2021	2020	3	3	3	3
	0.03 ± 0.00	84.87 ± 0.69	92.72 ± 0.55	99.05 ± 0.21	97.07 ± 0.37	99.95 ± 0.05	0.15 ± 0.09	100.00 ± 0.00	100.00 ± 0.00	100.00 ± 0.00
CMUP-CMX	2507	2286	2247	2234	2158	2157	2	2	2	1
	0.03 ± 0.00	91.18 ± 0.57	98.29 ± 0.27	99.42 ± 0.16	96.60 ± 0.38	99.95 ± 0.05	0.09 ± 0.07	100.00 ± 0.00	100.00 ± 0.00	50.00 ± 35.36
CMUP-CMU	831	797	785	785	762	762	0	0	0	0
	0.01 ± 0.00	95.91 ± 0.69	98.49 ± 0.43	100.00 ± 0.00	97.07 ± 0.60	100.00 ± 0.00	0.00 ± 0.00	0.00 ± 0.00	0.00 ± 0.00	0.00 ± 0.00
CMUP-CMP	1132	1047	1012	1011	978	978	1	1	1	1
	0.01 ± 0.00	92.49 ± 0.78	96.66 ± 0.56	99.90 ± 0.10	96.74 ± 0.56	100.00 ± 0.00	0.10 ± 0.10	100.00 ± 0.00	100.00 ± 0.00	100.00 ± 0.00
CMUP-CMIO	1956	1677	1614	1592	1533	1533	2	2	1	1
	0.02 ± 0.00	85.74 ± 0.79	96.24 ± 0.46	98.64 ± 0.29	96.29 ± 0.47	100.00 ± 0.00	0.13 ± 0.09	100.00 ± 0.00	50.00 ± 35.36	100.00 ± 0.00
CMX-CMX	1114	907	796	794	774	773	0	0	0	0
	0.01 ± 0.00	81.42 ± 1.17	87.76 ± 1.09	99.75 ± 0.18	97.48 ± 0.56	99.87 ± 0.13	0.00 ± 0.00	0.00 ± 0.00	0.00 ± 0.00	0.00 ± 0.00
CMX-CMU	474	449	436	435	428	428	0	0	0	0
	0.01 ± 0.00	94.73 ± 1.03	97.10 ± 0.79	99.77 ± 0.23	98.39 ± 0.60	100.00 ± 0.00	0.00 ± 0.00	0.00 ± 0.00	0.00 ± 0.00	0.00 ± 0.00
CMX-CMP	524	487	480	480	465	465	0	0	0	0
	0.01 ± 0.00	92.94 ± 1.12	98.56 ± 0.54	100.00 ± 0.00	96.88 ± 0.79	100.00 ± 0.00	0.00 ± 0.00	0.00 ± 0.00	0.00 ± 0.00	0.00 ± 0.00
CMX-CMIO	811	685	670	666	629	629	1	1	1	0
	0.01 ± 0.00	84.46 ± 1.27	97.81 ± 0.56	99.40 ± 0.30	94.44 ± 0.89	100.00 ± 0.00	0.16 ± 0.16	100.00 ± 0.00	100.00 ± 0.00	0.00 ± 0.00
$\mu\mu$	12020	10602	10142	10079	9748	9745	9	9	8	6
	0.13 ± 0.00	88.20 ± 0.29	95.66 ± 0.20	99.38 ± 0.08	96.72 ± 0.18	99.97 ± 0.02	0.09 ± 0.03	100.00 ± 0.00	88.89 ± 10.48	75.00 ± 15.31
total	31595	27100	25566	25406	24636	23713	34	32	21	18
	0.34 ± 0.00	85.77 ± 0.20	94.34 ± 0.14	99.37 ± 0.05	96.97 ± 0.11	96.25 ± 0.12	0.14 ± 0.02	94.12 ± 4.04	65.62 ± 8.40	85.71 ± 7.64

Table 49: data acceptance table, assuming $M_H^{\rm SM} = 180$ GeV

Category	Lepton ID	Lep1 Isol	Lep2 Isol	$M_{\ell\ell} > 16$	jet veto	opp sign	$\not\!\!E_t$	$\not\!\!E_t$ || $\Delta\phi$	$M_{\ell\ell} < M_H/2$	$p^1 p^2 \not\!\!E_t < M_H$
TCE-TCE	9493 0.10 ± 0.00	7991 84.18 ± 0.37	7288 91.20 ± 0.32	7195 98.72 ± 0.13	6969 96.86 ± 0.21	6959 99.86 ± 0.05	5 0.07 ± 0.03	4 80.00 ± 17.89	2 50.00 ± 25.00	2 100.00 ± 0.00
TCE-PHX	8804 0.09 ± 0.00	8275 93.99 ± 0.25	7922 95.73 ± 0.22	7920 99.97 ± 0.02	7729 97.59 ± 0.17	6837 88.46 ± 0.36	4 0.06 ± 0.03	4 100.00 ± 0.00	3 75.00 ± 21.65	3 100.00 ± 0.00
PHX-PHX	0 0.00 ± 0.00	0 0.00 ± 0.00	0 0.00 ± 0.00	0 0.00 ± 0.00	0 0.00 ± 0.00	0 0.00 ± 0.00	0 0.00 ± 0.00	0 0.00 ± 0.00	0 0.00 ± 0.00	0 0.00 ± 0.00
ee	18297 0.20 ± 0.00	16266 88.90 ± 0.23	15210 93.51 ± 0.19	15115 99.38 ± 0.06	14698 97.24 ± 0.13	13796 93.86 ± 0.20	9 0.07 ± 0.02	8 88.89 ± 10.48	5 62.50 ± 17.12	5 100.00 ± 0.00
TCE-CMUP	403 0.00 ± 0.00	86 21.34 ± 2.04	81 94.19 ± 2.52	79 97.53 ± 1.72	69 87.34 ± 3.74	68 98.55 ± 1.44	3 4.41 ± 2.49	3 100.00 ± 0.00	2 66.67 ± 27.22	2 100.00 ± 0.00
TCE-CMX	250 0.00 ± 0.00	48 19.20 ± 2.49	42 87.50 ± 4.77	42 100.00 ± 0.00	38 90.48 ± 4.53	37 97.37 ± 2.60	4 10.81 ± 5.10	4 100.00 ± 0.00	3 75.00 ± 21.65	3 100.00 ± 0.00
TCE-CMU	13 0.00 ± 0.00	8 61.54 ± 13.49	6 75.00 ± 15.31	6 100.00 ± 0.00	5 83.33 ± 15.21	5 100.00 ± 0.00	0 0.00 ± 0.00	0 0.00 ± 0.00	0 0.00 ± 0.00	0 0.00 ± 0.00
TCE-CMP	34 0.00 ± 0.00	12 35.29 ± 8.20	11 91.67 ± 7.98	11 100.00 ± 0.00	9 81.82 ± 11.63	9 100.00 ± 0.00	1 11.11 ± 10.48	1 100.00 ± 0.00	0 0.00 ± 0.00	0 0.00 ± 0.00
TCE-CMIO	419 0.00 ± 0.00	34 8.11 ± 1.33	31 91.18 ± 4.86	31 100.00 ± 0.00	29 93.55 ± 4.41	29 100.00 ± 0.00	3 10.34 ± 5.66	3 100.00 ± 0.00	2 66.67 ± 27.22	1 50.00 ± 35.36
PHX-CMUP	70 0.00 ± 0.00	22 31.43 ± 5.55	21 95.45 ± 4.44	21 100.00 ± 0.00	19 90.48 ± 6.41	10 52.63 ± 11.45	0 0.00 ± 0.00	0 0.00 ± 0.00	0 0.00 ± 0.00	0 0.00 ± 0.00
PHX-CMX	39 0.00 ± 0.00	17 43.59 ± 7.94	17 100.00 ± 0.00	17 100.00 ± 0.00	17 100.00 ± 0.00	11 64.71 ± 11.59	0 0.00 ± 0.00	0 0.00 ± 0.00	0 0.00 ± 0.00	0 0.00 ± 0.00
PHX-CMU	1 0.00 ± 0.00	0 0.00 ± 0.00	0 0.00 ± 0.00	0 0.00 ± 0.00	0 0.00 ± 0.00	0 0.00 ± 0.00	0 0.00 ± 0.00	0 0.00 ± 0.00	0 0.00 ± 0.00	0 0.00 ± 0.00
PHX-CMP	7 0.00 ± 0.00	2 28.57 ± 17.07	2 100.00 ± 0.00	2 100.00 ± 0.00	2 100.00 ± 0.00	2 100.00 ± 0.00	2 100.00 ± 0.00	2 100.00 ± 0.00	1 50.00 ± 35.36	1 100.00 ± 0.00
PHX-CMIO	42 0.00 ± 0.00	3 7.14 ± 3.97	3 100.00 ± 0.00	3 100.00 ± 0.00	2 66.67 ± 27.22	1 50.00 ± 35.36	1 100.00 ± 0.00	1 100.00 ± 0.00	1 100.00 ± 0.00	1 100.00 ± 0.00
$e\mu$	1278 0.01 ± 0.00	232 18.15 ± 1.08	214 92.24 ± 1.76	212 99.07 ± 0.66	190 89.62 ± 2.09	172 90.53 ± 2.12	14 8.14 ± 2.08	14 100.00 ± 0.00	9 64.29 ± 12.81	8 88.89 ± 10.48
CMUP-CMUP	2671 0.03 ± 0.00	2267 84.87 ± 0.69	2102 92.72 ± 0.55	2082 99.05 ± 0.21	2021 97.07 ± 0.37	2020 99.95 ± 0.05	3 0.15 ± 0.09	3 100.00 ± 0.00	3 100.00 ± 0.00	3 100.00 ± 0.00
CMUP-CMX	2507 0.03 ± 0.00	2286 91.18 ± 0.57	2247 98.29 ± 0.27	2234 99.42 ± 0.16	2158 96.60 ± 0.38	2157 99.95 ± 0.05	2 0.09 ± 0.07	2 100.00 ± 0.00	2 100.00 ± 0.00	1 50.00 ± 35.36
CMUP-CMU	831 0.01 ± 0.00	797 95.91 ± 0.69	785 98.49 ± 0.43	785 100.00 ± 0.00	762 97.07 ± 0.60	762 100.00 ± 0.00	0 0.00 ± 0.00	0 0.00 ± 0.00	0 0.00 ± 0.00	0 0.00 ± 0.00
CMUP-CMP	1132 0.01 ± 0.00	1047 92.49 ± 0.78	1012 96.66 ± 0.56	1011 99.90 ± 0.10	978 96.74 ± 0.56	978 100.00 ± 0.00	1 0.10 ± 0.10	1 100.00 ± 0.00	1 100.00 ± 0.00	1 100.00 ± 0.00
CMUP-CMIO	1956 0.02 ± 0.00	1677 85.74 ± 0.79	1614 96.24 ± 0.46	1592 98.64 ± 0.29	1533 96.29 ± 0.47	1533 100.00 ± 0.00	1 0.07 ± 0.07	1 100.00 ± 0.00	0 0.00 ± 0.00	0 0.00 ± 0.00
CMX-CMX	1114 0.01 ± 0.00	907 81.42 ± 1.17	796 87.76 ± 1.09	794 99.75 ± 0.18	774 97.48 ± 0.56	773 99.87 ± 0.13	0 0.00 ± 0.00	0 0.00 ± 0.00	0 0.00 ± 0.00	0 0.00 ± 0.00
CMX-CMU	474 0.01 ± 0.00	449 94.73 ± 1.03	436 97.10 ± 0.79	435 99.77 ± 0.23	428 98.39 ± 0.60	428 100.00 ± 0.00	0 0.00 ± 0.00	0 0.00 ± 0.00	0 0.00 ± 0.00	0 0.00 ± 0.00
CMX-CMP	524 0.01 ± 0.00	487 92.94 ± 1.12	480 98.56 ± 0.54	480 100.00 ± 0.00	465 96.88 ± 0.79	465 100.00 ± 0.00	0 0.00 ± 0.00	0 0.00 ± 0.00	0 0.00 ± 0.00	0 0.00 ± 0.00
CMX-CMIO	811 0.01 ± 0.00	685 84.46 ± 1.27	670 97.81 ± 0.56	666 99.40 ± 0.30	629 94.44 ± 0.89	629 100.00 ± 0.00	1 0.16 ± 0.16	1 100.00 ± 0.00	1 100.00 ± 0.00	1 100.00 ± 0.00
$\mu\mu$	12020 0.13 ± 0.00	10602 88.20 ± 0.29	10142 95.66 ± 0.20	10079 99.38 ± 0.08	9748 96.72 ± 0.18	9745 99.97 ± 0.02	8 0.08 ± 0.03	8 100.00 ± 0.00	7 87.50 ± 11.69	6 85.71 ± 13.23
total	31595 0.34 ± 0.00	27100 85.77 ± 0.20	25566 94.34 ± 0.14	25406 99.37 ± 0.05	24636 96.97 ± 0.11	23713 96.25 ± 0.12	31 0.13 ± 0.02	30 96.77 ± 3.17	21 70.00 ± 8.37	19 90.48 ± 6.41